Intelligent and Sustainable Manufacturing

SCIEPublish

Review

Electrospun Scaffolds for Spinal Cord Injury Repair: Mechanisms, Strategies, and Advances

Cheng Yang [1], Sijia Zhu [1], Chuankun Li [1], Min Yang [1,*], Yusuf Suleiman Dambatta [2,3], Xiaotian Zhang [2], Yongxing Zang [4], Yanbin Zhang [1], Xiao Ma [1], Peng Yao [5] and Changhe Li [1]

[1] Key Laboratory of Industrial Fluid Energy Conservation and Pollution Control (Ministry of Education), Qingdao University of Technology, Qingdao 266520, China; 13793913215@163.com (C.Y.); 18837627296@163.com (S.Z.); 17685471508@163.com (C.L.); yanbin_zhang@qut.edu.cn (Y.Z.); maxiao@qut.edu.cn (X.M.); lch@qut.edu.cn (C.L.)

[2] School of Mechanical and Electrical Engineering, Qingdao Binhai University, Qingdao 266555, China; ysidambatta@yahoo.com (Y.S.D.); zxt350871607@163.com (X.Z.)

[3] Department of Mechanical Engineering, Ahmadu Bello University, No 210 Sarduna Crescent, Area Bz Samaru, Zaria 810010, Nigeria

[4] Baoding Lizhong Wheel Manufacturing Co., Ltd., No. 948, East Qiyi Road, Baoding 071000, China; yongxing.zang@lzwheel.com (Y.Z.)

[5] Key Laboratory of High Efficiency and Clean Mechanical Manufacture, Shandong University, Ministry of Education, Jinan 250061, China; yaopeng@sdu.edu.cn (P.Y.)

* Corresponding author. E-mail: min_yang@qut.edu.cn (M.Y.)

Received: 16 January 2026; Revised: 31 March 2026; Accepted: 11 May 2026; Available online: 28 May 2026

ABSTRACT: Spinal cord injury (SCI) is a devastating and irreversible damage to the central nervous system that can result in permanent disability or even death. Electrospinning technology, as a specialized fiber preparation method, possesses unique advantages such as high porosity, adjustable pore size, and an extremely high surface area-to-volume ratio. Despite the widespread attention this technology has garnered for its potential application in the treatment of SCI, there is still a lack of comprehensive and up-to-date reviews in the existing literature, and specific clinical treatment guidelines are also scarce. As a result, researchers and clinicians lack targeted guidance for practical implementation. To address this gap, the present article systematically summarizes the mechanisms by which electrospun scaffolds facilitate SCI repair and their current therapeutic applications. First, this review provides an in-depth analysis of the five core mechanisms underlying electrospinning therapy for SCI, including extracellular matrix (ECM) mimicry, axonal-extension guidance, multimodal signal regulation, drug loading and sustained release, and physical support and protection. Next, this review examines how key electrospinning parameters (fiber diameter, alignment, surface chemistry, biodegradation rate, and nanomorphology) influence these therapeutic mechanisms. Finally, this review explores the state-of-the-art applications of electrospun scaffolds in SCI treatment, including purely structural conduits, biochemical functionalization (drug loading and controlled release, immunomodulation and anti-inflammation, and coaxial electrospinning), and multi-component composite materials (hydrogel–electrospun hybrids, cell- and growth-factor co-delivery systems, and cell electrospinning).

Keywords: Electrospinning; Spinal cord injury; Nanofiber scaffold

1. Introduction

SCI, as a complex and serious medical condition, can be traced back to various external and internal factors, including but not limited to severe trauma, long-term inflammatory infiltration, spinal cord tumor occupying space, vascular disease obstruction, *etc*. These unfavorable factors work together in the human body, causing damage to the structural integrity of the spinal cord, a key nerve center, and leading to its comprehensive decline in function [1–3]. This type of injury profoundly affects the intricate neural transmission network within the spinal cord, resulting in a series of serious clinical consequences in the body segments below the site of injury, such as loss of motor ability, decreased or even disappeared sensory function, autonomic dysfunction, and frequent pathological reflexes, seriously disrupting the patient's daily life and psychological state [4–6].

Globally, although the incidence rate of SCI fluctuates due to differences in regions, statistical methods, and time periods, it is generally estimated that it is between 3.6 and 195.4 cases/million people, of which the proportion of male patients is significantly higher than that of female patients, accounting for about 78% of the total cases [7,8]. This gender difference has been verified in many research reports around the world. In China, SCI also poses a health challenge that cannot be ignored [8–10]. Its incidence rate is between 25 and 60 cases/million people, and the patient population is mainly middle-aged men, mostly aged between 40 and 60 years old [11,12].

Currently, the primary treatment options for SCI encompass drug therapy, surgical intervention, stem cell transplantation, as well as the utilization of electrospinning techniques [13–15]. The specific implementation methods and their respective advantages and disadvantages are shown in Table 1. According to the comparison in the table, although there are many treatment methods for SCI, neither medication nor surgery has been able to cure it completely. Electrospinning technology can customize nanofiber scaffolds [16,17], accurately simulate the spinal cord microenvironment [18,19], and promote nerve cell repair and regeneration. Moreover, its high porosity, adjustable pore size, and high surface volume ratio [20–22] facilitate cell migration, proliferation, and differentiation. And by selecting biocompatible materials [23,24], immune reactions and toxicity can be avoided, protecting the spinal cord. In addition, its fiber morphology resembles ECM [24–26], promoting the growth and regeneration of nerve cells and supporting SCI repair [27,28].

Table 1. SCI treatment methods and characteristics.

Treatment Method	Implementation Method	Advantage	Disadvantage
Medication	Corticosteroid hormone (MP) High-dose methylprednisolone was administered in early SCI (within 8 h after injury)	Significantly enhanced motor and sensory functionalities in SCI patients.	MP can affect the intrinsic repair capacity of the spinal cord.
	Injection of gangliosides (GM-1) [1]	GM-1 has not only therapeutic effects but also certain preventive effects on SCI.	The application of ganglioside can not effectively promote the restoration of spinal cord function.
	Erythropoietin (EPO) injection [2,3]	EPO also has a certain therapeutic effect on SCI. EPO also has potent effects against brain lipid peroxidation.	EPO lacks clinical trials to clarify its efficacy in humans.

Operative treatment	Through decompression, fixation, fusion and other means to restore spinal stability, reduce spinal cord compression	Surgical decompression and stabilization can relieve spinal cord compression, eliminate chronic stimulation of spinal cord, improve blood supply, and facilitate the recovery of spinal cord function [4].	Difficult to directly promote the regeneration and repair of nerve cells.
Stem cell transplantation	Subarachnoid injection of lumbar puncture, intravenous infusion, internal spinal injection under open surgical incision (*in situ* transplantation at the injured site), puncture cell transplantation at the upper and lower ends of the SCI site under CT guidance, *etc*. [5].	Stem cells can differentiate into neurons, replace the original damaged cells, and reconstruct the motor and sensory transmission pathways of SCI [29,30].	There is a lack of unified reference standards for stem cell therapy corresponding to SCI at different stages and injury sites; The survival and differentiation efficiency of stem cells still need to be further improved [7].
Electrostatic spinning	3D electrospinning controllable nanofiber catheter, hydrogel stent, composite nanostent, *etc*.	Electrospun fiber scaffolds have a similar structure to ECM and can provide a favorable environment for cell growth, which helps promote the growth and differentiation of cells in the damaged area [20,31].	It is difficult to accurately control the influence of various characteristic parameters of electrospinning

As illustrated in Figure 1, substantial efforts have been devoted to understanding the roles of electrospinning parameters and their applications in SCI repair [8–10]. Current studies primarily focus on the design of electrospun nanofibrous scaffolds—such as conduit-based systems, multifunctional scaffolds, and microenvironment-responsive immunomodulatory platforms—as well as their integration with complementary strategies including cell therapy, growth factor delivery, and other biomaterials [11,12]. These advances have significantly propelled scaffold-based approaches for SCI repair [32,33].

However, electrospun scaffolds should be regarded not as direct therapeutic agents, but as structural and functional platforms that regulate the cellular microenvironment and guide tissue regeneration. In this context, increasing attention has been paid to the relationship between scaffold design parameters and biological outcomes. Nevertheless, two major challenges remain: (i) the synergistic effects of electrospinning parameters (e.g., fiber diameter, alignment, and degradation kinetics) on SCI repair are not yet fully understood, and (ii) the integration of multiple functionalities—such as immunomodulation, controlled drug release, and mechanical support—within a single scaffold system remains difficult.

Concurrently, emerging biofabrication approaches are beginning to address intrinsic limitations of conventional electrospun scaffolds, particularly the restricted cell infiltration within densely packed fibrous networks. Among these, cell electrospinning (C-ES) represents a shift from post-seeding strategies toward *in situ* cell incorporation. Since its initial demonstration in 2006, C-ES has evolved from proof-of-concept studies to a developing platform capable of controllable cell encapsulation, fiber alignment, and multilayer scaffold construction [34]. Although its application in SCI remains at an early stage, its ability to integrate structural guidance with cellular delivery suggests significant potential for next-generation neural scaffolds.

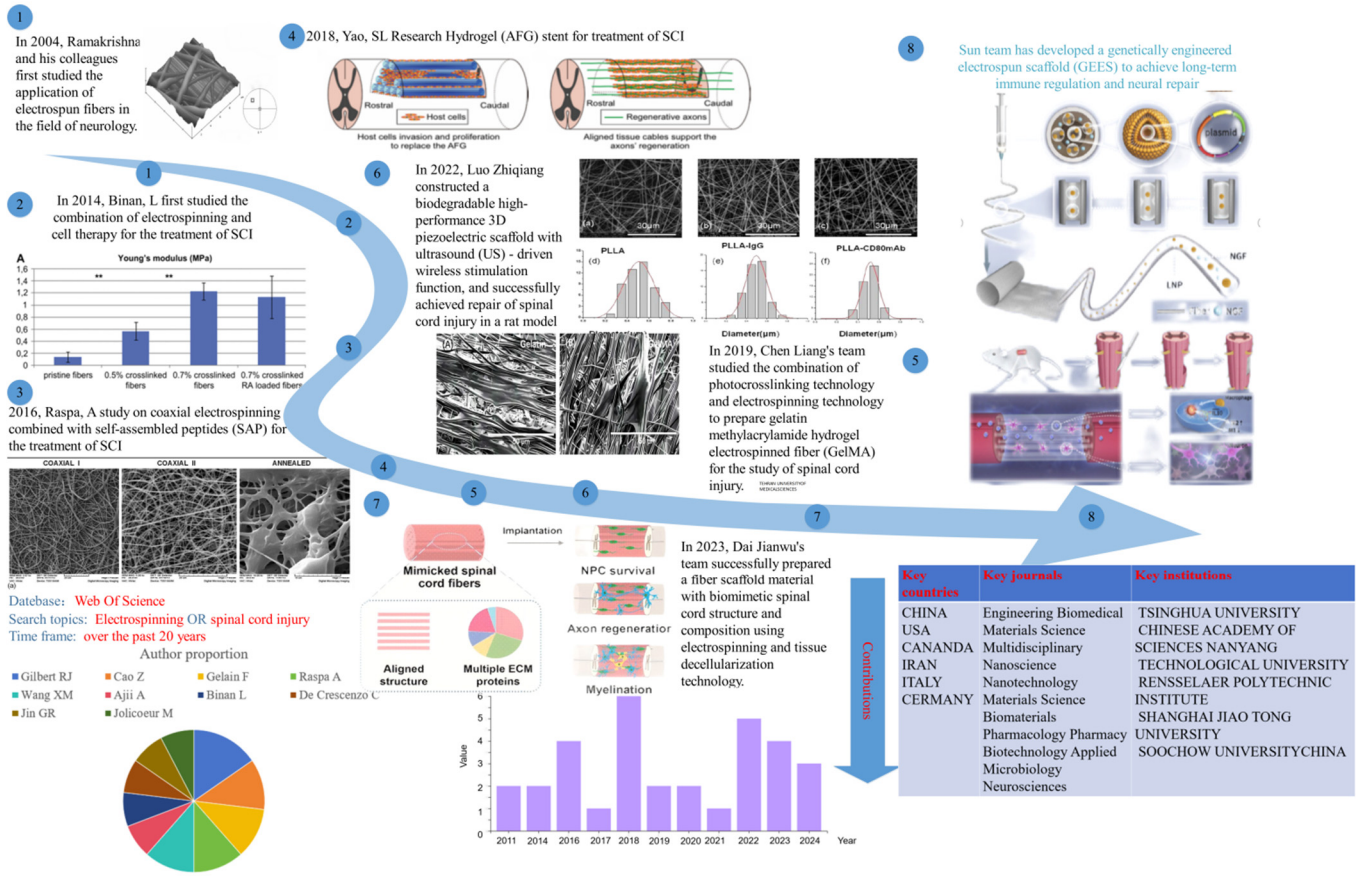

Figure 1. Overview of the development and applications of electrospinning in SCI repair. The evolution of electrospinning-based strategies for SCI is illustrated from early exploratory studies to recent advanced multifunctional systems. Initial work focused on the application of electrospun fibers in neural tissue engineering and their combination with cell therapy. Subsequent developments introduced coaxial electrospinning, biomimetic scaffold design, and integration with bioactive molecules and hydrogels. More recent advances include 3D-printed and stimuli-responsive electrospun scaffolds, as well as genetically engineered systems for immunomodulation and neural regeneration. In parallel, electrospun scaffolds have been designed to mimic spinal cord architecture, promote neural progenitor cell survival, support axonal regeneration, and enhance myelination. The figure also summarizes global research trends, highlighting key contributing countries, research fields, and institutions over the past two decades.

The research approach is illustrated in Figure 2. The initial focus is on analyzing the core mechanism of electrospinning for SCI treatment, followed by examining the dose-response relationship between material parameters and biological effects. Based on different parameters, five groups are identified: fiber diameter, arrangement method, biocompatibility and degradability, surface activity and biological activity, and nanostructure. Multi-parameter optimization has been analyzed. The key scientific challenge lies in applying electrospinning to SCI treatment and integrating it with other advanced technologies to achieve better outcomes. This study provides a detailed overview of how electrospinning parameters influence SCI, their application, and integration with other cutting-edge technologies, aiming to address current issues in electrospinning for SCI treatment.

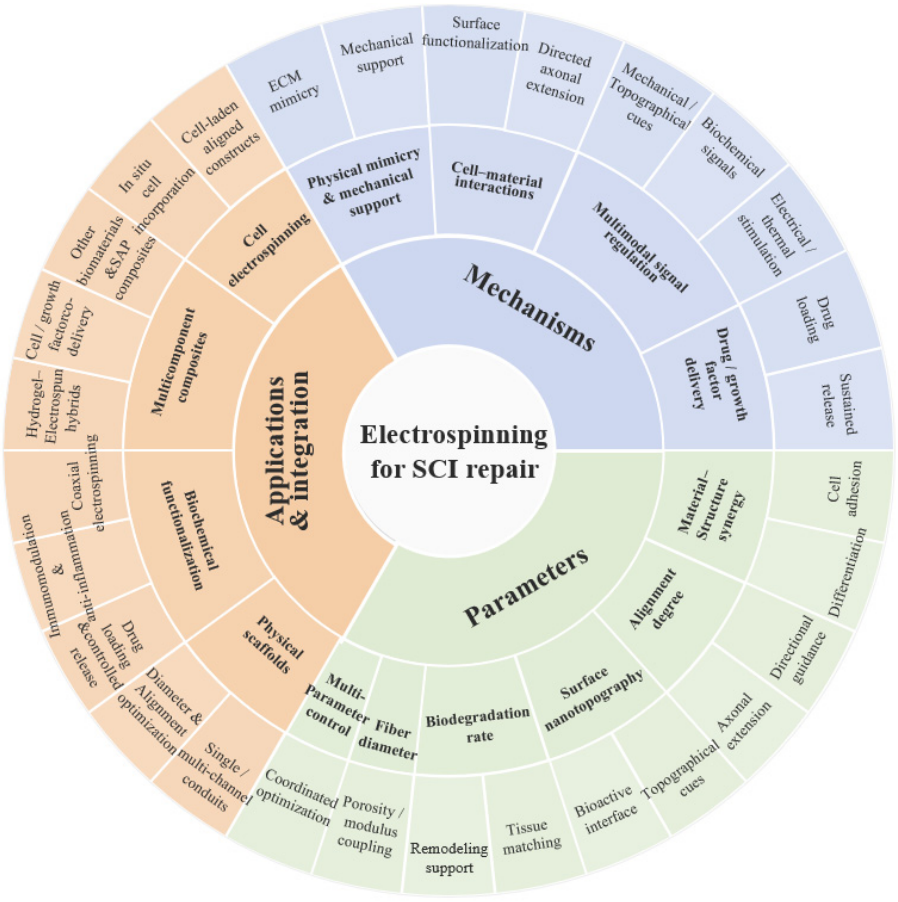

Figure 2. Onion Figure. Blue: Mechanism of Electrospinning Therapy for SCI; Green: The impact of electrospinning parameters on the treatment of SCI; Orange: Application of Electrospinning in SCI Treatment and Its Combination with Other Technologies.

According to Table 1, it can be learned that the influence of various characteristic parameters of electrospinning is difficult to accurately control at present; the existing literature lacks a systematic review and relatively few reference experience in clinical treatment, leading to the lack of targeted guidance in practical application. This paper reveals the core mechanism of electrospinning technology for SCI, systematically reviews the current application progress of the technology in SCI treatment, clarifies the influence of characteristic parameters on the repair effect, and summarizes the broad prospect of electrospinning technology combined with other advanced technologies. Finally, the challenges of SCI clinical treatment strategies based on electrospinning technology and the future directions are explored and discussed. It aims to provide technical guidance and theoretical support for the clinical application of electrospinning for SCI, and jointly promote the innovative development of electrospinning technology in the field of SCI therapy.

2. The Mechanism of Electrospinning for Spinal Cord Injury Treatment

Electrospun scaffolds promote SCI repair through a coordinated set of mechanisms rather than a single isolated effect. Their therapeutic value arises from the ability to mimic the extracellular matrix, provide directional guidance for axonal extension, regulate cellular responses through mechanical and biochemical cues, and deliver bioactive factors in a controlled manner. These mechanisms are interdependent: physical architecture establishes the initial structural niche, surface chemistry and topology modulate cell–material interactions, and drug-loading strategies further reshape the post-injury microenvironment. Therefore, the function of electrospun scaffolds in SCI should be understood as a hierarchical repair process that integrates structural support, biological signaling, and local microenvironmental regulation.

2.1. Physical Mimicry and Mechanical Support

A central advantage of electrospun scaffolds is their ability to approximate the fibrous architecture of the native ECM while providing temporary mechanical support across the lesion site. In SCI, tissue continuity is disrupted not only at the level of neuronal pathways but also at the level of the extracellular scaffold that normally organizes cells, molecules, and mechanical forces. Electrospun fibers can partially restore this lost architecture by creating a porous and anisotropic network that supports cell adhesion, migration, and tissue bridging. Compared with bulk materials, electrospun structures more closely resemble the nanoscale organization of the spinal cord microenvironment, thereby offering a more permissive substrate for regeneration [35,36].

Among the structural parameters that determine scaffold performance, fiber diameter and porosity are particularly important. Nanoscale fibers offer a large surface area-to-volume ratio and increase the density of cell-contact sites, which is favorable for adhesion and early neurite attachment. At the same time, pore size and inter-fiber spacing determine whether cells can infiltrate deeply into the scaffold and whether nutrients and metabolites can diffuse effectively. If the scaffold is too dense, the network may act as a barrier to cellular penetration; if it is too open, the scaffold may lose mechanical integrity and fail to provide stable guidance [37–40]. Therefore, scaffold design must balance structural mimicry with mass transport and mechanical robustness rather than maximizing any single parameter in isolation.

Mechanical support is another essential function of electrospun scaffolds. After SCI, the lesion cavity is exposed to mechanical instability, inflammatory infiltration, and secondary tissue collapse, all of which can further aggravate neural loss [41]. Electrospun conduits and three-dimensional fiber constructs can fill part of the defect space, reduce cavity collapse, and provide a temporary bridge for regenerating axons. In addition, the elastic modulus and overall compliance of the scaffold influence how host cells perceive the material. A scaffold that is too stiff may trigger a foreign-body-like response, whereas one that is too soft may collapse before tissue integration occurs. For this reason, mechanical matching with the spinal cord environment is a key design consideration in translational scaffold engineering [42,43]. As shown in Figure 3, electrospun scaffolds mimic the native extracellular matrix and provide mechanical support across the SCI lesion site, thereby creating a permissive microenvironment for tissue bridging and axonal regeneration.

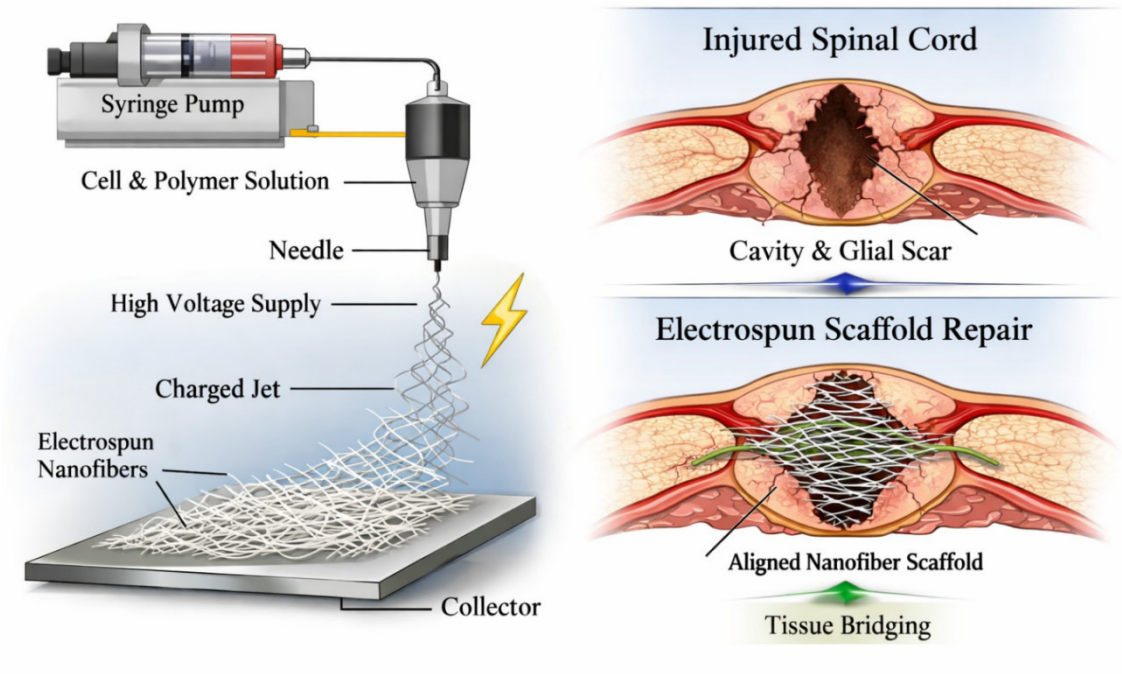

Figure 3. Physical Mimicry and Mechanical Support of Electrospun Scaffolds in SCI.

2.2. Cell–Material Interactions

Beyond structural support, electrospun fibers exert a profound influence on cell behavior through contact guidance and receptor-mediated signaling. In the injured spinal cord, neurons, glial cells, and stem/progenitor cells encounter a hostile microenvironment characterized by inflammation, inhibitory ECM components, and poor alignment of regenerative cues [44,45]. Electrospun fibers can partially counteract these barriers by presenting anisotropic topography that directs cell orientation and by providing an adhesive surface that supports cell attachment and spreading. In this sense, the scaffold does not merely occupy the lesion cavity; it actively instructs how cells organize and respond [46–48].

One of the most studied phenomena is fiber alignment. Aligned electrospun fibers can guide neurite extension along a preferred axis, thereby mimicking the longitudinal organization of nerve tissue [49]. This contact-guidance effect is especially relevant in SCI, where directed axonal growth is required to reconnect discontinuous neural pathways. In contrast, random fibers may support general cell attachment but usually provide weaker directional cues. The difference between aligned and random architectures highlights an important point: a scaffold's biological function is determined not only by its material composition, but also by the spatial organization of its micro- and nano-topology [50–52].

Surface chemistry further modulates cell behavior. Functional groups, peptide motifs, and ECM-derived ligands can be incorporated onto fiber surfaces to enhance the interaction between cells and the scaffold. Such modifications may improve adhesion, promote cytoskeletal reorganization, and activate signaling pathways related to survival, migration, and differentiation. For example, biomimetic ligands can enhance integrin engagement and trigger downstream responses that support neurite outgrowth and progenitor cell fate commitment. In SCI repair, these effects are particularly valuable because the lesion environment is typically unfavorable for spontaneous cell attachment and extension [53,54].

As shown in Figure 4, the biological responses of cells to electrospun scaffolds are governed by fiber alignment, surface functionalization, and receptor-mediated signaling, which collectively regulate adhesion, polarity, and neurite extension.

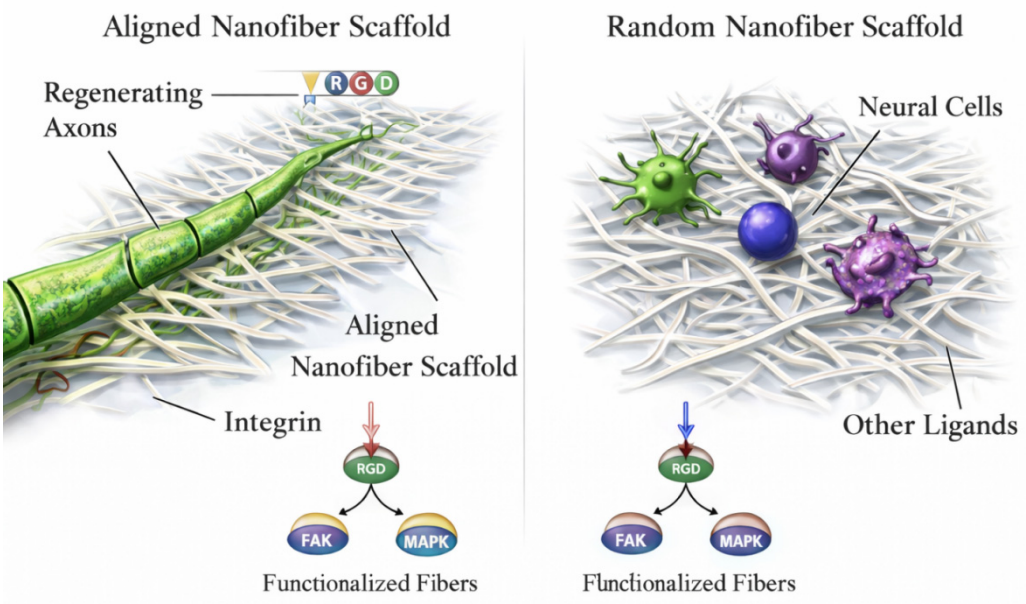

Figure 4. Cell-Material Interactions with Electrospun Scaffolds in SCI.

Importantly, cell–material interactions should be interpreted in a context-dependent manner. A design strategy that works well for one cell type or one injury phase may not be optimal for another. For instance, a scaffold that promotes early adhesion may not necessarily support long-term maturation or remyelination.

Similarly, the needs of transplanted stem cells may differ from those of resident glial cells or regenerating neurons. Therefore, a critical review of electrospun scaffolds must move beyond simply listing "good effects" and instead discuss how topography, chemistry, and cell type jointly determine biological outcomes.

2.3. Multimodal Signal Regulation

Electrospun scaffolds are particularly attractive because they can integrate multiple regulatory cues within a single platform. In SCI, tissue repair is governed by a complex interplay of mechanical injury, inflammatory cascades, glial scarring, and impaired axonal regeneration. A successful scaffold must therefore do more than provide passive support; it must also participate in shaping the biochemical and biophysical environment of the damaged tissue. Electrospun systems can achieve this by combining mechanical guidance, biochemical functionalization, and, in some cases, electrically or thermally responsive behavior [55–57].

Mechanical and topographical cues are the most immediate signals delivered by electrospun scaffolds. Fiber diameter, surface roughness, and alignment all influence how cells spread, migrate, and polarize. These cues can regulate the morphology of astrocytes, the directional growth of axons, and the behavior of stem cells within the damaged tissue. The significance of these effects lies in the fact that SCI repair depends not only on cell survival, but also on the restoration of organized tissue architecture. By offering a defined physical template, electrospun scaffolds help convert a disordered lesion into a more structured regenerative niche [17,58,59].

Biochemical cues can be introduced by loading growth factors, cytokines, small molecules, or immunomodulatory agents into the fibers. Such functionalization allows the scaffold to interact with inflammatory and regenerative processes in a stage-dependent manner. During the acute phase of SCI, anti-inflammatory signals may help limit secondary damage and reduce glial scar formation. During later phases, neurotrophic or pro-regenerative cues can promote neuronal survival, neurite extension, and remyelination. This temporal dimension is important: the ideal scaffold is not static but rather adapts its influence to the changing biological needs of the lesion [60].

As shown in Figure 5, electrospun scaffolds can integrate mechanical, biochemical, and electrical/thermal cues to modulate the post-injury microenvironment and enhance SCI repair.

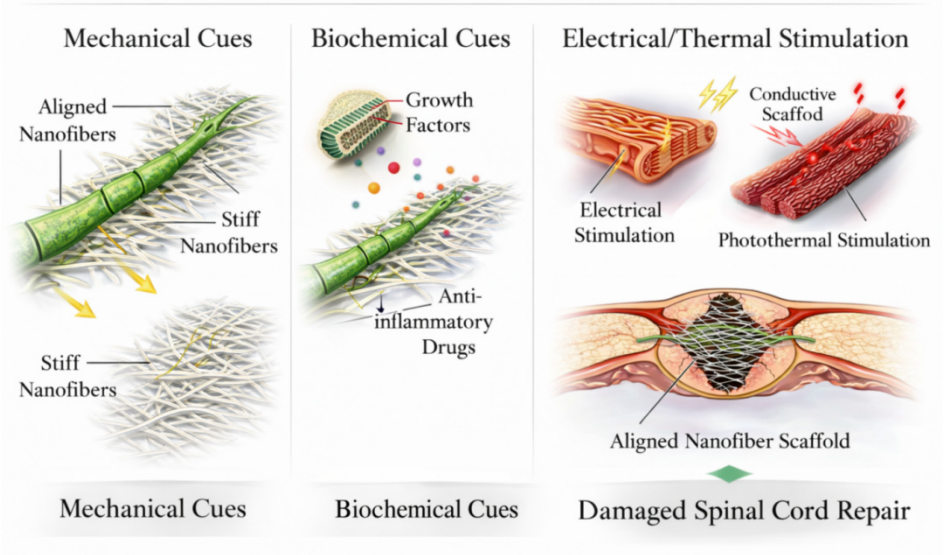

Figure 5. Multimodal Signal Regulation by Electrospun Scaffolds in SCI.

In some studies, electrospun scaffolds are further combined with electrical, photothermal, or piezoelectric components to create more sophisticated multimodal systems. These designs aim to provide

additional levels of control over cell behavior and material performance. However, such complexity should not be introduced for its own sake. In a review focused on SCI, it is more useful to emphasize how multimodal regulation helps reproduce the dynamic, heterogeneous, and evolving nature of the post-injury microenvironment. The value of electrospinning in this context is its ability to integrate several cues into one material platform without losing the basic structural function of a scaffold.

2.4. Drug and Growth-Factor Loading & Sustained Release

Architectural design and material composites enable multi-phase, stimuli-responsive release of bioactive molecules, precisely matching the evolving therapeutic demands of SCI repair . Electrospun scaffolds also function as local delivery systems for drugs and growth factors. This capability transforms them from passive conduits into active therapeutic platforms that modulate inflammation, support cell survival, and promote regeneration over extended time periods. In SCI, where pathological processes unfold in stages, controlled release is especially important because the biological needs of the tissue change over time. An agent that is useful in the acute phase may not be sufficient in the chronic phase, and vice versa .

Various electrospinning strategies have been developed to regulate release behavior. Core–shell fibers are particularly effective for protecting sensitive cargo and extending release duration. Nanoparticle incorporation, multilayer structures, and stimulus-responsive systems can further tailor the temporal profile of delivery. These approaches allow electrospun scaffolds to deliver anti-inflammatory compounds early after injury, followed by neurotrophic factors or other pro-regenerative molecules during later stages. Such sequential delivery is conceptually well suited to SCI because it mirrors the transition from inflammation control to tissue reconstruction [61].

Controlled release also has an important structural implication. A scaffold that merely loads a therapeutic agent without preserving fiber architecture may fail to provide the intended physical guidance. Conversely, a structurally robust scaffold without therapeutic cargo may not sufficiently modulate the hostile injury environment. The strength of electrospun systems lies in their ability to combine these two functions. This dual role is especially relevant in SCI, where regeneration depends on both creating a permissive microenvironment and physically directing new tissue growth [62,63]. As shown in Figure 6, electrospun scaffolds can serve as controlled delivery platforms for drugs and growth factors, enabling staged release in accordance with the evolving phases of SCI pathology.

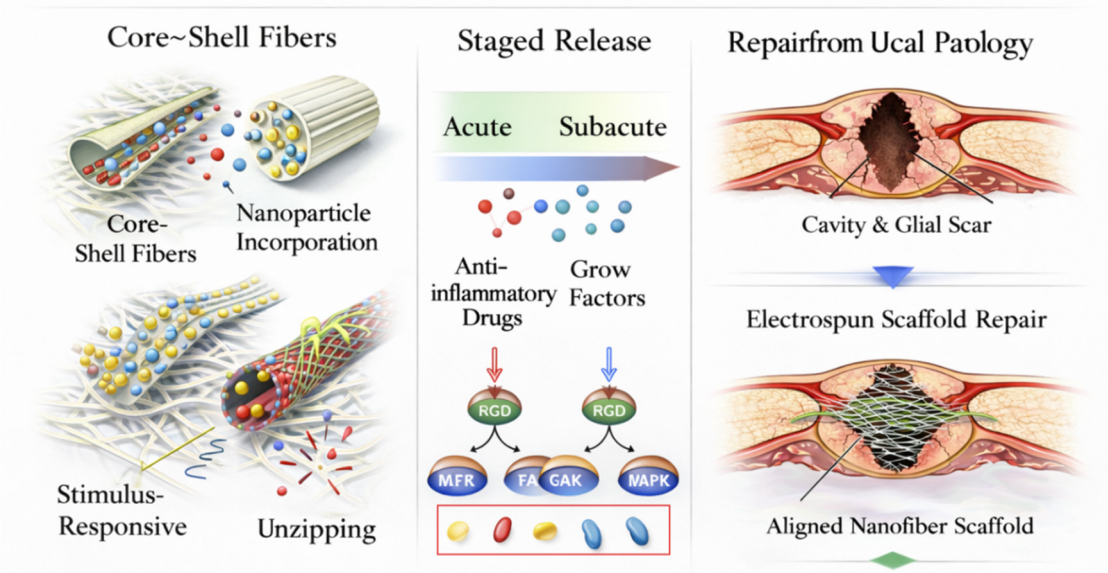

Figure 6. Drug and Growth Factor Loading & Sustained Release from Electrospun Scaffolds in SCI. (The red boxes represent different types of bioactive payloads, used to illustrate the ability of electrospun scaffolds to achieve staged delivery of anti-inflammatory and pro regenerative factors in spinal cord injury repair).

Nevertheless, the design of drug-loaded electrospun scaffolds should be evaluated critically. Not every release profile is clinically meaningful, and not every drug benefits from encapsulation in a fibrous matrix. Factors such as burst release, degradation kinetics, bioactivity retention, and manufacturing reproducibility must be considered. For this reason, an effective review should not simply enumerate loaded molecules, but should explain how the release strategy relates to the injury stage, the target cell population, and the intended biological effect.

2.5. Conclusions

Taken together, electrospun scaffolds support SCI repair through a layered mechanism that combines ECM mimicry, directional cell guidance, multimodal regulation, and controlled therapeutic release. The earliest and most fundamental contribution of these scaffolds is structural: they provide a fibrous framework that can bridge the lesion and guide cell organization. On this basis, surface chemistry, topography, and cargo delivery further amplify biological responses by influencing cell adhesion, migration, survival, and differentiation. The resulting repair effect is therefore not the product of any single material property, but of the coordinated interaction between scaffold architecture and the evolving post-injury microenvironment.

This mechanistic understanding also explains why electrospun scaffold design remains challenging. A scaffold optimized for one function may compromise another, and the best-performing system *in vitro* may not necessarily translate into durable *in vivo* repair. For this reason, future research should focus on integrated design strategies that balance structure, mechanics, bioactivity, and degradation behavior. Such a perspective is essential for developing electrospun platforms that are not only scientifically interesting but also genuinely relevant to clinical SCI repair.

3. Mechanism of Influence of Electrospinning Parameters on Spinal Cord Injury Repair

The core advantage of electrospinning lies in its capacity to precisely reconstruct the spinal cord's native microenvironment by tuning fiber-level structural parameters. These intrinsic scaffold properties—fiber diameter, alignment, biocompatibility, and degradation rate, and surface nanotopography—act in concert across multiple dimensions of mechanical support, cell-adhesion guidance, and multimodal signal regulation to direct tissue repair. In particular, structural parameters (diameter and alignment) define the scaffold's physical topology and thus establish the foundation for cell–material interactions, while chemical functionalization (bioactive-molecule loading and surface-group modification) endows the scaffold with dynamic control over the local microenvironment. By delineating a systematic "design window" that spans single-parameter optimization to multiparameter synergy, this chapter provides clear, quantitative guidelines for the engineering of electrospun scaffolds.

3.1. Structural Parameters: Fiber Diameter

Among the various electrospinning parameters, fiber diameter represents a fundamental structural dimension that directly influences cell–material interactions by modulating surface area, mechanical cues, and topographical scale [64,65].

Small diameter fibers (200–500 nm) promote the differentiation of neural stem cells (NSC): Christopherson et al. [66] demonstrated that 200–500 nm electrospun fibers significantly enhanced neural stem cell (NSC) adhesion and neuronal differentiation by increasing specific surface area, as evidenced by SEM imaging of rNSCs exhibiting superior attachment and axial alignment on 283 nm fibers compared to flat cells, As shown in Figure 7. This study quantitatively validated the "200–500 nm" diameter range as a critical determinant for early NSC differentiation. However, limitations included: Polymer specificity confined to PES systems, with unverified universality in alternative materials (e.g., PLCL, PCL); Exclusive focus on *in vitro* short-term assays, lacking long-term *in vivo* validation in chronic injury models or clinical samples; and omission of systematic

analysis on the impact of fiber diameter distribution heterogeneity (e.g., standard deviation) on cellular responses. While advancing mechanistic understanding, these constraints restrict translational applicability.

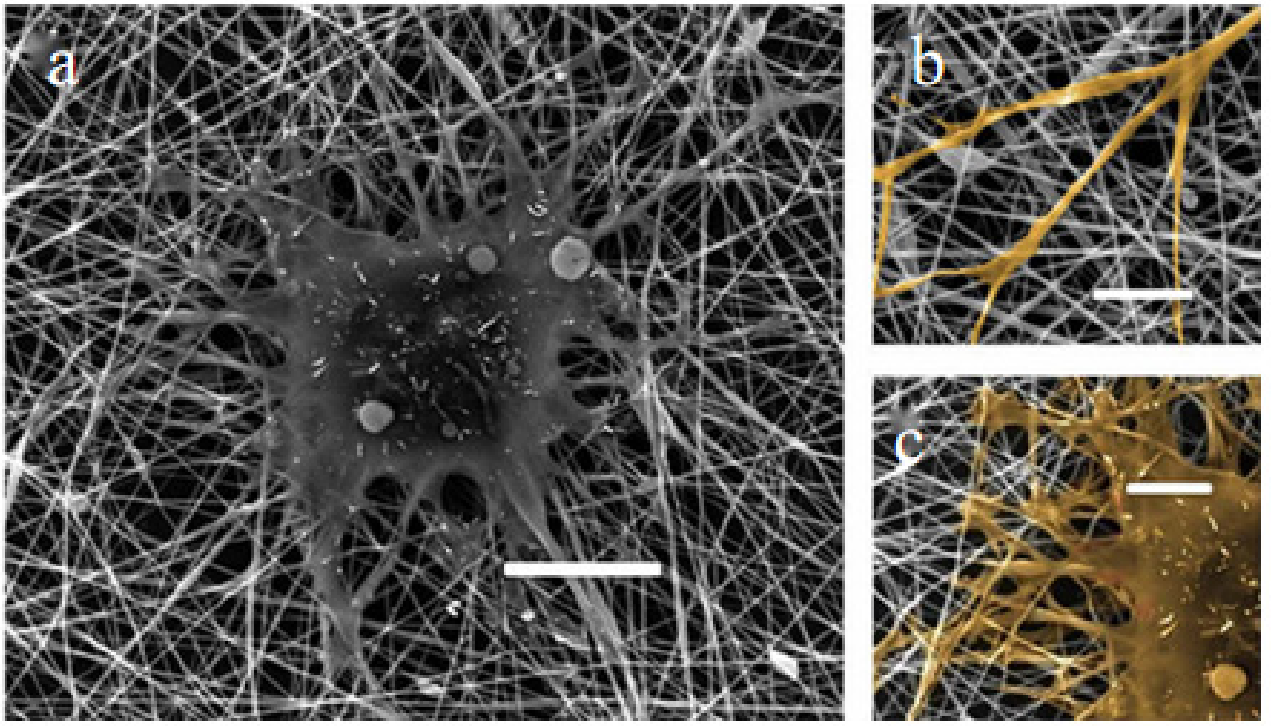

Figure 7. (**a**–**c**) Cells on 283-nm fiber mesh (cells are highlighted in yellow in (**b**,**c**)); Scale bars for (**a**) are 10 mm, for (**b**,**c**) are 5 mm.

Medium diameter fibers (800–1200 nm) support astrocyte (AC) function: Zhang et al. [67] found that fibers with diameters of 800–1200 nm were more conducive to the elongation of astrocytes (AC), which helped to form supportive glial networks. As shown in Figure 8A–D, GFAP, positive cells (green) are significantly stretched along the fiber direction on the SF:PLCL nanofiber scaffold with a diameter of approximately 900 nm, forming a mesh-like structure. In contrast, similar cells in the control group (glass substrate) exhibit a classic star-like pattern without directional extension. This figure intuitively demonstrates that nanofibers in the range of 800–1200 nm facilitate the elongation of AC along the fiber direction, thereby constructing a supportive glial network. By precisely regulating the electrospinning parameters, a quantitative relationship between fiber diameter and biological function was established, which provided an important paradigm for the design of neural tissue engineering scaffolds. This work clarifies the biological effects of medium diameter fibers in “glial scaffolds”, but additional *in vivo* experiments are needed to verify their practical significance for functional recovery.

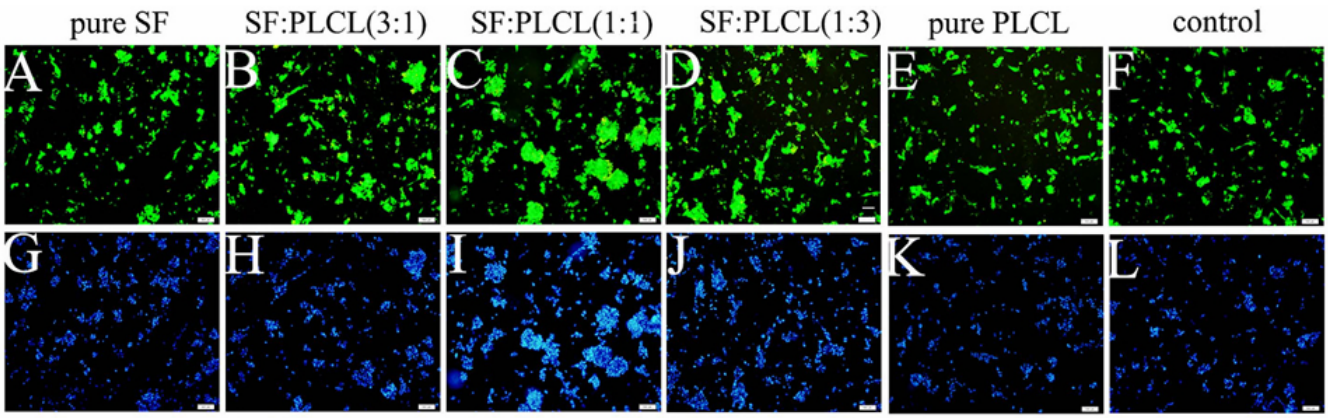

Figure 8. Morphology of RPCs seeded on electrospun SF/PLCL nanofibrous scaffolds. (**A**–**L**): Fluorescent micrographs of GFP grown on pure SF, SF:PLCL (3:1), SF:PLCL (1:1), SF:PLCL (1:3) and pure PLCL nanofibrous scaffolds under proliferation conditions for 3 days, and the cell nuclei were counterstained with DAPI. The RPCs cultured on SF:PLCL (1:1) showed the highest cell density. Scale bars: 100 μm.

Liu et al. [68] prepared collagen nanofibers with an average diameter of 208.2 ± 90.4 nm using electrospinning technology and found that fibers of this size can effectively inhibit the over-activation of astrocytes. *In vitro* experiments showed that oriented collagen fibers significantly promoted the directed growth of dorsal root ganglion (DRG) axons compared to randomly arranged fibers. Additionally, after *in vivo* implantation, the scaffold's helical structure remained intact for 30 days, supporting continuous nerve fiber regeneration. As shown in Figure 9, the average diameter of the electrospun collagen nanofibers is 208.2 ± 90.4 nm (Figure 9a,b), and their ordered arrangement (aligned fibers) promotes DRG axon growth along the fiber axis through contact guidance mechanisms (Figure 9c). This diameter range has been proven to inhibit astrocyte activation (reduced GFAP expression by 72%) while supporting neuronal adhesion and differentiation. This case is a breakthrough in natural biomaterials, but it still needs to be combined with more complex models to examine long-term degradation and immune compatibility.

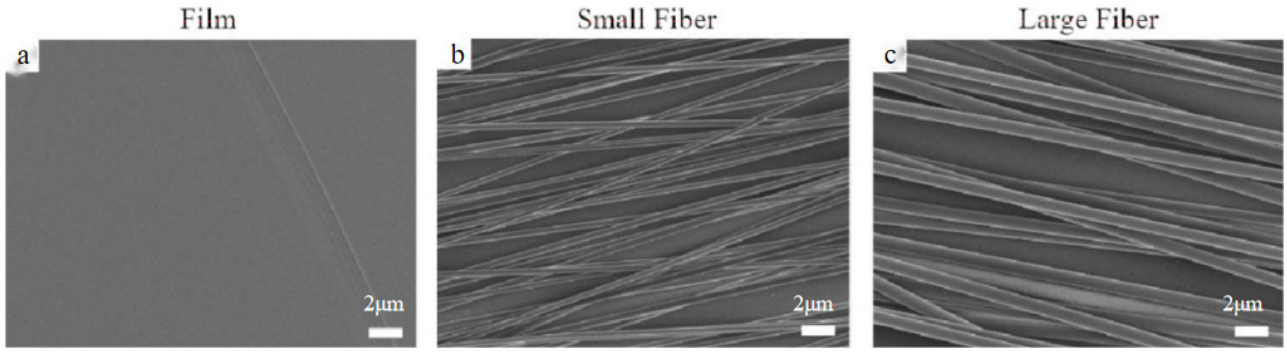

Figure 9. Analysis of electrospun fibers with low PLLA content (7%) and high PLLA content (12%). SEM of (**a**) a film, (**b**) fibers with small diameters, and (**c**) fibers with large diameters.

Johnson et al. [69] research shows that 808 nm large-diameter fibers enhance the morphological polarity and GLT-1 expression of astrocytes, while optimizing axon guidance efficiency and neuroprotective capabilities, providing crucial parameter references for the design of spinal cord injury repair scaffolds. Figure 10 displays scanning electron microscope images of two electrospun fibers, showing diameters of 386 nm and 808 nm, respectively. The consistency in fiber surface roughness and pore structure indicates that the diameter difference is the only variable. The conclusion that 808 nm large diameter promotes glial cell polarity and neuroprotection is innovative, but there are deficiencies in *in vivo* verification and parameter optimization.

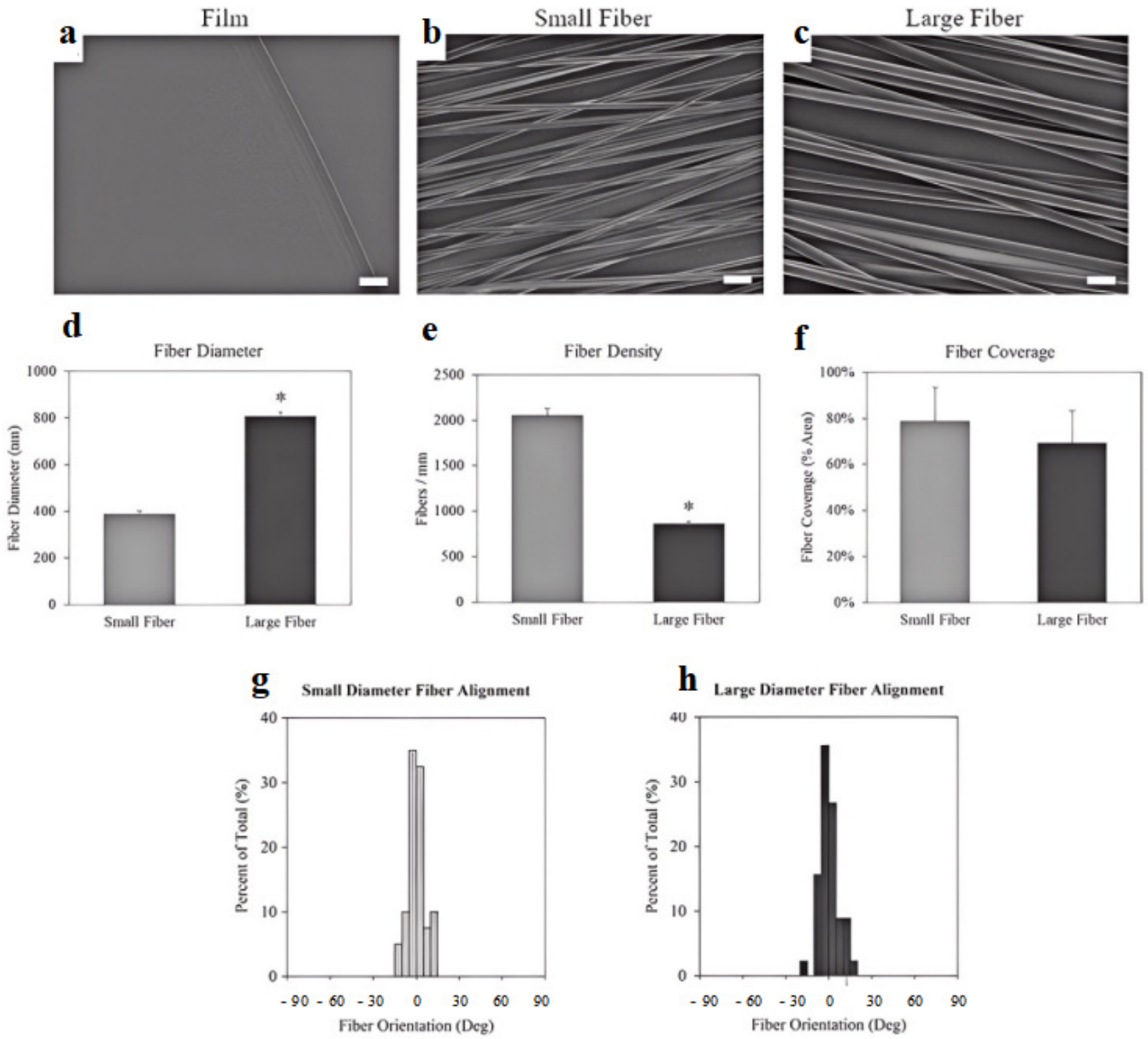

Figure 10. Characterization of small (7% PLLA) and large (12% PLLA) electrospun fibers. Scanning electron micrographs of (**a**) film, (**b**) small diameter fibers, and (**c**) large diameter fiber surfaces. Scale bar = 2 µm. (**d**) The scaffold's mean fiber diameter. (**e**) Fiber density or the fibers per mm on each scaffold. (**f**) The fiber surface coverage. The alignment of the (**g**) small fibers and (**h**) large fibers. The * indicates statistical significance ($p < 0.05$). Statistical differences in fiber alignment were not observed.

Chen et al.[70] found that Gelatin methacryloyl (GelMA) fiber scaffolds with a diameter of 1.1 ± 0.13 µm have better orientation and mechanical properties than Gelatin scaffolds with a diameter of 1.4 ± 0.13 µm, As shown in Figure 11. This study provides important data for the diameter optimization of GelMA-based electrospun scaffolds, but further breakthroughs are needed in material diversity, mechanism depth, and transformation validation to promote its clinical application potential in spinal cord injury repair.

A comparative summary is provided in Table 2, which links diameter ranges to cellular behavior and clinical relevance. While fiber diameter governs the cellular interface at the microscale, it is the spatial organization—or alignment—of these fibers that determines the directionality of axonal regrowth, which is critical for functional neural circuit reconstruction [71–73]. This leads to the next key parameter: fiber orientation.

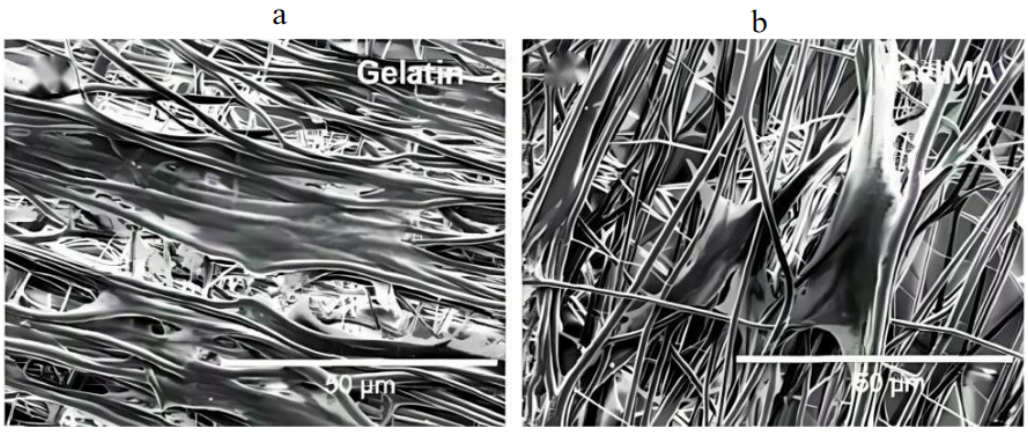

Figure 11. (**a**) Cells after implantation of Gelatin. (**b**) GelMA fiber scaffold.

Table 2. Effects of fiber diameter gradient on neuronal behavior.

Parameter Range	Mechanism of Action	Biological Effect	Clinical Relevance
200–500 nm	High specific surface area → integrin clustering → FAK/ERK activation	NSC adhesion↑, Less glial differentiation↑	Early axon regeneration guidance
800–1200 nm	Mechanical support enhancement to star-shaped glial polarization	GFAP arrange↑, Meaullation↑	Late functional reconstruction

"↑" indicates an increase or upregulation of the indicated biological effect.

3.2. Arrangement Parameters: Orientation Degree

Following the determination of fiber diameter, the next critical parameter is fiber alignment, as it directly regulates axon guidance, directional mechanical properties, and scaffold anisotropy [74].

Orientation fibers promote axonal orientation and extension: Hurtado et al. [39] placed randomly arranged and directionally arranged electrospun left-handed PLLA nanofibers in a rat spinal cord transection model, and found that after 4 weeks of implantation, the directionally arranged group (2055 μm ± 150 μm) had a longer protrusion extension distance compared to the randomly arranged group (1162 μm ± 87 μm), and the difference was statistically significant. As shown in Figure 12, the immunofluorescence imaging of aligned and random fiber groups visually compared the growth of NF H labeled axons on the two scaffolds. "It has been widely accepted that high orientation significantly improves axon regeneration and functional recovery", but further optimization is needed in large size preparation and multi-directional mechanical matching.

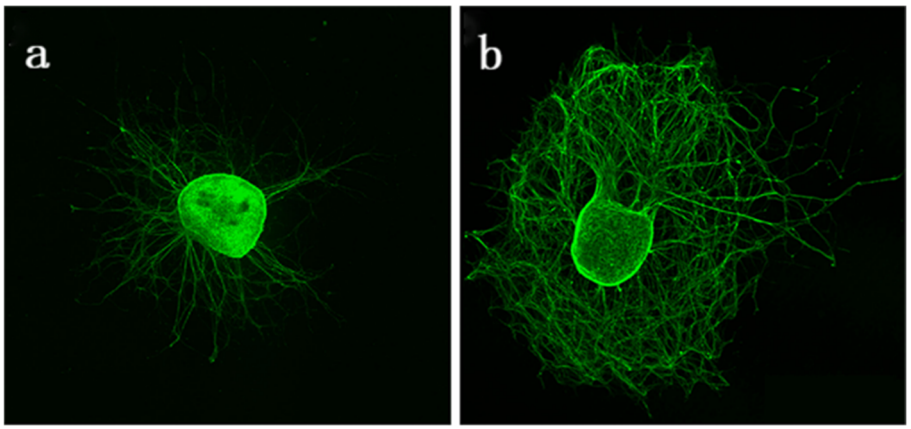

Figure 12. (**a**) (Random) The axon is marked (green) and grows in a disordered manner; (**b**) (Aligned) the axon extends significantly along the fiber direction and forms a bundle structure.

Random fiber induced multi-directional differentiation: Xia et al. [75] found that in polymethyl methacrylate (PMMA) electrospun nanofibers, astrocytes cultured in the oriented arrangement group formed longer, highly oriented protrusions along the matrix fiber axis compared to the randomly arranged group, As shown in Figure 13. This study provides important experimental evidence for the regulation of astrocyte behavior by oriented nanofiber scaffolds, but it needs to be deepened in the aspects of material degradability, multi-cell interaction and transformation verification, so as to break through the gap between the current "cell-scaffold" binary model and the complex SCI microenvironment.

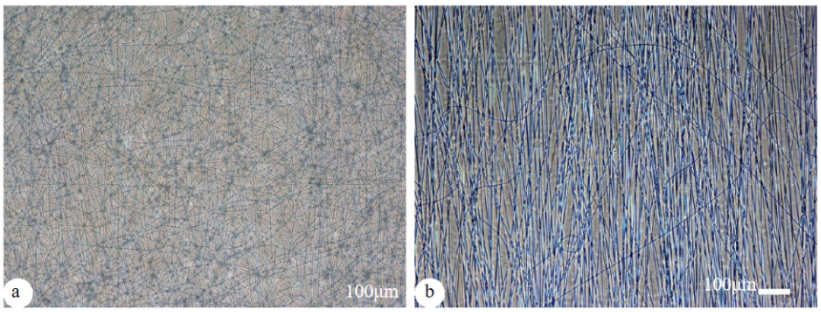

Figure 13. Microscopic images of electrospun PMMA nanofibers: (**a**) Random and (**b**) Aligned.

Subramanian et al. [76] developed a collector-based method to fabricate oriented PLGA-PCL nanofibers (230 ± 63 nm) and quantified alignment via fiber angle distribution. Compared to random fibers, oriented scaffolds exhibited significantly reduced pore size, Young's modulus, and degradation rate ($p < 0.05$). *In vitro* evaluation demonstrated that axial alignment enhanced Schwann cell adhesion and proliferation ($p < 0.05$), As shown in Figure 14. Although there are shortcomings in *in vivo* validation and mechanism elucidation, the systematic material design and cell behavior research have laid a solid foundation for subsequent translational applications.

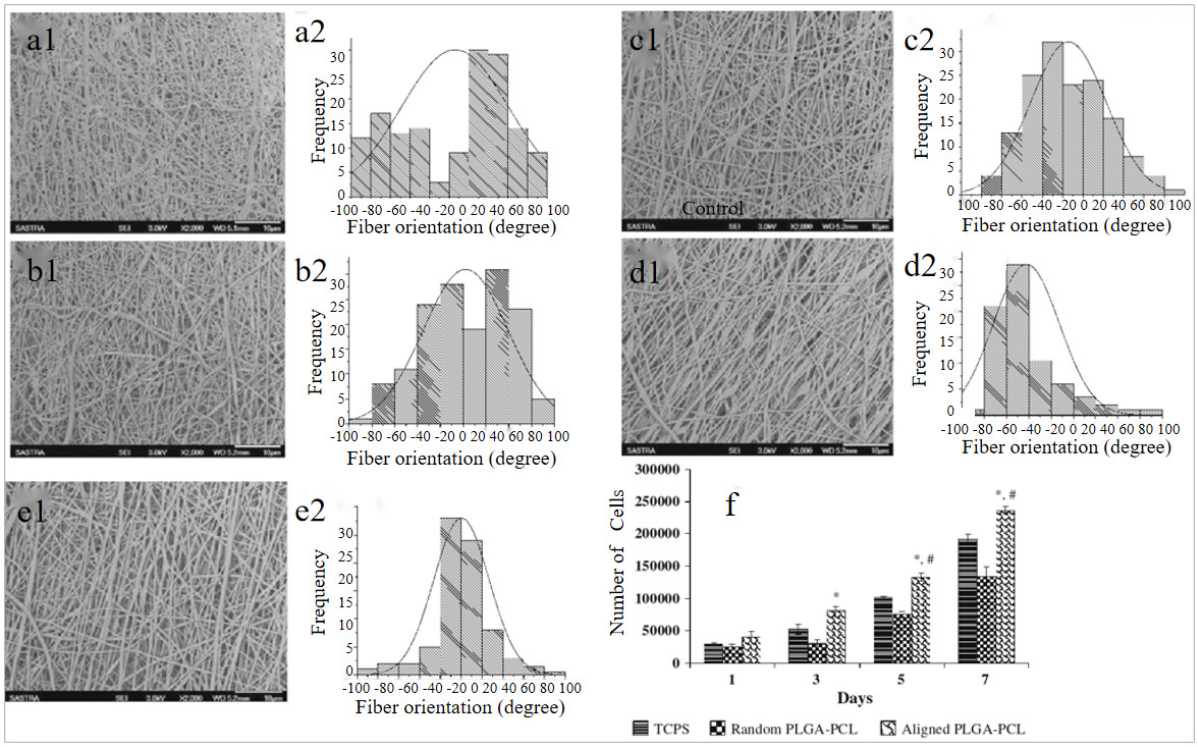

Figure 14. PLGA-PCL nanofibers at different rotational speeds (**a1**,**a2**) of 1000 rpm; (**b1**,**b2**) 1500 rpm; (**c1**,**c2**) 2000 rpm; (**d1**,**d2**) 2500 rpm; (**e1**,**e2**) 3000 rpm; (**f**) Cell proliferation on the surface of random and aligned PLGA–PCL nanofibers. (*, # indicates the statistical sig- nificance between orientation and samples with respect to TCPS, control, respectively at $p < 0.05$).

Key distinctions between aligned and random fiber effects are summarized in Table 3. Although alignment provides structural guidance, its effectiveness is greatly enhanced when combined with appropriate biochemical signals. Therefore, the next section explores how surface chemistry and nanotopography can further modulate cellular responses through ligand presentation and topographical cues.

Table 3. The differential effect of fiber arrangement direction on axon guidance.

Degree of Orientation	Mechanism of Mechanical Signal Transmission	Cell Behavior Response	Function Output
Bias in statistics <10	Contact guidance leads to the arrangement of stress fibers in the cytoskeleton	Axons extend in a directed manner up to 2 times	Neural bridge efficiency improved
Random permutation	Homogeneous stress distribution	Nerve fiber diffusion increased, myelin thinning	Function integration is difficult

3.3. Surface Parameters: Nano-Topological Structure

Beyond physical parameters, the biochemical landscape of electrospun fibers—such as surface ligand functionalization and nanoscale texture—plays a pivotal role in directing cell fate, particularly via integrin signaling and cytoskeletal reorganization.

Nanotube structure regulates cell behavior: Sánchez et al. [77] added curcumin dissolved in dimethyl sulfoxide (DMSO) to the electrospinning solution and functionalized the PLA electrospun membrane during the electrospinning process, altering the surface morphology of the nanofibers, guiding and supporting axonal elongation in neuronal culture, and providing neuroprotection and enhanced neuroplasticity when implanted into a half cut spinal cord *in vivo*. In Figure 15, functionalized PLA-curcumin nanofibers showed enhanced neuroplasticity. This study is the first to integrate "nano-topology + drug", but it needs to be strengthened in terms of drug release timing and long-term stability.

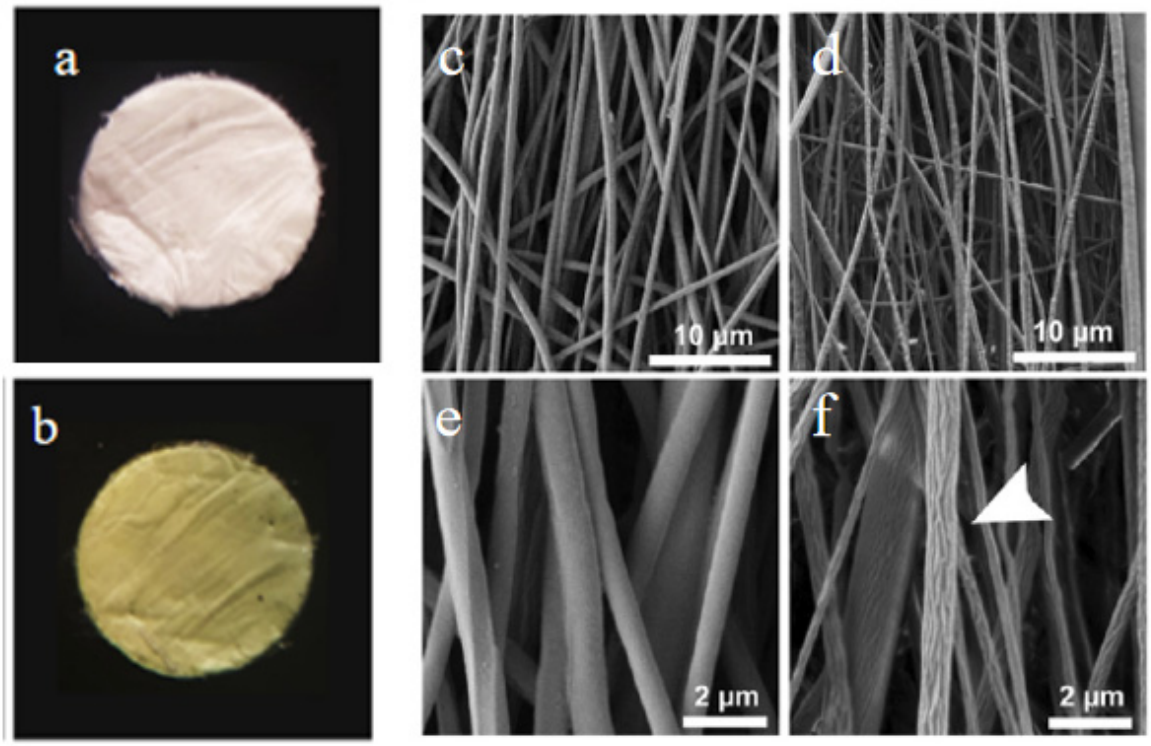

Figure 15. Characterization of electrospun PLA and polylactate-curcumin membranes. Macroscopic images of PLA (**a**) and PLA-curcumin (**b**) ring membranes with 8 mm diameter, FESEM images of PLA (**c**,**e**) and PLA-curcumin (**d**,**f**) membranes at low and high magnification.

Micropores promote angiogenesis: Liao et al. [78] found that Tubastatin A (TUBA) is a stable and efficient selective histone deacetylase 6 (HDAC6) inhibitor, with much higher selectivity than any other isoenzymes, which can accelerate cell autophagy and apoptosis. Loading TUBA into multi-channel bioactive silk nanofiber conduits can pharmacologically inhibit HDAC6, enhance axonal regeneration, and restore functionality in mice that have undergone injury. Reducing inflammation stabilizes the damaged microenvironment, promoting neuronal regeneration and functional recovery. The role of multi-channel stents loaded with bioactive agents is illustrated in Figure 16. Its core value lies in the close combination of basic research and clinical needs to confirm that local sustained release TUBA can reshape the damaged microenvironment and promote functional recovery.

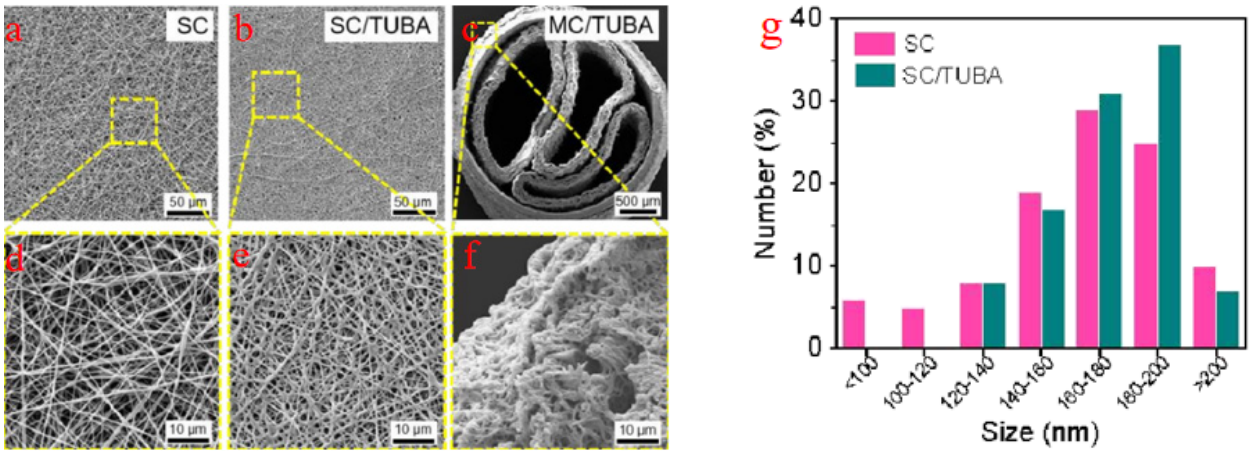

Figure 16. Catheter stent characterization. (**a**) The diameter spacing between single channel (SC) and (**b**) SC/TUBA nanofibers is approximately 140–200 nm. (**b**) Catheter stent, SC/TUBA: single channel bioactive nanofiber catheter stent equipped with TUBA, (**c**) MC/TUBA: multi-channel bioactive nanofiber catheter stent equipped with TUBA. (**d**) Local enlarged image of SC; (**e**) SC/TUBA partial enlarged view; (**f**) MC/TUBA partial enlarged view; (**g**) SC and SC/TUBA diameter gap.

Johnson et al. [44] Several pure physical morphologies have been compared, but the results are consistent with Maria et al. at the pure surface topology level. Topographical regulation mechanisms are summarized in Table 4, detailing cell responses to nanoscale surface features.

Table 4. The regulation of cell behavior by surface nano-topological structure.

Surface Topography	Cell Sensing Mechanism	Molecular Response	The End of the Story
Nanotraps	F-actin depolymerization → inhibition of RhoA/ROCK pathway	Nerve branch ↑, myelin thickness ↑	Motor function recovered
Micron holes	Macrophage pseudopod anchoring to M2 polarization	Anti-inflammatory factor (IL-10) ↑	Gliosis scar reduction

"↑" indicates an increase or upregulation of the indicated biological effect.

However, for long-term therapeutic efficacy, scaffolds must also undergo controlled biodegradation and sustained bioactive release. The following section thus addresses how material biocompatibility and degradation dynamics modulate the inflammatory microenvironment and scaffold longevity.

3.4. Biodegradation Parameters: Degradation Rate

The *in vivo* performance of electrospun scaffolds depends not only on their initial structure and function but also on their degradation profile, which affects immune responses, drug delivery, and tissue integration over time.

Degradation rate regulates inflammatory response: Wu et al. [79] fabricated aligned electrospun poly(vinylidene fluoride-trifluoroethylene) (PVDF-TrFE) scaffolds and demonstrated that their intrinsic piezoelectric properties enable the conversion of mechanical stimulation into electrical signals. This electroactive behavior significantly promoted Schwann cell alignment, neurite extension, and myelination in vitro, As shown in Figure 17. These findings indicate that PVDF-TrFE scaffolds can regulate neural cell behavior through an electro-mechanical coupling mechanism, providing an alternative strategy to enhance neural regeneration that is fundamentally different from degradation-mediated bioactivity in conventional biodegradable scaffolds.

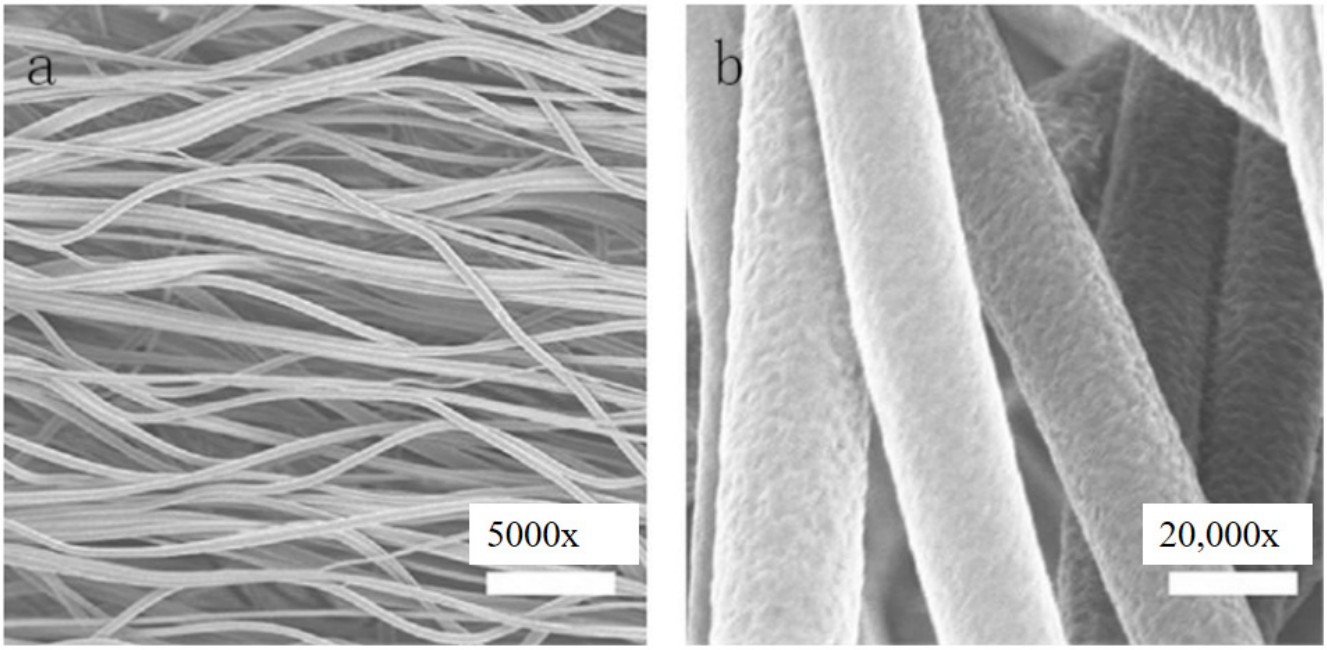

Figure 17. SEM characterization of the oriented fiber structure of PVDF-TrFE stent. (**a**) 5000×; (**b**) 20,000× magnification.

Extended factor activity of the sustained release system: Sun et al. [80] studies have shown that the electroactive scaffold based on hydroxyapatite/carbon nanofibers (HAp/CNF) achieves controlled degradation through the following mechanisms: the carbonization of PVDF releases HF, which causes slight expansion of the fibers (Figure 18g), increasing the specific surface area and accelerating medium permeation; during physiological activities (such as spinal movement), the piezoelectric effect generates microcurrents in the scaffold, promoting local ROS production and accelerating material decomposition; HAp doping provides a continuous release function for Ca^{2+}, with its lattice defects (Figure 18i) enhancing the charge distribution on the material surface, promoting osteoblast adhesion and differentiation. Scanning electron microscopy reveals that the scaffold has three-dimensional interconnected pores (with pore sizes of about 500 nm) and a high aspect ratio structure (Figure 18a–e), and the HAp/CNF composite design significantly upregulates the expression of osteogenic markers such as Runx2 and OCN. This scaffold holds potential for multi-trauma repair but requires further validation through the synergistic effects of multiple mechanisms and targeted verification for pure spinal cord injury.

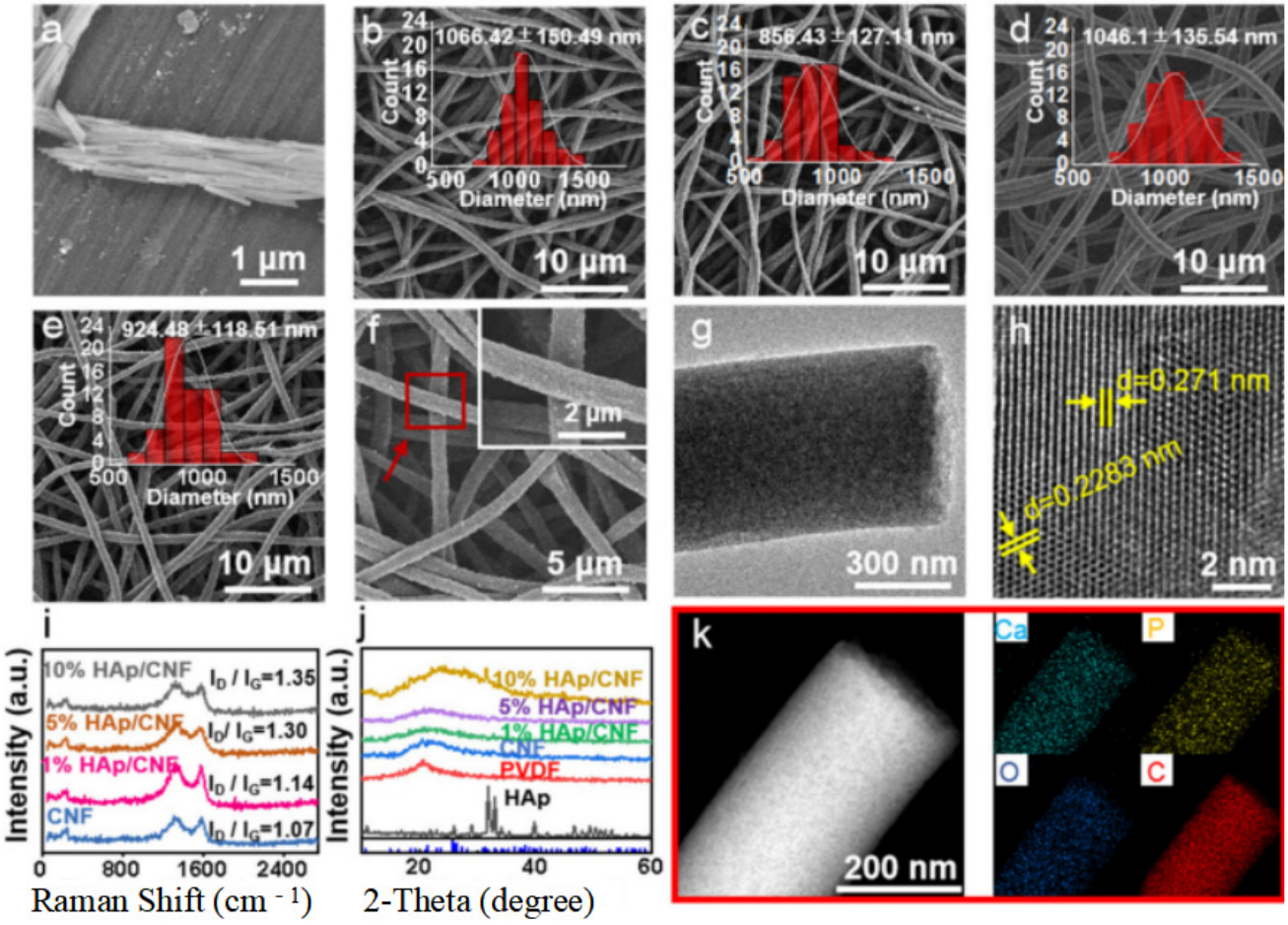

Figure 18. Structural and functional characterization of HAp/CNF scaffolds: SEM (**a**–**e**) & TEM (**h**) morphology, XRD (**j**) & Raman (**i**) crystallinity, EDS (**k**) elemental mapping, (**f**) SEM images of 10% HAp/CNF atdifferent magnifications and degradation-related porosity (**g**).

For a comparison of degradation cycles and immune effects, refer to Table 5. As degradation progresses, scaffold porosity and mechanical properties evolve [81,82]. Hence, a thorough understanding of porosity and modulus matching is essential to support vascularization and maintain structural integrity, which is the focus of the next section.

Table 5. The relationship between the degradation rate and the dynamic response of the inflammatory microenvironment.

Degradation Cycle	Microenvironmental Regulation Mechanism	Immune Modulation Effect	Organize a Regeneration Window
2–4 months	Slow degradation to maintain mechanical support	M1 → M2 macrophage transformation increased	Adaptation to chronic regeneration
>6 months	Rapid disintegration → inflammatory factor explosion	TNF-α↑, IL-6↑	The risk of re-injury is increased

"↑" indicates an increase or upregulation of the indicated biological effect.

3.5. Synergistic Design of Biological Material Properties and Structural Parameters

Porosity and mechanical compliance are key characteristics of electrospun scaffolds. By regulating nutrient diffusion gradients, cell migration kinetics, and host-scaffold interface mechanical matching, the microenvironment for angiogenesis and axonal regeneration can be synergistically optimized, significantly promoting spinal cord injury repair [83].

Cnops et al. [40] found that high-density fiber scaffolds have good host integration performance. Fiber density has no effect on cell infiltration, and effective vascular growth may require larger gaps between fibers or faster fiber degradation, offering an optimal environment for nerve regeneration post-SCI.SEM and vascular infiltration data are shown in Figure 19, where scaffold gap size influences host integration. The "density-vascularization" mechanism was quantitatively analyzed, but to truly guide the design of SCI stents, the coupling evaluation of "vascular maturity-neurological function" should be supplemented.

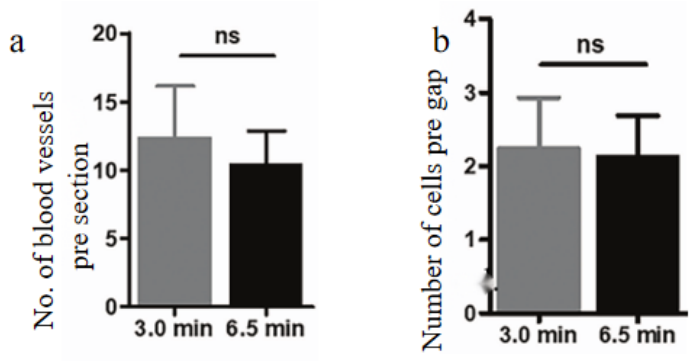

Figure 19. Influence of gap size on blood vessel ingrowth and cell infiltration into the scaffold. (**a**) Effect of electrospinning time on the number of blood vessels in the scaffold. (**b**) Effect of electrospinning time on cell infiltration. Although a shorter electrospinning time resulted in larger gaps, the average number of cells. ns, not significant.

Zhao et al. [84] through a spinal cord injury rat model, the PHBV/PLA+COL electrospun scaffold loaded with AC significantly improved biocompatibility. After implantation, the inflammatory response was reduced, the area of spinal cord cavities shrank, glial scar formation was inhibited, and neuronal regeneration capacity was enhanced, ultimately promoting the recovery of hind limb motor function (Figure 20). Cell experiments showed an increased cell proliferation rate on the scaffold surface, indicating its ability to support cell adhesion and expansion. Although degradability was not explicitly mentioned, the copolymer structure of PHBV/PLA typically has controllable degradation properties, potentially degrading gradually through hydrolysis to meet tissue repair needs. The study explored the "synthetic + natural composite" synergistic approach.

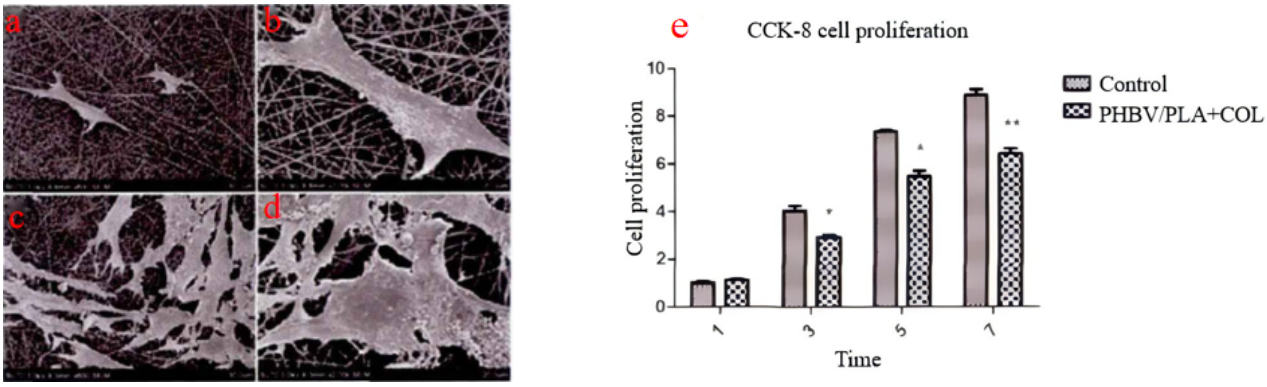

Figure 20. (**a**) 600× and (**b**) 2000× images of electrospun PHBV/PLA+COL scaffolds inoculated with AC for 7 days, (**c**) 600× and (**d**) 2000× images of materials inoculated with AC for 14 days, and (**e**) The effect of electrospun reverse transcription receptors inoculated with AC on cell proliferation rate.* $p > 0.05$;** $p < 0.01$.

Zheng et al. [85] through live and dead cell staining and cell counting kit-8 (CCK-8) experiments, confirmed that 0.5% and 1.0% ceria nanofiber scaffolds (NS@COP) Nanofiber scaffolds have good biocompatibility, no obvious cytotoxicity, and do not affect cell proliferation. *In vivo*, 0.5%, 1.0% by h&e staining NS@COP The nanofiber scaffolds did not cause pathological tissue changes to the important

organs of the body at 8 weeks after surgery, indicating its good biological safety. Nanofiber scaffold NS@COP It not only has degradability, but also has good biosafety, slow-release of loaded nanoparticles, simple preparation process, high feasibility and low cost. As shown in Figure 21.

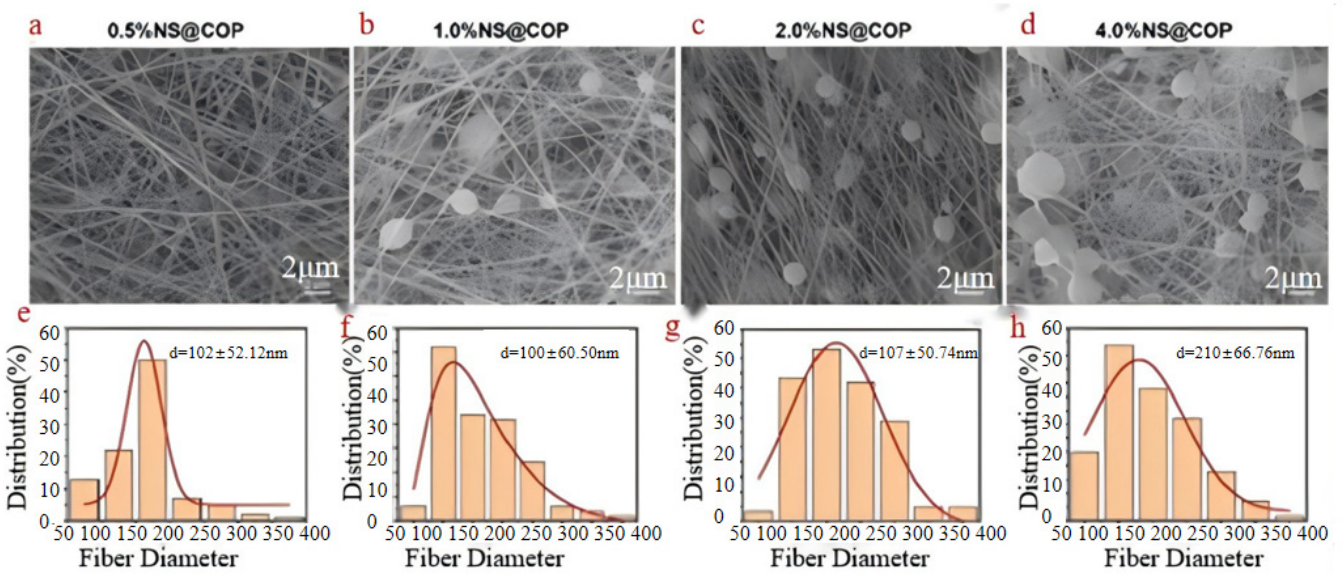

Figure 21. Different concentrations NS@COP Observation of the microstructure and fiber diameter distribution of nanofiber scaffolds. (**a**–**d**) the surface morphology of nanofiber scaffolds. (**e**–**h**) Statistical chart of diameter distribution of nanofiber scaffolds. (**a**,**e**) 0.5%; (**b**,**f**) 1.0%; (**c**,**g**) 2.0%; (**d**,**h**) 4.0% NS@COP.

Given the interdependence among diameter, alignment, chemistry, degradation, and porosity, the final section integrates these parameters into a synergistic strategy, outlining how multi-parameter optimization can be achieved in practice.

3.6. Multi-Parameter Coordinated Control Strategy

To move beyond single-parameter tuning, this section synthesizes the preceding findings into an integrative framework, identifying optimal combinations and trade-offs among electrospinning variables to design functionally robust scaffolds [86,87].

Optimization and regeneration of diameter-oriented composite stent: He et al. [88] created a unique electrospun PLLA scaffold (oriented and randomly oriented) with a diameter range of 300–900 nanometers and increments of 200 nanometers. C17.2 cells cultured on a scaffold with an average fiber diameter of 500 nm induced the longest neuroinflammation elongation and the maximum neuronal differentiation. Unlike previous studies, C17.2 differentiation is highly dependent on fiber arrangement, as there are more cells differentiating into neuronal lineages on arranged fibers regardless of fiber diameter. This result led He et al. to conclude that fibers with a diameter of 500 nm are optimal for guiding neuroinflammation. However, the researchers acknowledge that their observations may result from the high neuronal differentiation of C17.2 cells, as neuroinflammation is longest on scaffolds with the highest neuronal differentiation. Diameter-alignment combinations and their influence on neuronal differentiation are illustrated in Figure 22. “500 nm + high orientation” has been established as the optimal unit for early neuronal differentiation, but to build a truly “globally optimal” scaffold, more dimensional parameters and *in vivo* validation are needed.

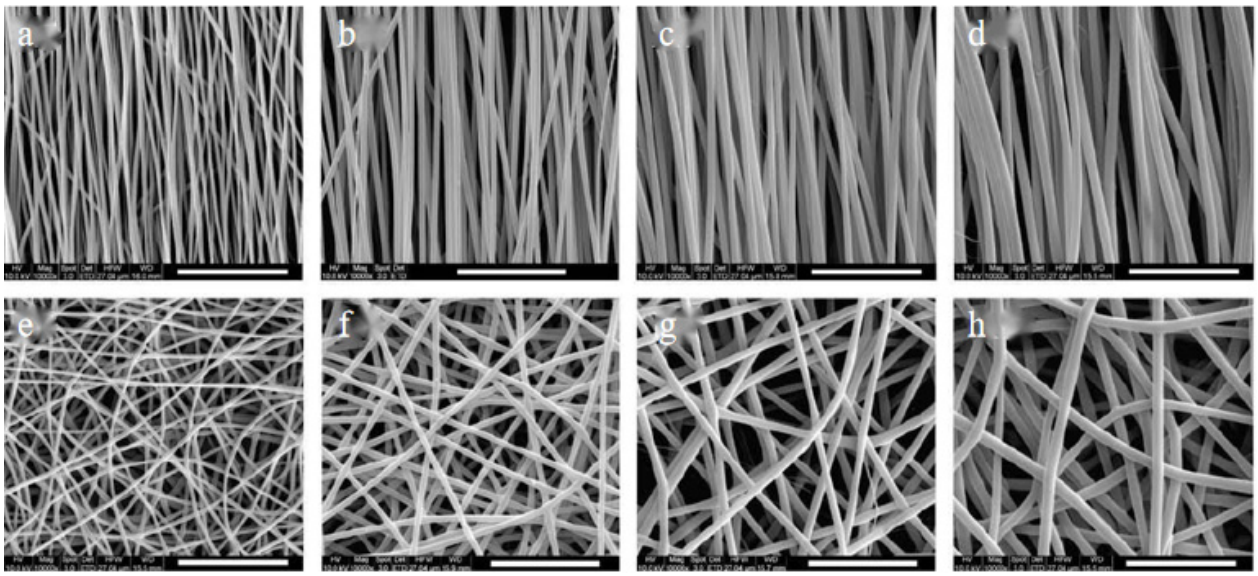

Figure 22. PLLA electrospun fibers of different sizes and arrangements. Directional arrangement: (**a**) 307 ± 47 nm; (**b**) 500 ± 53 nm; (**c**) 679 ± 72 nm; (**d**) 917 ± 84 nm; Random arrangement: (**e**) 327 ± 40 nm; (**f**) 545 ± 54 nm; (**g**) 746 ± 82 nm; (**h**) 1150 ± 409 nm.

Topological-drug synergistic enhancement of functional recovery: Singh et al. [89] developed a novel method of delivering a UA locally from biomaterials and demonstrated that the Uric acid (UA)-PCL fibers successfully protected excitotoxic lesions in an *in vitro* spinal cord tissue injury model. Both fibers protected neurons and reduced the reactive oxygen species (ROS) produced by Glutamate-induced excitotoxicity (GIE) in organospinal cord slice cultures. Its findings have implications for the treatment of SCI and further support the feasibility of UA as an effective therapeutic agent. Topological–pharmacological synergy effects are shown in Figure 23. The research shows high scientific value in parameter design, mechanism interpretation, and function verification, but some key links still need to be further deepened.

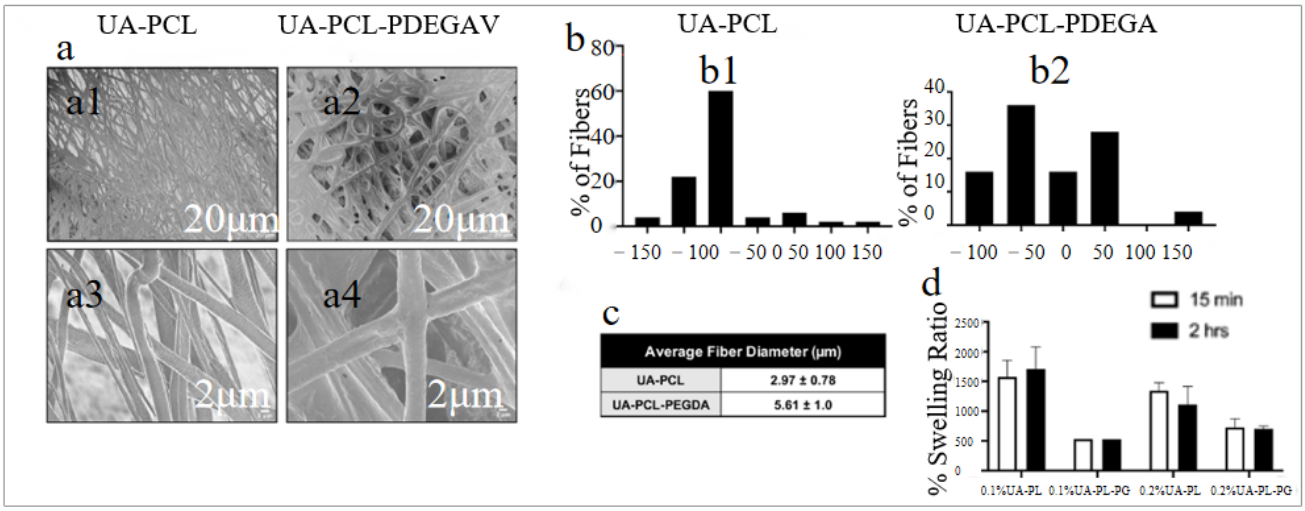

Figure 23. Fiber mat properties. (**a**) Uncoated cross-sections of UA-PCL and UA-PCL-poly (ethylene glycol) diacrylate (PEGDA) fibers. (**b**) Angle distributions of UA-PCL and UA-PCL-PEGDA fibers. (**c**) Average diameter of UA-PCL and UA-PCL-PEGDA fibers. (**d**) Percent swelling ratios of UA-PCL and UA-PCL-PEGDA fiber mats after 15-min and 2-h incubations in PBS.

In summary, the influence of key electrospinning parameters on spinal cord injury repair can be understood through a hierarchical, multiparametric framework. Fiber diameter exerts a first-order effect: nanoscale fibers (200–500 nm) maximize specific surface area to cluster integrins, activate FAK/ERK signaling, and thereby promote neural stem cell adhesion and early axonal extension, whereas larger fibers (800–1200 nm) favor astrocyte elongation and glial network formation to support later-stage tissue stabilization. Fiber alignment (<10° deviation) provides contact-guidance tracks that double axonal outgrowth relative to random mats, while simultaneously tuning directional stiffness without compromising porosity. Surface chemical functionalization—through RGD peptide or antibody grafting—and nanotopographical features (pits, pores) synergistically regulate integrin–MAPK pathways, reduce GFAP expression, and encourage neurite branching. Scaffold composition and molecular weight govern degradation kinetics (e.g., ~35% mass loss at 28 days), synchronizing mechanical support with sustained release of bioactive agents; degradation byproducts further modulate macrophage polarization from M1 to M2, extending the regenerative window. Finally, scaffold porosity (70–95%) and elastic modulus (0.1–1 MPa) must be co-optimized to facilitate vascular ingrowth and minimize interfacial shear stress. By integrating these single-parameter effects into a consolidated "design window" matrix, researchers can rationally engineer electrospun scaffolds that faithfully recapitulate spinal cord microarchitecture and dynamically orchestrate the repair milieu [90,91].

To visually consolidate the relationships described above, Figure 24 presents a schematic overview of the five principal electrospinning parameters, their optimized design ranges, biological effects, and interdependencies. This diagram captures both the direct cellular responses elicited by individual parameters (e.g., fiber alignment enhancing axonal extension) and the synergistic interactions required to balance structural, biochemical, and immunological functions *in vivo*. As such, it serves as a strategic framework for scaffold design, guiding the rational integration of multiple fiber-level cues into a unified, biomimetic solution for spinal cord injury repair. Table 6 summarizes the experimental validation of the effect of electrospinning parameters on therapeutic spinal cord injury.

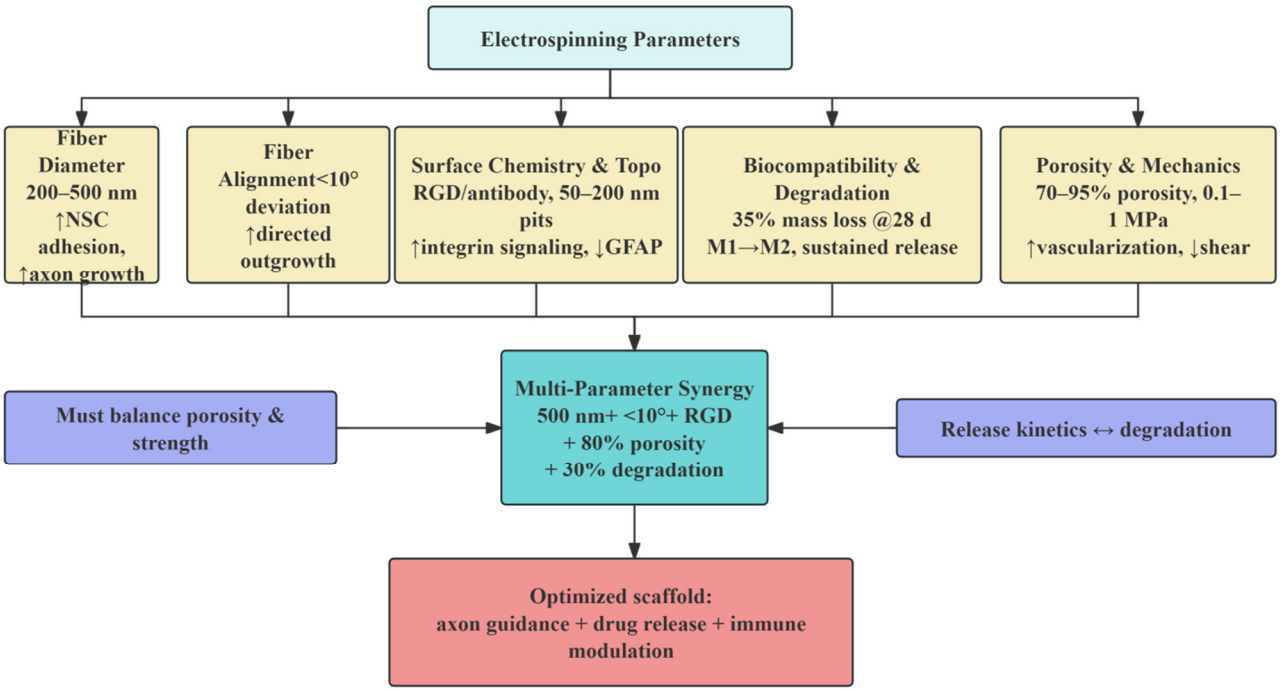

Figure 24. Synergistic framework of electrospinning parameters in spinal cord injury repair. "↑" indicates an increase or upregulation of the indicated biological effect. "↓" indicates a decrease, reduction, or inhibition.

Table 6. Experimental validation of the effects of electrospinning parameters on therapeutic SCI.

Parameter Category	Optimized Range/Design	Mechanistic Role	Biological Effect	Representative Study	Design Implication
Fiber diameter	200–500 nm	High surface area → integrin clustering → FAK/ERK activation	NSC adhesion↑, neuronal differentiation↑	Christopherson et al. [66]	Early-stage regeneration guidance
Fiber diameter	800–1200 nm	Enhanced mechanical support → cytoskeletal tension regulation	Astrocyte elongation↑, GFAP alignment↑	Zhang et al. [67]	Glial network formation
Fiber diameter	~200 nm (collagen)	Contact guidance + reduced astrocyte activation	DRG axon alignment↑, GFAP↓	Liu et al. [68]	Anti-glial scarring + axon growth
Fiber diameter	~800 nm	Cytoskeletal polarization	Astrocyte polarity↑, GLT-1↑	Johnson et al. [44]	Neuroprotection enhancement
Fiber diameter	~1.1 μm	Mechanical optimization	Scaffold orientation↑, stability↑	Chen et al. [70]	Material optimization reference
Fiber alignment	<10° deviation	Contact guidance → cytoskeleton alignment	Axonal extension↑ (~2×)	Hurtado et al. [39]	Directional nerve regeneration
Fiber alignment	Random	Isotropic stress distribution	Disordered growth, myelin thinning	Xia et al. [75]	Not suitable for guided repair
Fiber alignment	Controlled alignment (collector-based)	Mechanical anisotropy tuning	Schwann cell adhesion↑, proliferation↑	Subramanian et al. [76]	Translational scaffold design
Surface topology	Nanostructured (curcumin-functionalized)	Integrin signaling + topology modulation	Neurite growth↑, neuroplasticity↑	Sánchez et al. [77]	Topology–drug synergy
Surface chemistry	Drug-loaded multi-channel fibers	HDAC6 inhibition → microenvironment regulation	Axon regeneration↑, inflammation↓	Liao et al. [78]	Clinical-oriented design
Surface topology	Pure morphology comparison	Cytoskeleton modulation	Consistent with topology-driven effects	Johnson et al. [69]	Validation of physical cues
Degradation behavior	Electroactive scaffold	Electro-mechanical coupling	Schwann cell alignment↑, myelination↑	Wu et al. [79]	Alternative to degradation control
Degradation + release	HAp/CNF composite	Piezoelectric + ion release synergy	Osteogenic markers↑, regeneration support	Sun et al. [80]	Multi-functional degradation system
Porosity & density	Controlled fiber density	Nutrient diffusion + vascular infiltration	ngiogenesis↑, integration↑	Cnops et al. [40]	Host integration optimization
Composite scaffold	PHBV/PLA + collagen	Biocompatibility + immune modulation	Inflammation↓, axon regeneration↑	Zhao et al. [84]	Hybrid material strategy
Nanoparticle-loaded scaffold	Ceria nanofibers	ROS scavenging + slow release	Biocompatibility↑, safety↑	Zheng et al. [85]	Safe translational design
Multi-parameter coupling	Diameter (~500 nm) + alignment	Structure–function synergy	Neuronal differentiation↑	He et al. [88]	Optimal early-stage design
Topology + pharmacology	UA-loaded fibers	ROS suppression	Neuron protection↑	Singh et al. [89]	Oxidative stress targeting

"↑" indicates an increase or upregulation of the indicated biological effect. "↓" indicates a decrease, reduction, or inhibition.

4. Results of Electrospinning in Spinal Cord Injury Therapy and Its Combination with Other Techniques

Electrospun scaffolds have been explored in SCI repair from a translational perspective because they can simultaneously provide physical bridging, directional guidance, and a platform for biochemical functionalization. Compared with single-component biomaterials, electrospun systems are especially attractive in SCI because they can be engineered at multiple levels: macroscopically, they can fill lesion cavities and reconstruct continuity across the injury site; microscopically, they can regulate cell adhesion, migration, and axonal extension; and functionally, they can be combined with drugs, cells, growth factors, and hydrogels to reshape the hostile post-injury microenvironment. Nevertheless, the reported studies differ widely in scaffold geometry, material composition, cell-loading strategy, and animal model, making direct comparison difficult and highlighting the need for critical synthesis rather than simple enumeration.

4.1. Physical Scaffolds

Physical scaffolds are the most direct and foundational application of electrospinning in SCI repair. Their core purpose is to reconstruct a permissive bridge across the lesion cavity and to provide a structural template that can support axonal extension, host-cell infiltration, and tissue integration. In this category, the central design logic is relatively consistent across studies: electrospun conduits or three-dimensional fiber constructs are used to recreate the anisotropic architecture of the spinal cord ECM, while the specific implementation varies in terms of conduit geometry, pore structure, material composition, and degree of structural hierarchy. As a result, the reported systems differ substantially in translational maturity, even when they share a similar regenerative intent [17].

4.1.1. Single-/Multi-Channel Conduits

Single- and multichannel conduits are designed to provide a macroscale physical bridge across the injury site and to convert the lesion cavity into a more organized regeneration space. The common rationale is that a channelized scaffold can reduce collapse of the injured region, restrict fibrotic invasion, and guide axons along a preferred direction. In practice, however, the biological benefit of such constructs depends not only on the presence of a conduit but also on whether the conduit maintains sufficient porosity, wall stability, and internal organization to support host integration over time.

Among the reported examples, Wang et al. [92] developed a 3D-printed bionic scaffold incorporating plant-derived exosomes extracted from *Lycium barbarum* L. and loaded with isoliquiritigenin (ISL). The authors showed that the plant-derived exosomes possessed anti-inflammatory activity and promoted neuronal differentiation, and that ISL-loaded plant-derived exosomes (ISL@PE) further enhanced these effects compared with exosomes derived from ectomesenchymal stem cells. By combining ISL@PE with a biomimetic 3D-printed scaffold, the study aimed to modulate the inflammatory response after spinal cord injury, facilitate axonal restoration, and improve neurological function， As shown in Figure 25. This work is notable because it introduces a novel plant-exosome-based delivery route for an insoluble drug and demonstrates a composite 3D-bioprinted strategy for SCI repair, although further mechanistic clarification and long-term translational validation are still needed.

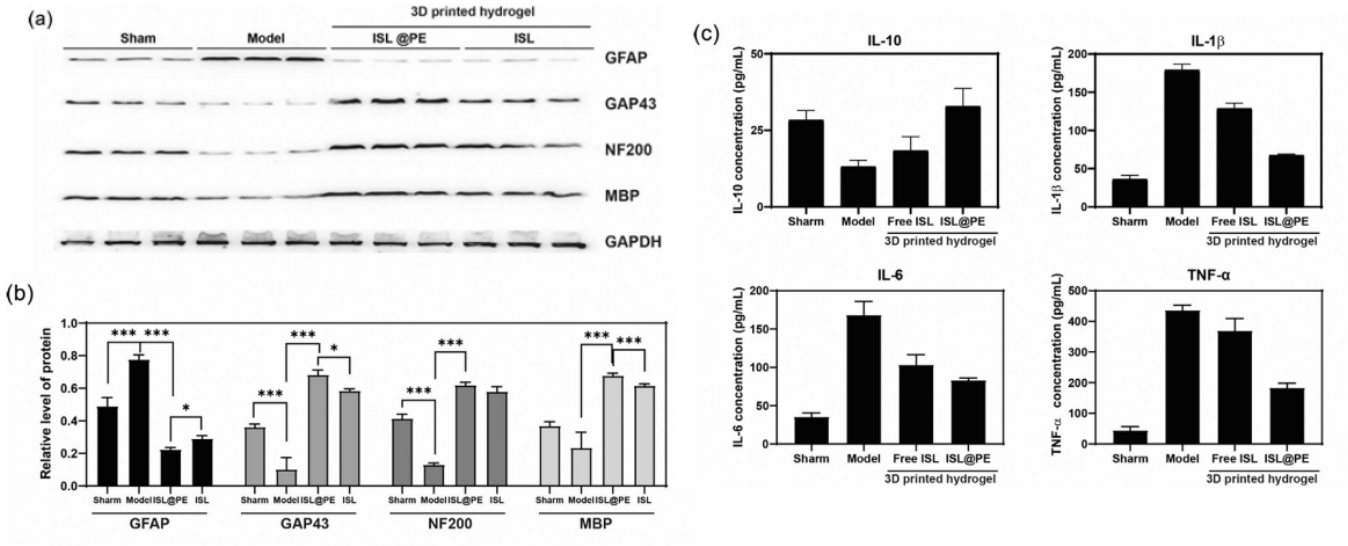

Figure 25. Relative expression levels of GFAP, GAP43, NF200, and MBP, as well as GAPDH protein in the spinal cord of injured patients across different treatment groups. Western blot protein expression data (**a**) and quantitative analysis of GFAP, Tuj1, and NF200 (**b**) support the Nestin, MAP2, and MBP groups, respectively. (**c**) Quantitative data of IL-10, IL-1β, IL-6, and TNF-α in spinal cord injury treatment groups under different conditions. * $p > 0.05$;*** $p < 0.001$.

A different design strategy was used by Li et al. [42], who combined gas foaming with electrospinning to fabricate three-dimensional PCL/PPDO nanofiber sponge scaffolds with controllable hierarchical structure and high porosity. Their study emphasized that the value of a conduit lies not merely in filling the lesion space, but in reproducing a native ECM-like fiber profile while allowing tissue ingrowth and exogenous neural stem cell support, As shown in Figure 26. This work is important because it addresses a major limitation of many densely packed electrospun mats, namely, insufficient three-dimensional infiltration. However, the clinical relevance of this approach still depends on whether the scaffold degradation rate and structural persistence can be matched to the dynamic phases of SCI repair.

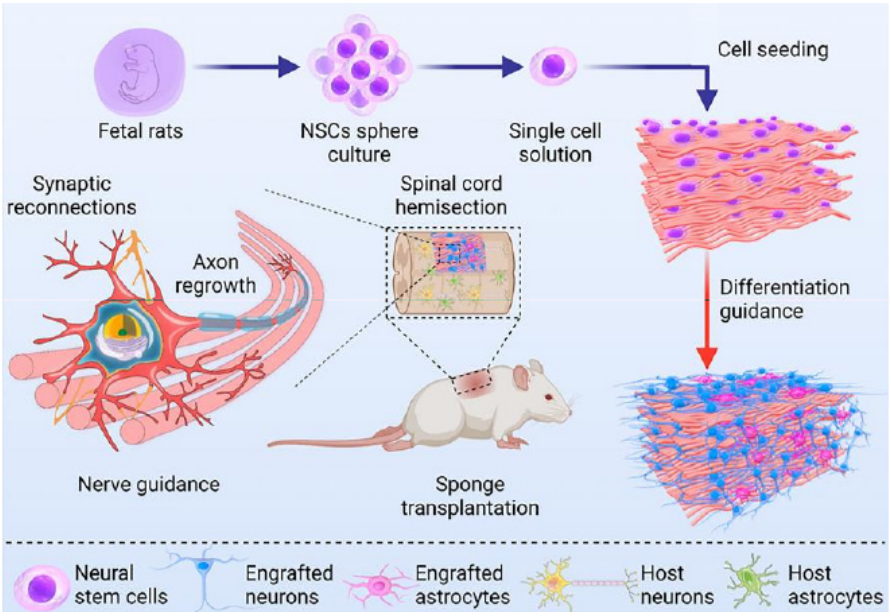

Figure 26. Schematic diagram of 3D PCL/PPDO nanofiber sponge loaded with exogenous NSCs for treating spinal cord injury in rats.

The translational potential of channel-based scaffolds was further strengthened by Zeng et al. [93], who evaluated a three-dimensional gelatin sponge scaffold in a non-human primate SCI model. In this study,

the scaffold supported robust tissue remodeling, with evidence of cell migration into the regenerated tissue, matrix deposition, nerve fiber regeneration, myelination, vascularization, and electrophysiological improvement, As shown in Figure 27. This is one of the most clinically relevant studies in the present review because it moves beyond rodent-only evidence and demonstrates that a cell-supportive scaffold can also perform in a primate model. Nevertheless, the system is not without limitations: although the tissue response was encouraging, additional work is still needed to determine whether the scaffold can sustain long-term biomechanical integrity and whether similar outcomes can be achieved in more severe or chronic injuries.

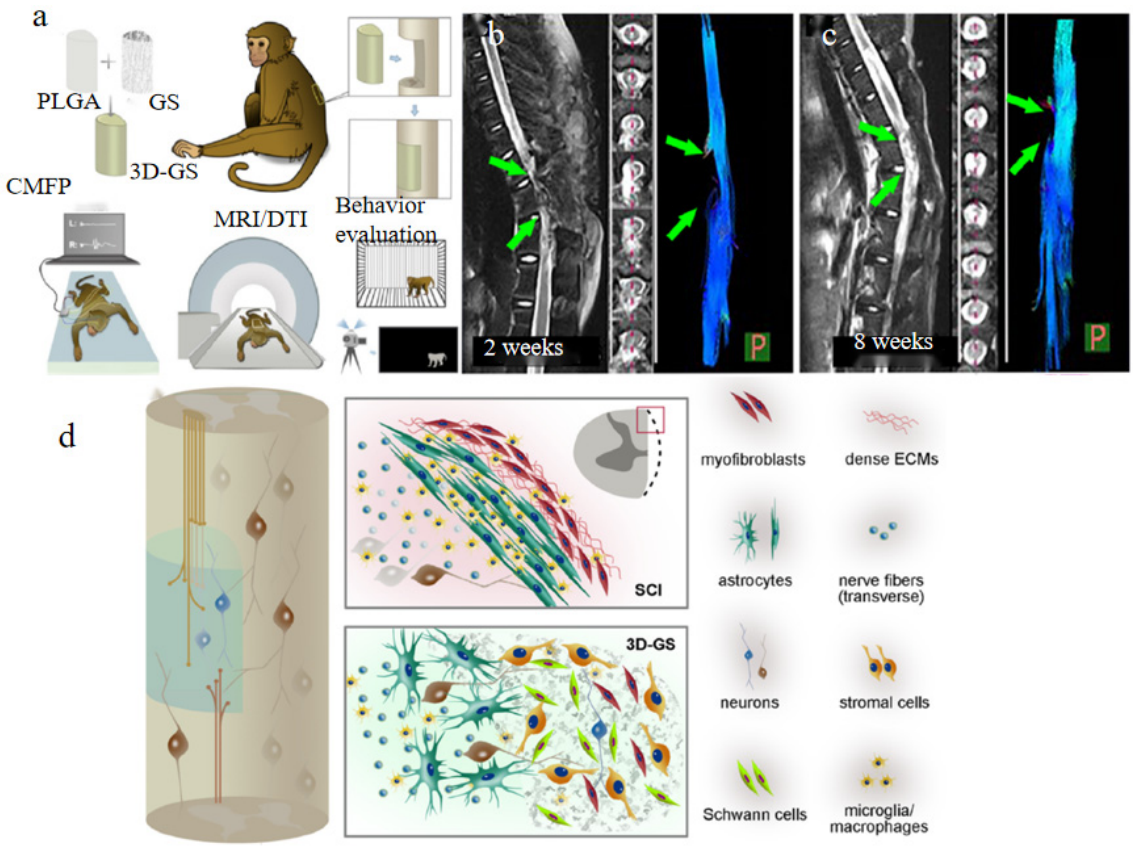

Figure 27. Structural repair of the injured spinal cord following implantation of 3D-GS. (**a**) Schematic showing experimental procedures. (**b**) Images generated by magnetic resonance imaging (MRI)/diffusion tensor tractography (DTT) showing tissue defects in the injured spinal cords 2 weeks after hemisection. (**c**) MRI/DTT showing tissue restoration and nerve fiber regeneration in the injured areas of the spinal cords 2 weeks after 3D-GS implantation. (**d**) A schematic diaphragm showing.

Taken together, these studies suggest that single- and multichannel conduits are best understood as lesion-bridging platforms whose value depends on the balance between geometry, porosity, degradation, and biological loading. The main advancement in this subfield is no longer simply whether a conduit can be fabricated, but whether it can be engineered to maintain internal organization, support cell retention, and remain mechanically competent long enough to influence meaningful regeneration.

4.1.2. Diameter & Alignment Optimization

Once the overall conduit architecture is established, fiber diameter and alignment are the key variables that determine how effectively the scaffold guides cell behavior and axonal regrowth. These two parameters act together: diameter influences surface area, compliance, and cell-contact density, whereas alignment determines whether the scaffold provides directional cues for neurite extension and cellular polarity. The major message from the literature is that physical guidance is not a binary property; rather, it is a graded

response that depends on the interactions among topography, mechanics, and the specific cell types present in the lesion environment [94].

A representative body of work has established fiber alignment as a key determinant of axonal guidance in electrospun scaffolds. Hurtado et al. [39] provided a classic demonstration of the importance of orientation by implanting aligned PLLA electrospun microfibers into a rat complete spinal cord transection model. Their results showed that aligned fibers promoted axonal regeneration along the fiber axis through contact guidance, with axonal extension reaching 2055 ± 150 μm, compared with 1162 ± 87 μm for random fibers and 413 ± 199 μm for the film control,As shown in Figure 28. This study remains highly influential because it clearly established that aligned electrospun fibers can provide a directional track for regenerating axons and can partially reconstruct the ordered architecture required for functional recovery. However, the work also illustrates a recurring limitation in the field: while directional growth was evident histologically, translating that structural success into durable long-term functional restoration remains challenging.

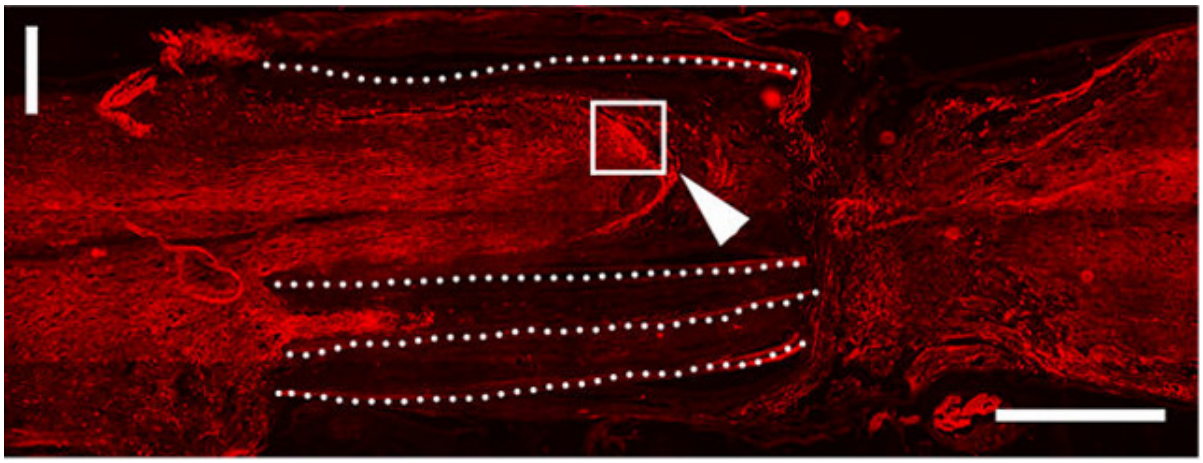

Figure 28. Long distance, linear arrangement of RT97+ axons (red) can be seen in the targeted PLA scaffold, indicating the key role of topology in axon orientation.

Building on this foundation, subsequent studies have expanded the role of alignment beyond neuronal guidance to include glial regulation and mechanical adaptation. Subramanian et al. [76] extended this logic by developing a directed PLGA-PCL nanofiber scaffold that mimicked the Büngner-band structure of peripheral nerves. *In vitro*, Schwann cells aligned longitudinally on the oriented fibers, with their cytoskeleton organized in the same direction as the scaffold, and *in vivo*, the scaffold promoted axonal regeneration and accelerated myelination, As shown in Figure 29. This study is important because it shows that alignment affects not only neurons but also glial cells that are essential for regeneration and remyelination. It also highlights a more nuanced design principle: the best scaffold is not simply the one with the highest alignment, but the one whose mechanical properties and cell response are compatible with the tissue it aims to reconstruct. The measured reduction in Young's modulus compared with the random scaffold indicates that structural alignment can be accompanied by a softer, more nerve-like mechanical profile. Even so, the field still lacks sufficient comparative data to determine the optimal level of alignment under different injury conditions and scaffold compositions.

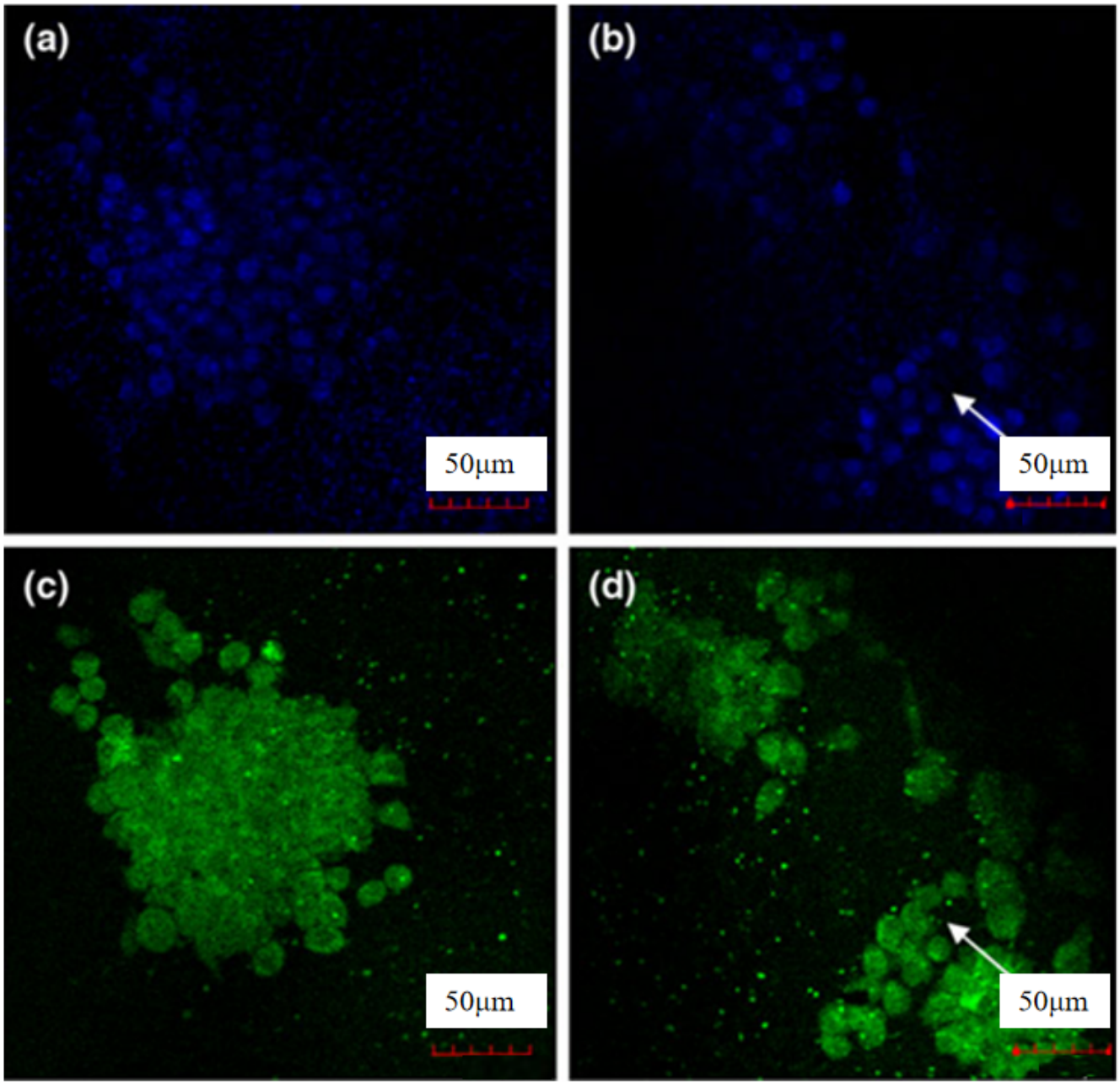

Figure 29. Fluorescence images of Shewan cells on PLGA-PCL nanofiber scaffolds: (**a**) oriented arrangement (Hirst staining); (**b**) Random arrangement (Hirst staining); (**c**) Directional alignment (F-actin); (**d**) Random arrangement (F-actin) arrow: indicates the direction of fibers.

Additional studies reinforce the same conclusion from different material systems. For example, Tai et al. [41] collagen-based aligned electrospun fibers were reported to be more suitable for SCI repair than random counterparts, and dECM-derived aligned versus random fibers have been investigated for mesenchymal stem cell-based SCI treatments. These studies collectively show that the directional effect is not material-specific, but rather emerges from the interaction between anisotropic geometry and cell adhesion dynamics, As shown in Figure 30. This also means that alignment should not be discussed as an isolated structural feature; instead, it should be considered together with diameter, porosity, and surface chemistry when evaluating scaffold performance.

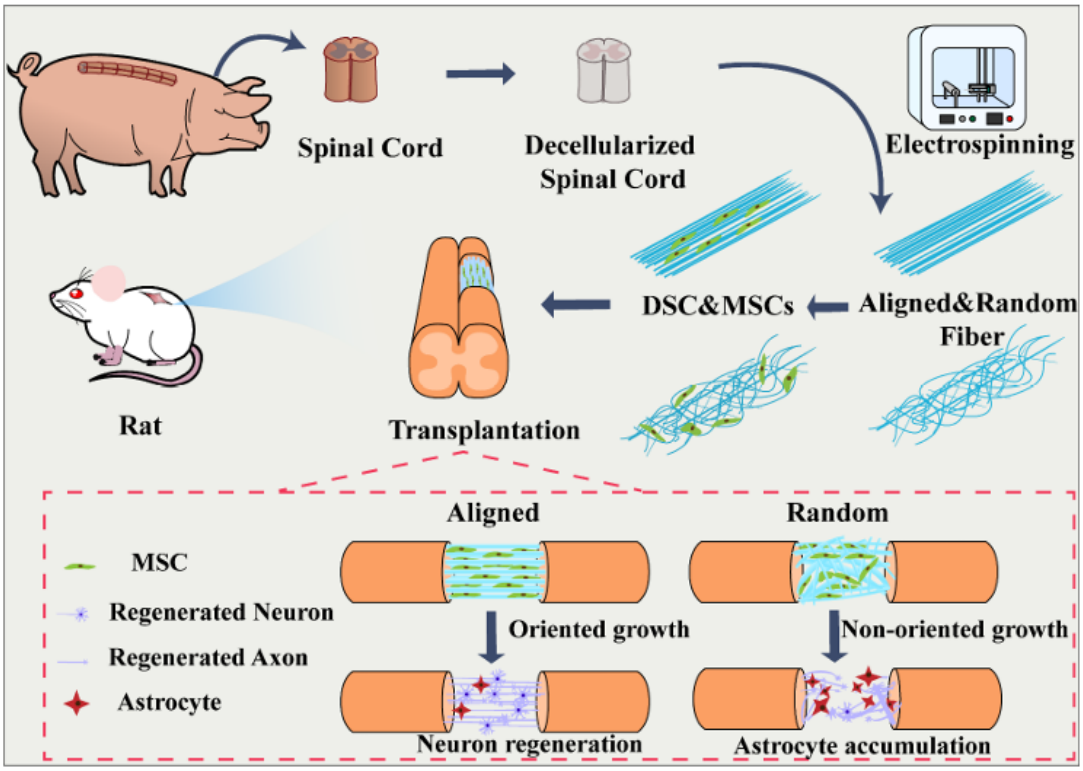

Figure 30. Preparation of aligned fibers and their application for SCI repair.

Overall, the physical scaffold literature shows a clear trend toward increasingly sophisticated architectures, moving from simple conduits to hierarchical, cell-supportive, and clinically more realistic systems. The remaining challenge is to establish design rules that connect scaffold geometry to reproducible biological outcomes across models, species, and injury stages.

4.2. Biochemical Functionalization

Biochemical functionalization represents the transition of electrospun scaffolds from passive structural supports to active therapeutic platforms. In SCI repair, this strategy is used to localize pharmacological agents, regulate inflammatory signaling, and provide spatiotemporally controlled release that matches the evolving phases of injury. Compared with purely physical scaffolds, chemically functionalized electrospun systems can more directly modulate the post-injury microenvironment; however, their effectiveness depends strongly on cargo stability, release kinetics, and the degree to which the biochemical function remains coupled to scaffold architecture rather than being added as an afterthought.

4.2.1. Drug-Loading & Controlled Release

A foundational step in this field was the demonstration that electrospun fibers can serve as localized, sustained delivery systems. For example, Xia et al. [95] developed poly(propylene carbonate) microfibers loaded with dbcAMP and showed that sustained release significantly promoted axonal regenerative sprouting and functional recovery after spinal cord hemisection, As shown in Figure 31. The key innovation of this study lies in proving that electrospun scaffolds can maintain long-term bioactive signaling at the injury site, which is essential for overcoming the transient nature of direct drug injection. However, the study primarily focused on a single signaling pathway, limiting its ability to address the multifactorial nature of SCI.

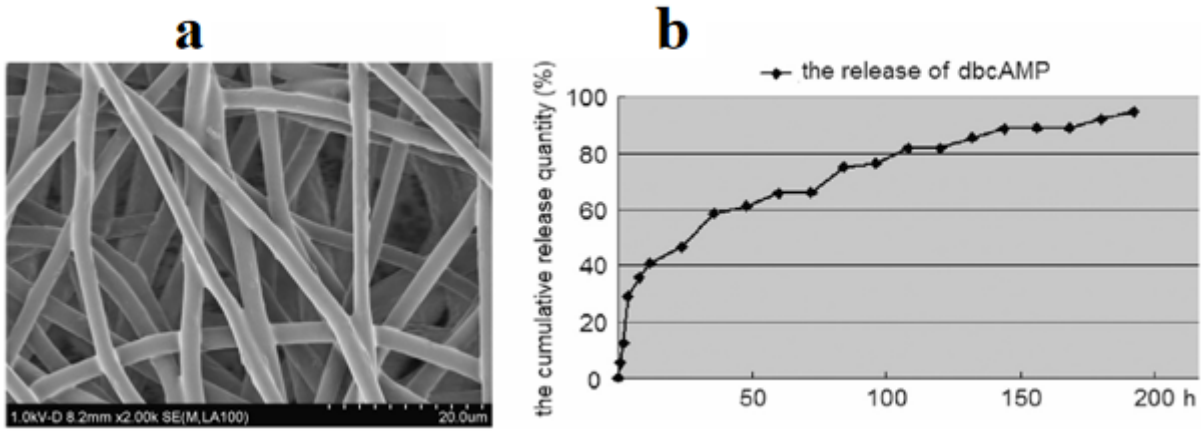

Figure 31. (**a**) Surface and morphology of the micron fbers. (**b**) Release curve of dbcAMP.

Building on this concept, Xia et al. [71] further developed a multi-drug delivery system by incorporating both dibutyryl cyclic AMP (db-cAMP) and chondroitinase ABC (ChABC) into electrospun fibers, aiming to simultaneously address intrinsic and extrinsic barriers to axonal regeneration. In this design, db-cAMP was used to enhance the intrinsic growth capacity of neurons, while ChABC enzymatically degraded chondroitin sulfate proteoglycans (CSPGs), which are major inhibitory components of the glial scar. By integrating these two agents into a single electrospun platform, the study demonstrated that electrospun fibers can function as dual-function delivery systems, enabling coordinated modulation of neuronal signaling and extracellular matrix remodeling, As shown in Figure 32. *In vitro* and *in vivo* results showed enhanced neurite outgrowth and improved axonal regeneration compared to single-factor treatments, highlighting the advantage of synergistic therapy. This work is particularly significant for SCI repair because it shifts the strategy from single-target intervention to multi-target modulation of the injury microenvironment. However, the study also revealed challenges associated with multi-drug systems, including the need for precise control over release kinetics, potential interactions between bioactive agents, and the lack of systematic optimization of dosage ratios for maximal therapeutic efficacy.

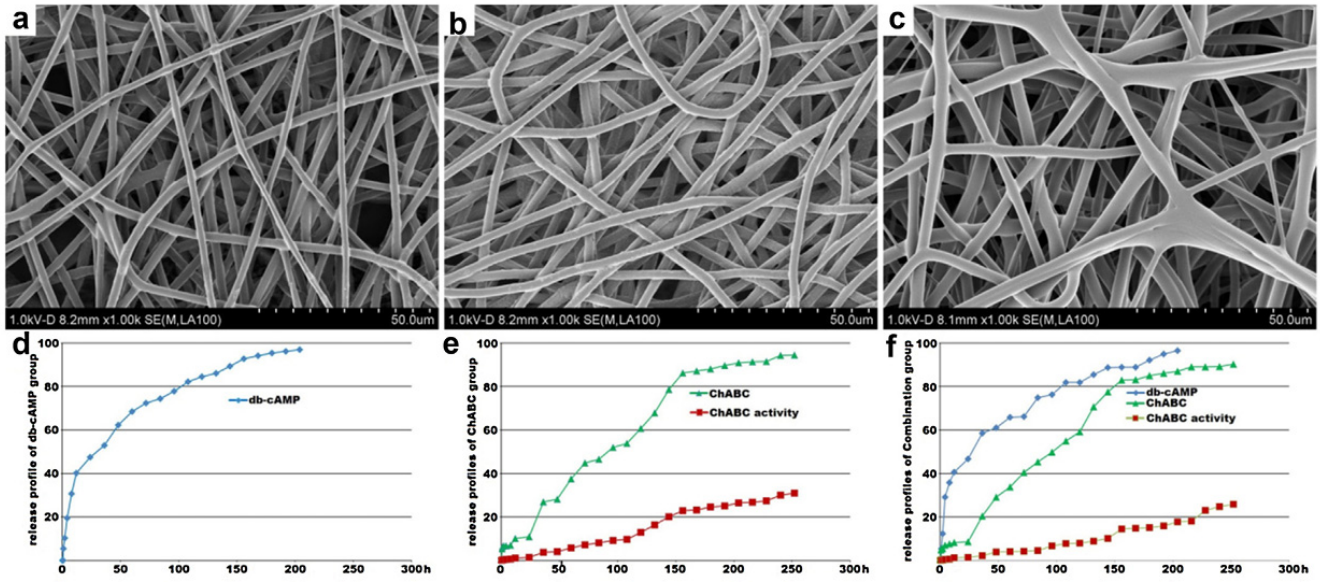

Figure 32. The SEM images and release profiles of the microfibres. Surface and morphology of the microfibres from the (**a**) db-cAMP. (**b**) ChABC, and (**c**) combination groups; (**d**) the release profile the db-cAMP in db-cAMP group; (**e**) the curves of ChABC release and its activity in the ChABC group; (**f**) the release profiles of db-cAMP and ChABC, and ChABC's activity curve.

A more clinically relevant strategy was explored by Rasti et al. [96], who developed electrospun PCL/gelatin nanofibrous scaffolds incorporating dexamethasone sodium phosphate (DEX-P) as an anti-inflammatory agent. In this system, the combination of hydrophobic PCL and hydrophilic gelatin enabled modulation of drug diffusion pathways, thereby reducing the typical burst release observed in many electrospun drug delivery systems. As a result, the scaffold achieved a more sustained and controlled release profile of DEX-P over time, which is critical for maintaining a prolonged anti-inflammatory effect during the early stages of spinal cord injury. Experimental results demonstrated that the controlled release of DEX-P effectively suppressed inflammatory responses and improved cellular compatibility, while the fibrous structure maintained sufficient mechanical integrity to serve as a supportive scaffold, As shown in Figure 33. This work is particularly relevant for SCI repair, where excessive inflammation is a major barrier to regeneration, and highlights the importance of engineering release kinetics to match the temporal dynamics of injury progression. However, the study remains limited by relatively short-term evaluation and lacks *in vivo* validation in complex SCI models, leaving questions regarding long-term efficacy and translational potential.

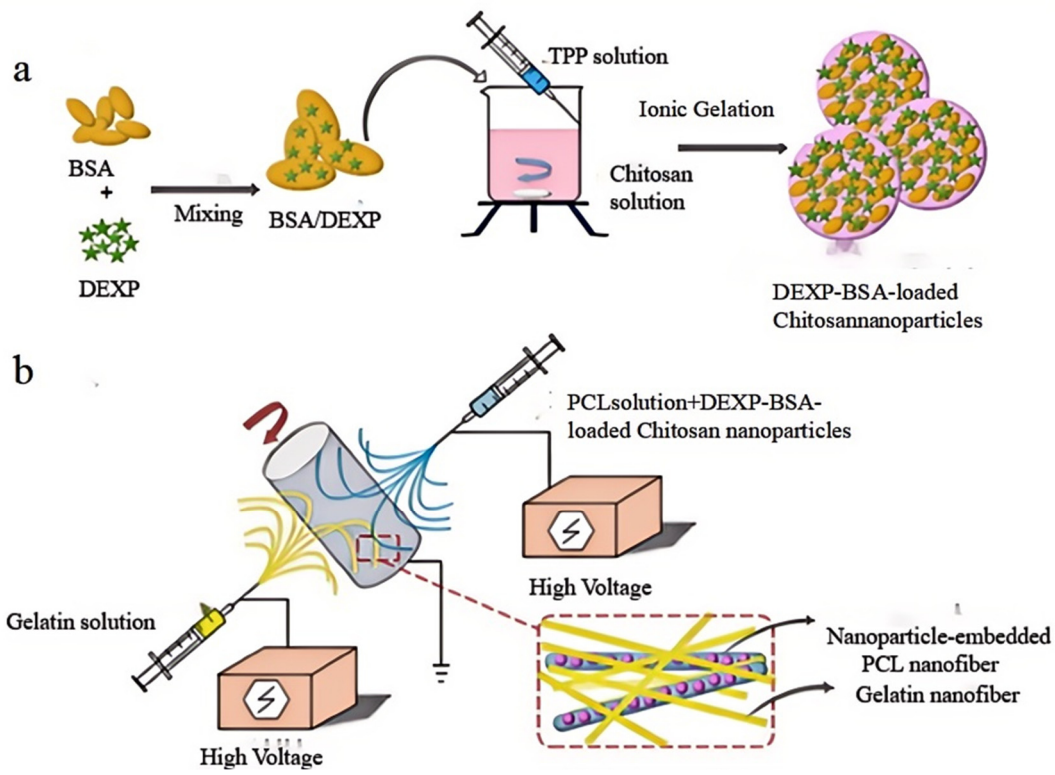

Figure 33. (**a**) Schematic illustration of DEXP-BSA-loaded chitosan nanoparticles (NPs) and (**b**) electrospinning procedure for the fabrication of chitosan NPs-embedded PCL and gelatin nanofiber.

Recent advances in electrospun scaffolds have increasingly focused on integrating immunomodulation with sustained delivery of neurotrophic or therapeutic agents to achieve synergistic repair. Sun et al. [55] developed a new drug delivery composite system named interleukin-10 plasmid (pIL10) wasloaded into lipid nanoparticles (pIL10-LNP) @PLA-HA, designed to steadily release pIL10-LNP and NGF over an extended duration. This system is adept at modulating the inflammatory response following SCI and accelerating nerve regeneration. It exhibits excellent biocompatibility, promotes cell growth, triggers M2 macrophage polarization, and sustains anti-inflammatory factor secretion, enhancing post-SCI inflammatory response. Gradual NGF release promotes NSC differentiation into neuronal cells, enhancing neural repair in Figure 34. This case linked "immune regulation + neurotrophic" and clarified the synergistic value of the two in SCI repair, but for safe transformation, more comprehensive safety studies of gene vectors and long-term follow-up of efficacy are needed.

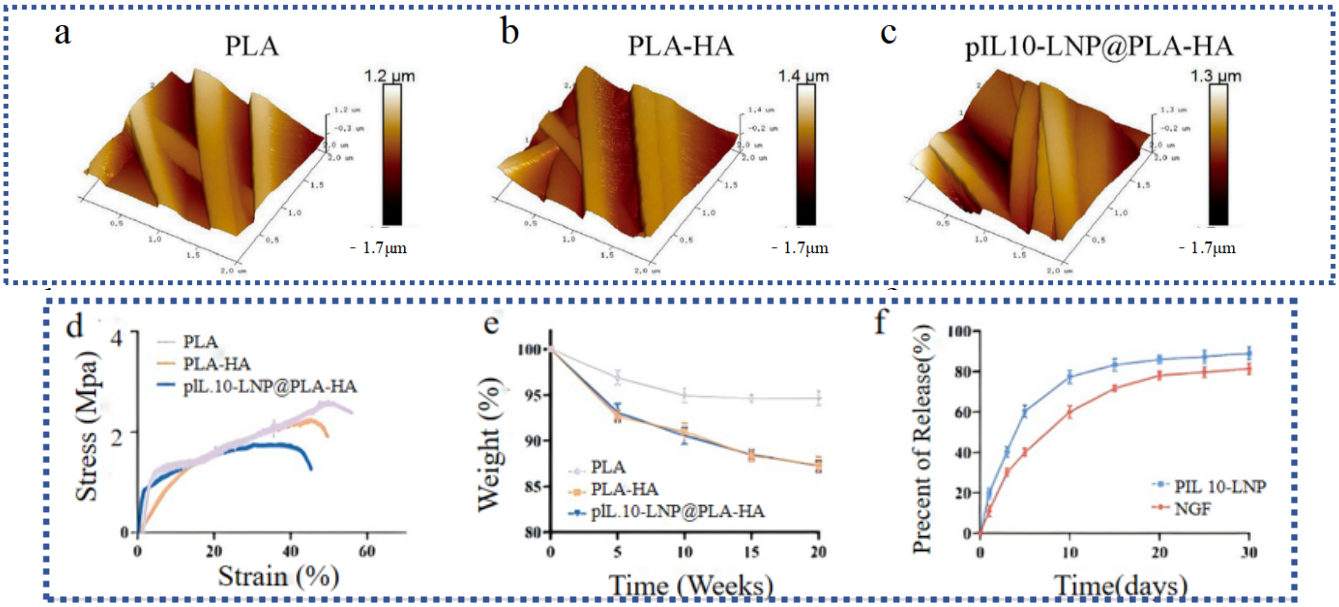

Figure 34. Roughness of various electrospun supports: (**a**) PLA; (**b**) PLA-HA; (**c**) pIL10-LNP@PLA-HA; (**d**) Stress-strain curves of various scaffolds; (**e**) Degradation curves of various scaffolds; (**f**) Release curves of pIL10-LNP and NGF of pIL10-LNP@PLA-HA scaffold.

Complementing gene-based strategies, other studies have explored immune-responsive delivery systems to achieve more precise temporal control over growth factor release. Mays et al. [97] studied the combination of growth factor loaded gelatin microspheres (GMS) with methyl methacrylate hyaluronic acid (MeHA) to produce GMS fibers (GMSF) through electrospinning technology, in order to achieve delayed release of growth factors. GMS successfully combined with MeHA to produce fibers with an average diameter of 365–10 nm and a fiber arrangement of 44–8%, As shown in Figure 35. The experiment tested the effect of GMSF loaded with NGF on isolated chicken dorsal root ganglion cells. A drug delivery biomaterial system triggered by an immune response has been developed, achieving more precise control and longer exposure time for encapsulated drugs. This immune-mediated drug release system is of great significance for targeted repair.

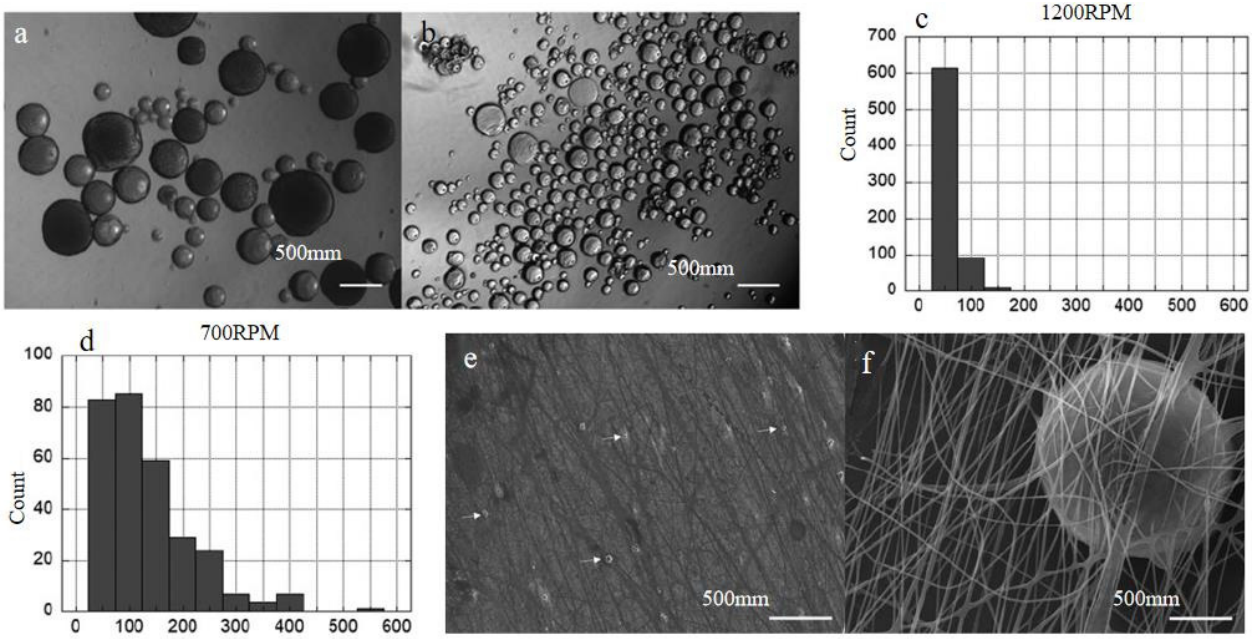

Figure 35. GMSF visualizedwith brightfield microscopyand histogram of micro-sphere sizes: (**a**,**c**) 1200 rpm; (**b**,**d**) 700 rpm. GMSF: (**e**) 20·magnfication of GMSF, arrows indicate a few GMS. (**f**) 2000·magnficationof a single GMS within the MeHA nanofibers.

Extending the concept of multifunctional delivery, pharmacological co-loading strategies have also been developed to address multiple pathological processes simultaneously. Dolci et al. [98] developed an innovative multidirectional pharmacological approach to acute injury of the central nervous system. By incorporating two complementary and potentially synergistic drugs, ibuprofen (Ibu) and triiodothyronine (T3), into a single polymer scaffold, this method accomplishes the dual therapeutic objectives of anti-inflammatory action and remyelination, As shown in Figure 36. Based on previous indoor studies and field experiments, the team determined the non-toxic and effective concentration of the two drugs when used simultaneously, and successfully loaded these drugs into nanofibers to make scaffolds that could continuously release the drugs. The dual drug sequential release strategy of this paper can be extended to more drug combinations, but more detailed *in vivo* pharmacokinetics and concentration-efficacy correlation studies are needed.

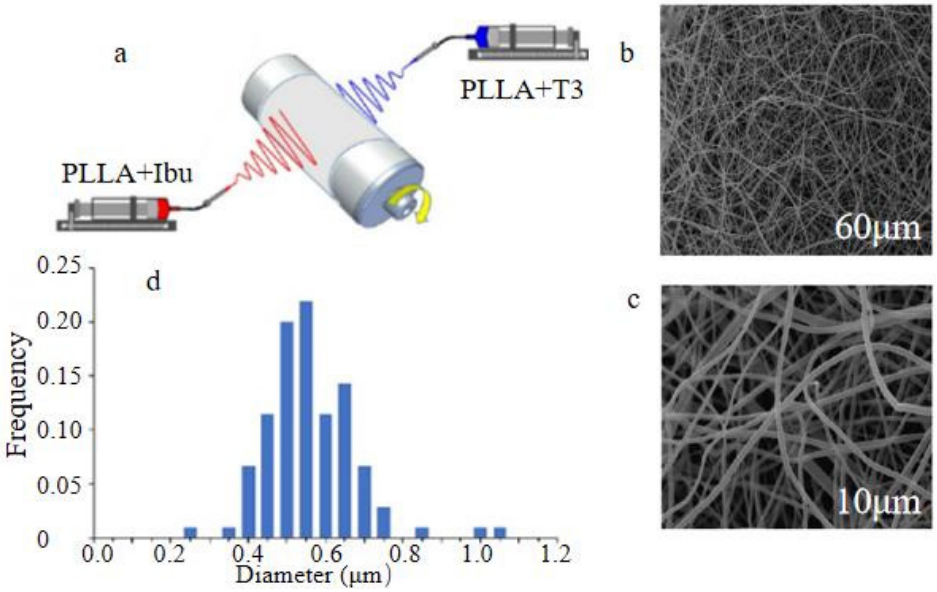

Figure 36. (**a**) Schematic of co-electrospinning apparatus for dual-drug delivery system with PLLA fibers loaded with 5% Ibu and 0.6% T3. (**b**,**c**) PLLA images with different magnifications. (**d**) Fiber diameter distribution.

Further advancing scaffold multifunctionality, Zhang et al. [57] designed a hybrid electrospun system composed of PCL, PSA, and MP, aiming to integrate structural, biochemical, and neuroprotective functions within a single platform. In this design, PCL provided mechanical support and structural stability, while the incorporation of PSA introduced bioactive cues that are known to modulate neural cell adhesion, migration, and axonal extension due to its role in neural development and plasticity. Meanwhile, MP, a clinically used anti-inflammatory agent, was incorporated to suppress the secondary inflammatory response following spinal cord injury. Through this combination, the scaffold simultaneously provided topographical guidance, anti-inflammatory regulation, and enhanced cell–material interactions, demonstrating the feasibility of multifunctional integration within electrospun systems, As shown in Figure 37. Experimental results showed improved neuronal compatibility and reduced inflammatory responses compared to non-functionalized scaffolds, highlighting the synergistic effect of combining structural and biochemical components. This work is particularly significant as it represents a shift from single-function scaffolds toward integrated therapeutic platforms that more closely mimic the complex requirements of SCI repair. However, the increased compositional complexity also introduces challenges, including potential variability in degradation behavior, difficulty in precisely controlling component interactions, and uncertainties regarding large-scale fabrication and clinical translation.

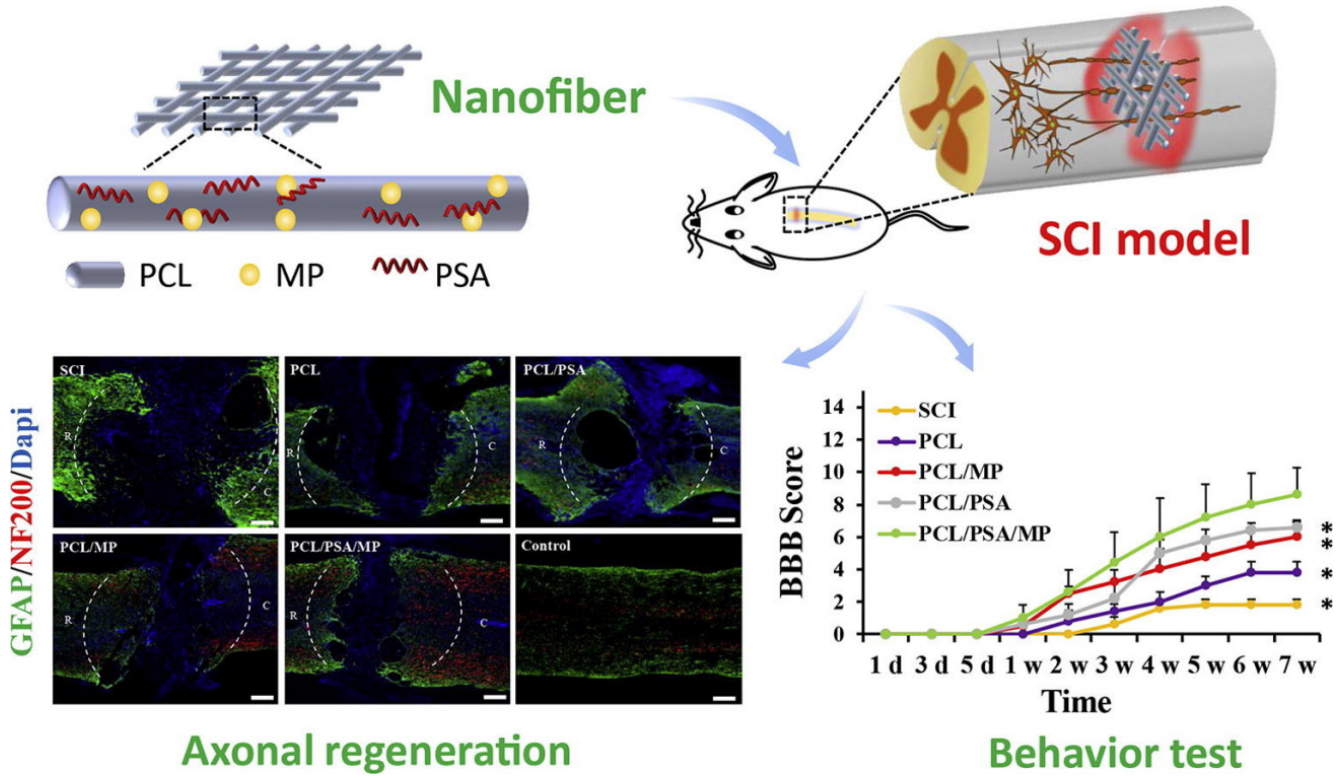

Figure 37. Structural Design of Multifunctional PCL/PSA/MP Electrospun Scaffolds and Functional Validation for Spinal Cord Injury Repair (Axonal Regeneration and Behavioral Assessment).*P* values are calculated using repeated-measures ANOVA with Bonferroni's post hoc test; * $p < 0.05$ is significantly different (versus PCL/PSA/MP group).

In parallel, several studies have explored alternative bioactive agents to expand the therapeutic scope of electrospun systems. For instance, Singh et al. [89] developed uric acid-loaded electrospun fibers aimed at reducing oxidative stress, a key pathological factor in secondary spinal cord injury, and demonstrated improved cellular protection under oxidative conditions. Similarly, María et al. designed curcumin-loaded electrospun membranes combined with neural progenitor cell transplantation, showing that the antioxidant and anti-inflammatory properties of curcumin could mitigate neuronal degeneration and enhance the regenerative microenvironment, As shown in Figure 38. These studies highlight the flexibility of electrospinning as a platform for delivering a wide range of therapeutic molecules targeting different aspects of SCI pathology, including oxidative stress, inflammation, and neuronal loss. However, despite variations in the choice of bioactive agents, most of these approaches follow similar design principles—namely, drug incorporation into electrospun matrices for sustained release—and therefore contribute primarily as incremental or confirmatory advancements rather than introducing fundamentally new therapeutic paradigms.

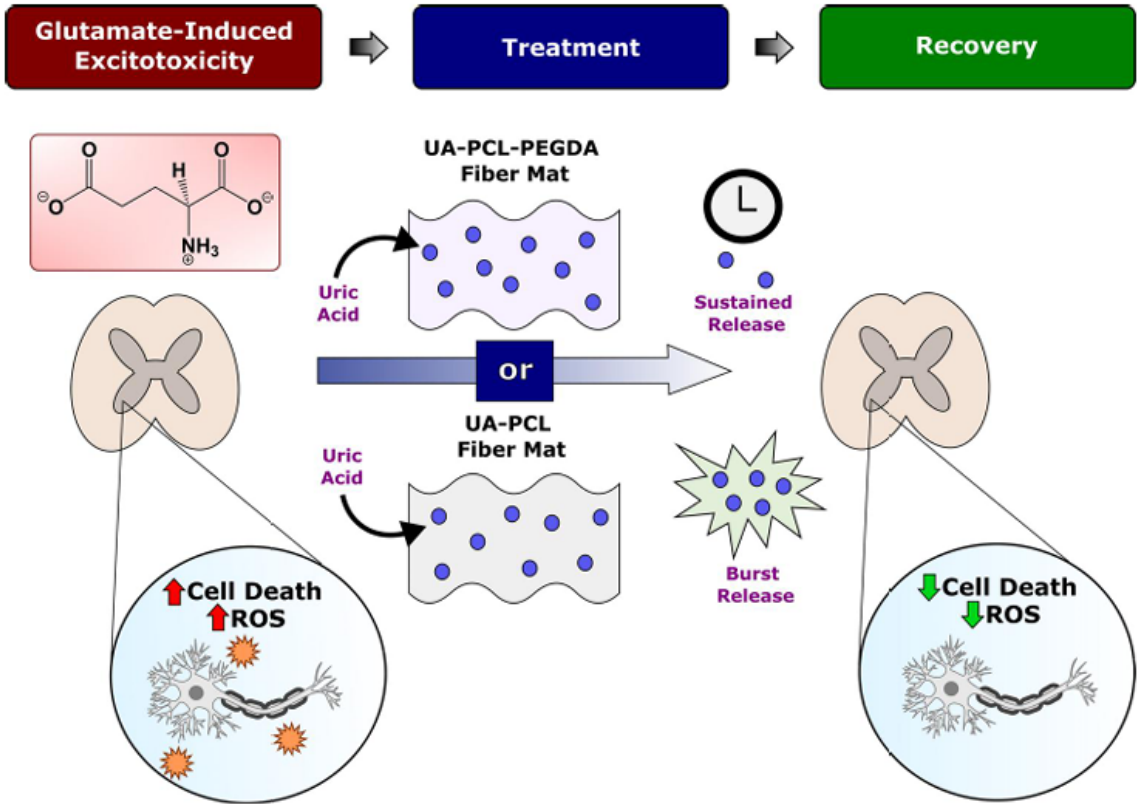

Figure 38. Model of the effects of UA fibers on secondary SCI. After the primary mechanical impact occurs during SCI and damages spinal cord tissue, GIE and secondary signaling cascades further exacerbate cell death, and ROS release both proximal to and distal to the lesion site. UA released from PCL fibers reduces cell death and ROS levels in spinal cord tissue subjected to GIE and represents a promising therapeutic platform for the treatment of SCI.

Notably, recent work continues to advance electrospun drug-delivery systems toward clinically relevant applications. For example, Ullrich et al. [65] developed a riluzole-releasing electrospun implant for spinal cord injury, demonstrating sustained local drug delivery and improved neuroprotective outcomes, As shown in Figure 39. Given that riluzole is a clinically investigated neuroprotective agent, this study highlights the translational potential of electrospinning-based delivery platforms and underscores that this research direction remains actively evolving.

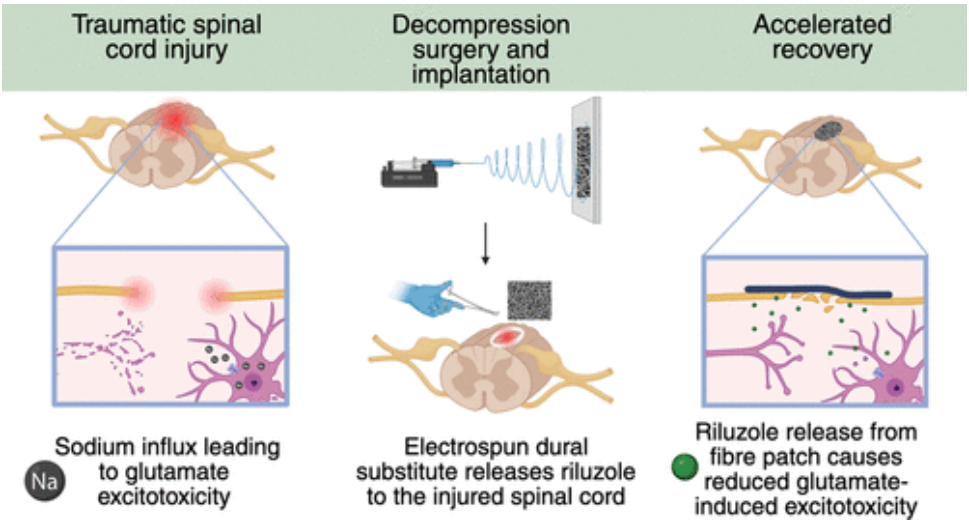

Figure 39. Schematic diagram of the neuroprotective mechanism of the electrospun riluzole delivery system in traumatic spinal cord injury.

Overall, while drug-loaded electrospun scaffolds have demonstrated clear therapeutic potential, a major limitation remains the lack of quantitative correlation between *in vitro* release behavior and *in vivo* therapeutic outcomes, as well as insufficient validation in chronic and clinically relevant SCI models.

4.2.2. Immune-Modulation & Anti-Inflammation

Recent advances have shifted attention from simple drug delivery to active regulation of the immune microenvironment, which plays a decisive role in SCI progression. Rather than merely suppressing inflammation, emerging strategies aim to reprogram immune responses toward a regenerative phenotype.

A representative breakthrough was reported by Xi et al. [99] who developed microenvironment-responsive immunoregulatory electrospun fibers that dynamically interact with the spinal cord injury microenvironment. In this system, the electrospun scaffold was engineered to respond to local pathological cues—such as inflammatory signals and oxidative stress—thereby enabling the controlled release of immunomodulatory factors in a stimuli-responsive manner. Mechanistically, the scaffold was designed to regulate macrophage polarization, shifting the balance from the pro-inflammatory M1 phenotype toward the pro-regenerative M2 phenotype, which is critical for creating a permissive environment for neural repair. As a result, the system not only reduced local inflammation but also promoted axonal regeneration and functional recovery *in vivo,* As shown in Figure 40. This work is particularly significant because it moves beyond passive or pre-programmed delivery systems and introduces the concept of adaptive biomaterials, in which therapeutic responses are dynamically tuned according to the evolving injury environment. However, the complexity of such responsive systems introduces challenges in reproducibility, precise control of responsiveness thresholds, and large-scale manufacturing, which may limit their translational potential.

From a pharmacological perspective, Liao et al. [78] prepared a multi-channel bioactive nanofiber catheter loaded with TUBA by dissolving TUBA in SF and mixing it with PGCL at a ratio of 5:5 using electrospinning technology, achieving controlled local release of TUBA over a long period of time. They constructed an MC/TUBA bioactive nanofiber catheter scaffold and induced SCI in T9-10 using a fully transverse large-span model. Compared with the SC/TUBA, SC, and SCI groups, local delivery of TUBA by MC/TUBA can significantly increase the number of nerve fibers, reduce glial scar formation, inhibit inflammation, reduce demyelination, and protect bladder tissue. Therefore, local administration of TUBA via MC/TUBA can effectively promote rehabilitation after SCI, As shown in Figure 41. In this case, precise anti-inflammatory effect was achieved at the level of “signal pathway + scaffold”, but to ensure the best efficacy in clinical application, TUBA dosage and carrier matching need to be further optimized.

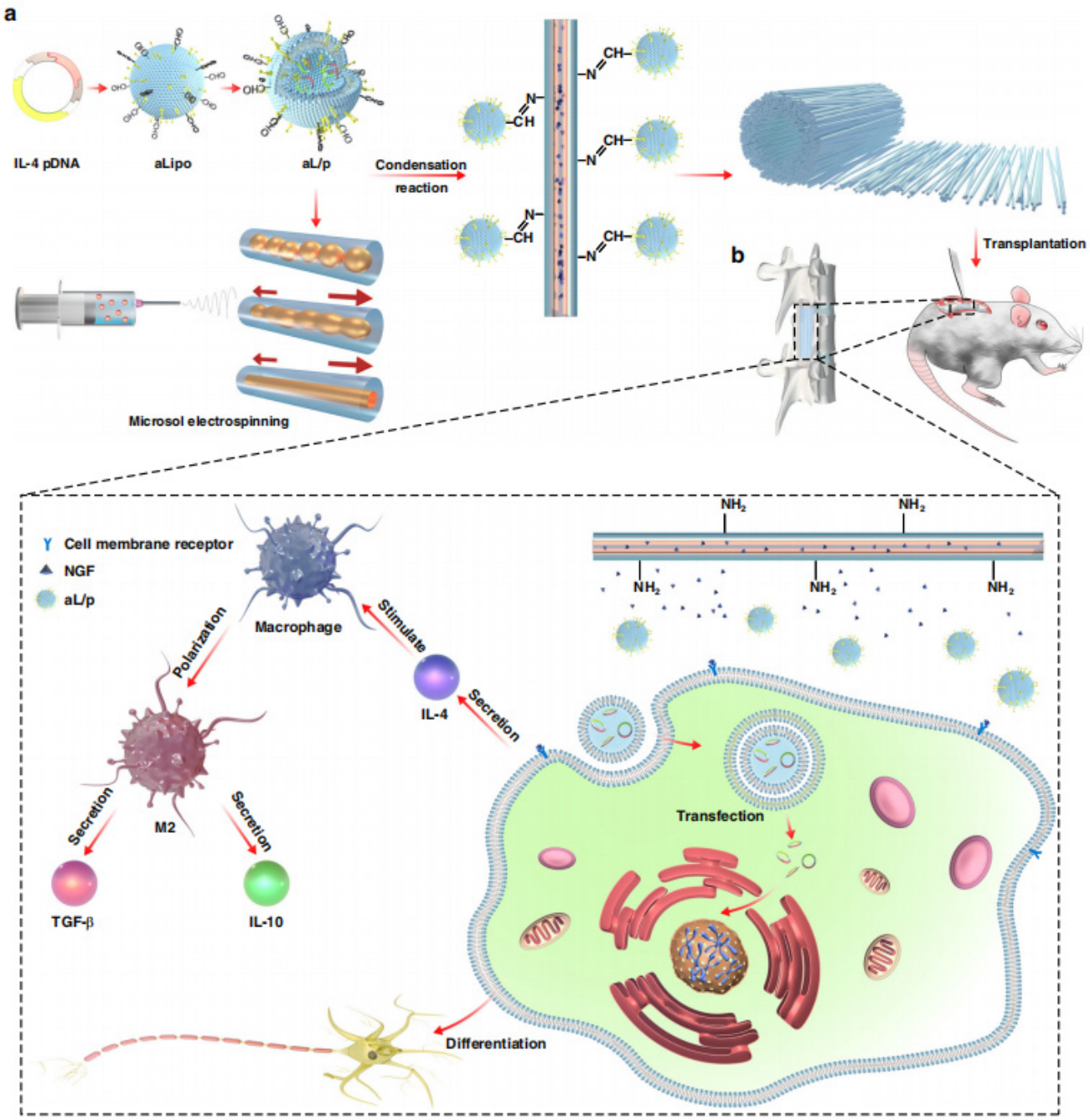

Figure 40. Construction and effect mechanism of composite fiber. Scheme illustration of (**a**) the construction of bioinspired composite scaffold for the treatment of spinal cord injury along with (**b**) its microenvironment-responsive immune regulation and nerve regeneration effect.

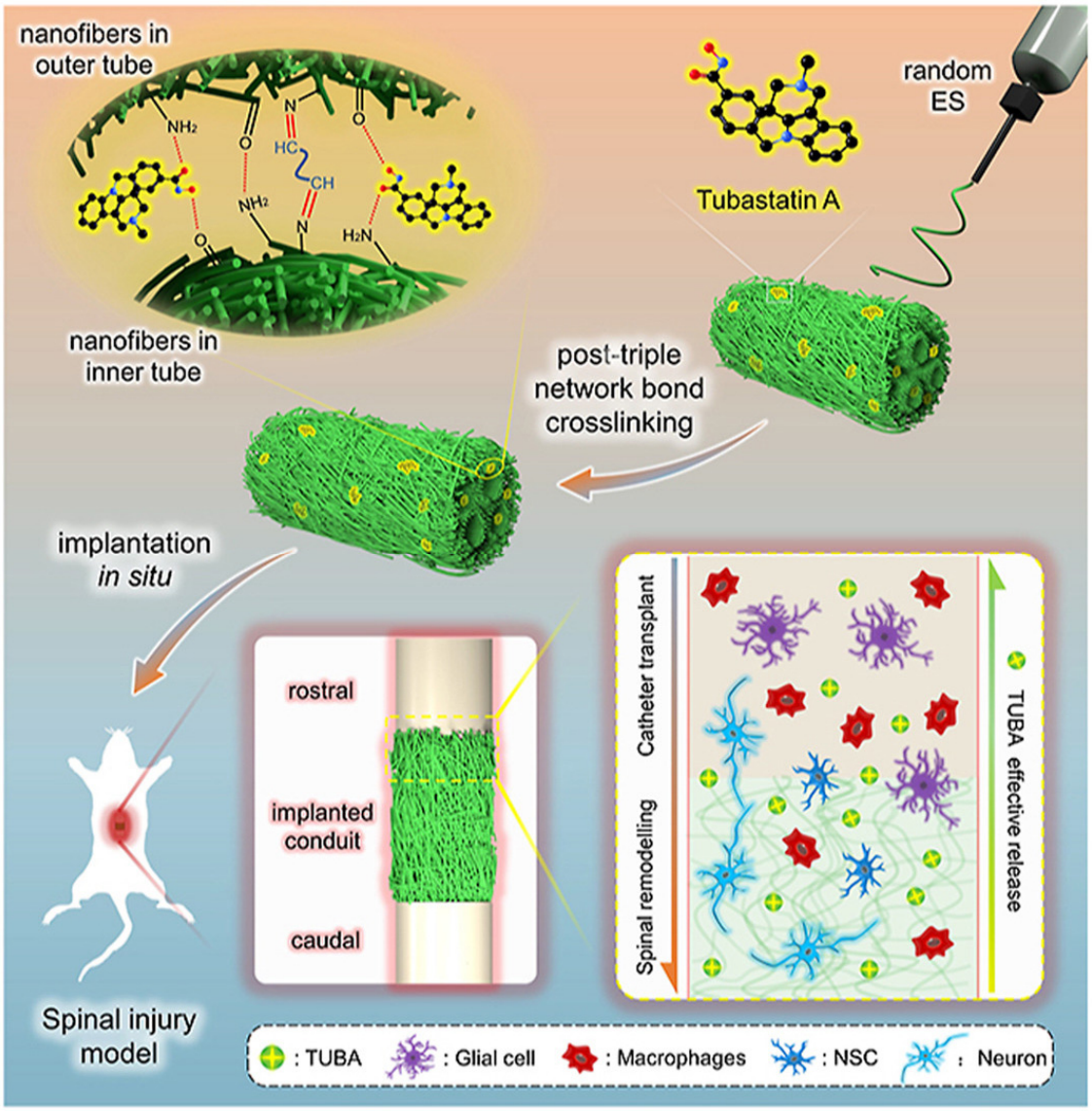

Figure 41. Schematic illustration of the preparation for the bionic multichannel nanofiber conduit carrying Tubastatin A (SC-TUBA(þ)) by random electrospinning and post-triple network bond crosslinking (amidation, Schiff based reaction, and hydrogen-bonding network densification) and its effective implantation in spinal injury model in rat.

In another innovative approach, Funnell et al. [100] designed magnetically responsive coaxial electrospun fibers for the controlled release of transforming growth factor beta 3 (TGFβ3), introducing an externally tunable system for regulating the spinal cord injury microenvironment. In this design, magnetic nanoparticles were incorporated into the coaxial fiber structure, enabling the release behavior of TGFβ3 to be modulated under an applied magnetic field. The core–shell architecture further facilitated sustained release, while the magnetic responsiveness provided an additional level of on-demand control over release kinetics. TGFβ3 was selected due to its known role in modulating astrocyte activity and reducing glial scar formation, which is a major inhibitory factor in SCI regeneration. As a result, the system demonstrated a reduction in astrocyte reactivity and a more permissive environment for neural repair, As shown in Figure 42. This work is particularly significant because it introduces the concept of externally controllable electrospun delivery systems, extending beyond passive and microenvironment-responsive platforms toward user-regulated therapeutic interventions. However, the reliance on external magnetic stimulation introduces practical challenges, including the need for precise field control, potential safety considerations, and increased complexity in clinical implementation, which may limit its translational feasibility.

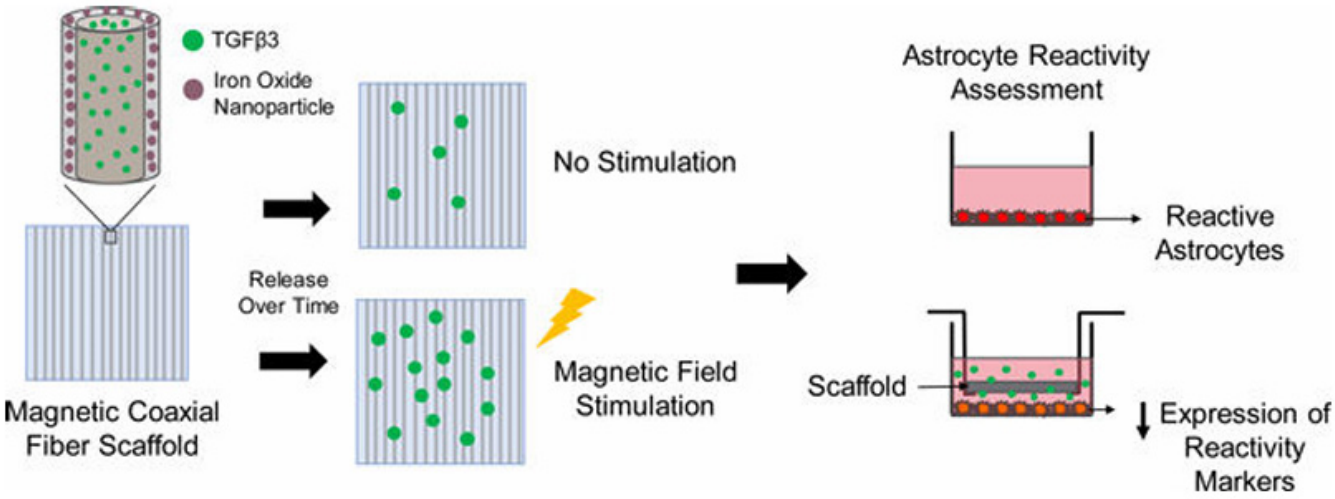

Figure 42. There is a need for treatments that restore function after spinal cord injury. Here, we fabricated magnetic core-shell fibers loaded with a growth factor that reduces spinal cord astrocyte reactivity. Magnetic field stimulation increased the release rate of the growth factor, which could be used in future studies to non-invasively tune delivery based on injury severity.

Extending this concept, Sun et al. [55] proposed a genetically engineered electrospinning strategy to regulate the immune microenvironment following spinal cord injury. In this approach, gene regulatory elements were incorporated into the electrospun scaffold to enable localized and sustained expression of therapeutic factors, thereby achieving gene-level modulation of the injury environment. Unlike conventional drug-loaded systems that rely on passive release, this strategy allows the scaffold to actively influence cellular behavior by inducing the expression of specific proteins associated with immunomodulation and tissue repair. Mechanistically, the system was shown to regulate key inflammatory pathways, including promoting macrophage polarization toward the pro-regenerative M2 phenotype while suppressing pro-inflammatory signaling, As shown in Figure 43. As a result, reduced inflammation, improved cellular compatibility, and enhanced regenerative outcomes were observed compared to non-genetically modified systems. This work is particularly significant as it advances electrospun scaffolds from passive or stimuli-responsive platforms toward active biological reprogramming systems, representing a new direction in scaffold design for SCI repair. However, the incorporation of gene delivery strategies also introduces important challenges, including potential safety concerns related to gene vectors, control over spatial and temporal expression levels, and uncertainties regarding long-term stability and clinical translation.

In addition, several studies—including those using dexamethasone-loaded or anti-inflammatory molecule-loaded electrospun scaffolds—have consistently shown reduced inflammatory markers and improved tissue response. While these works reinforce the importance of immunomodulation, they largely follow similar strategies and therefore serve as supporting validation rather than major conceptual advances.

Overall, immunomodulatory electrospun scaffolds represent a significant shift toward microenvironment engineering, but future studies must better establish causal links between immune regulation and long-term functional recovery, particularly in chronic SCI models.

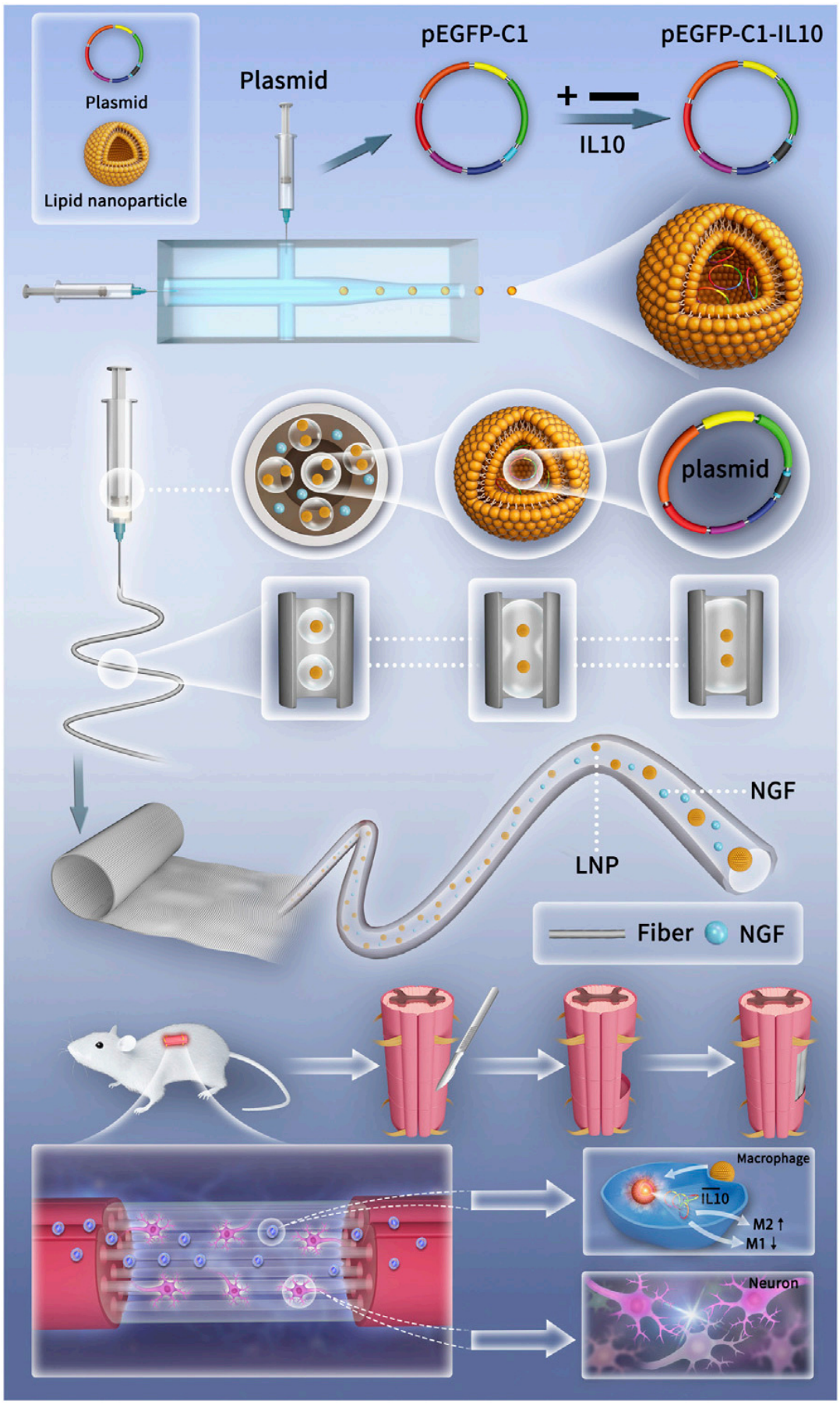

Figure 43. Schematicdiagramsofthepreparation of genetically engineered electrospun scaffolds and the mechanism of promoting SCI repair.

4.2.3. Coaxial Electrospinning

Coaxial electrospinning represents one of the most technically advanced approaches in biochemical functionalization, enabling the fabrication of core–shell structured fibers for improved cargo protection and controlled release. Its primary innovation lies in allowing spatiotemporal separation of multiple therapeutic agents, which is particularly relevant for the staged treatment requirements of SCI [101].

An early example of coaxial electrospinning for neural repair was provided by Reis et al. [102] who developed valproic acid (VPA)-loaded poly(lactic-co-glycolic acid) (PLGA) core–shell microfibers for central nervous system injury applications. In this system, the coaxial architecture enabled the encapsulation of VPA within a protective core, effectively improving the stability of the bioactive molecule and reducing premature degradation. At the same time, the surrounding shell layer acted as a diffusion barrier, allowing for a more controlled and sustained release profile, As shown in Figure 44. This study demonstrated that coaxial electrospinning can overcome key limitations of conventional electrospun systems—such as burst release and poor drug stability—thereby establishing it as a viable strategy for neural repair.

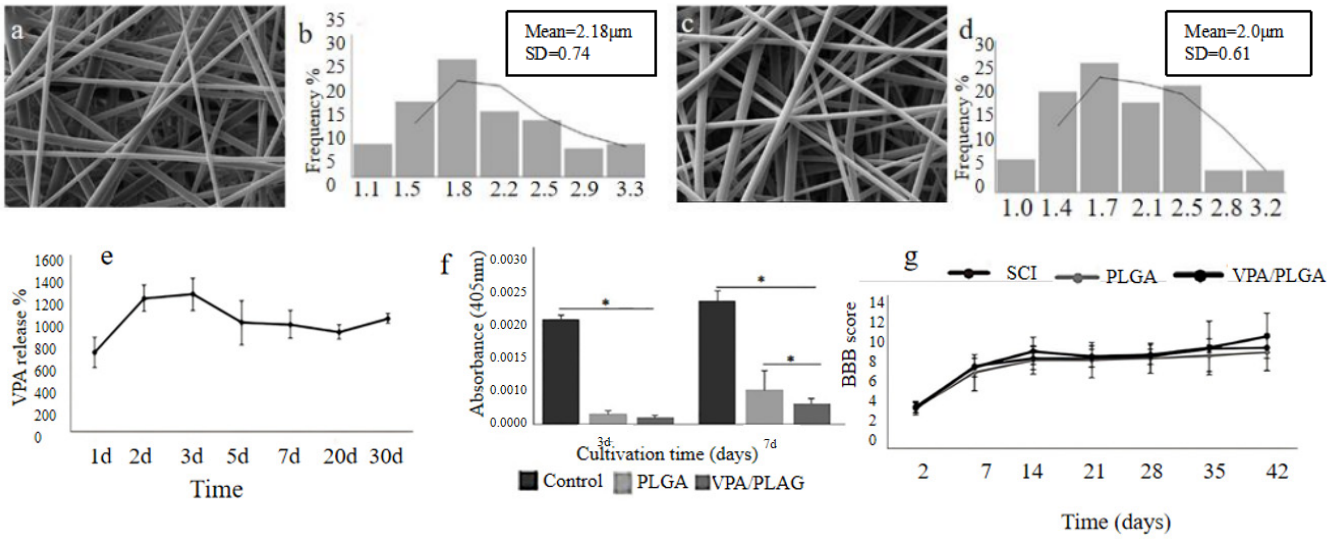

Figure 44. (**a**) PLGA coaxial electrospun fiber with an average diameter of 2.18 ± 0.74 μm; (**c**) VPA/PLGA coaxial microfibers with an average diameter of 2.0 ± 0.61 μm. Histogram of fiber diameter distribution: (**b**) PLGA; (**d**) VPA/PLGA. (**e**) Cumulative release curve of VPA from core-shell fiber determined by high performance liquid chromatography. (**f**) The viability of cells on PLGA and VPA/PLGA scaffolds was analyzed by WST-8 test. (**g**) Basso, Beatie and Bresnahan (BBB) open-field walking scores for the spinal cord injury (SCI, control), poly(lactic-co-glycolic acid) (PLGA), and valproic acid (VPA)/PLGA groups on the ipsilateral, lesioned side (n = 6 animals/group). Data are reported as means ± SD.* $p < 0.05$, one-way ANOVA.

A more structurally integrated strategy was demonstrated by Liu et al. [103] who developed aligned core–shell electrospun fibers capable of co-delivering docosahexaenoic acid (DHA) and BDNF. In this system, the core–shell architecture enabled spatial separation of the two bioactive agents, allowing for staged and sustained release profiles, while the aligned fiber structure provided directional guidance for axonal growth. DHA, incorporated primarily for its neuroprotective and anti-inflammatory properties, was shown to improve neuronal survival and modulate the injury microenvironment, whereas BDNF served as a potent neurotrophic factor, promoting neurite outgrowth and synaptic plasticity. By integrating these biochemical cues within an oriented fibrous scaffold, the study effectively coupled topographical guidance with controlled molecular signaling, resulting in enhanced neurite extension and improved regeneration outcomes compared to non-aligned or single-factor systems, As shown in Figure 45. This work is particularly significant because it advances the concept of spatiotemporal regulation in neural repair, in which the spatial organization of the scaffold and the temporal release of bioactive molecules are coordinated. However, the complexity of the

core–shell fabrication process introduces challenges in reproducibility and large-scale manufacturing, and precise control over release kinetics remains difficult to standardize across different experimental conditions.

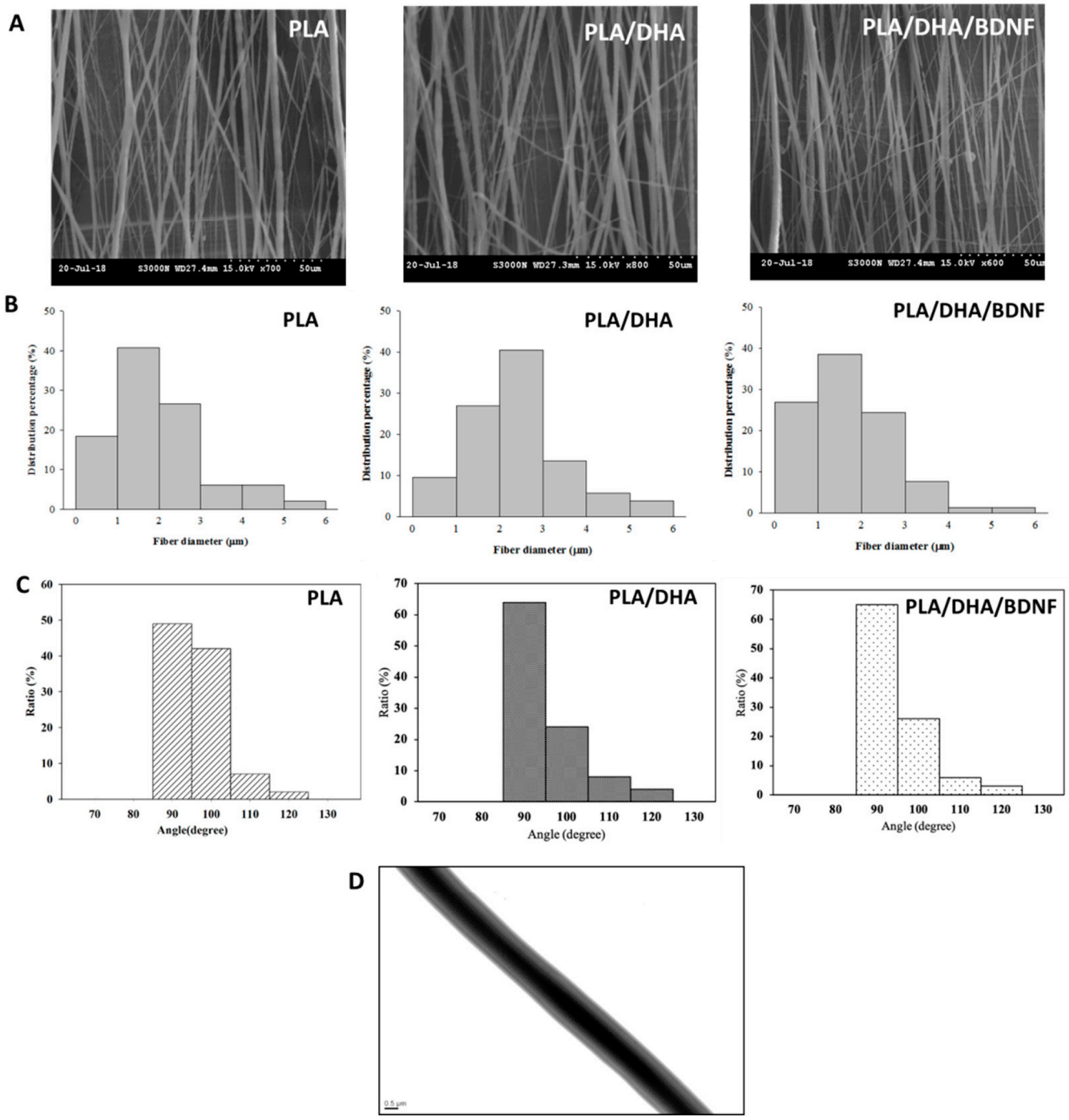

Figure 45. The SEM images (**A**), bar = 50 μm, the fiber diameter distribution (**B**), and the fiber angle distribution (**C**) of PLA, 777 PLA/DHA, and PLA/DHA/BDNF CSFMs. The TEM (**D**) bar = 0.5 μm, image of PLA/DHA/BDNF CSFMs.

Additional studies, including those using antioxidant or neuroprotective agents in core–shell fibers, further confirm the flexibility of this approach. However, these works generally follow similar design principles and therefore contribute primarily as technical extensions rather than fundamentally new concepts.

Despite its advantages, coaxial electrospinning faces significant challenges, including complexity in fabrication, reproducibility, and scalability. As a result, while it offers precise control over drug delivery, its practical application in clinical settings remains to be fully demonstrated.

4.2.4. Summary

In summary, biochemical functionalization has transformed electrospun scaffolds into multifunctional therapeutic systems for SCI repair. Key advances include sustained drug delivery (Xia et al. [71,95]), multifunctional scaffold integration (Zhang et al. [57]), immune microenvironment regulation (Xi et al. [99], Sun et al. [55]), and spatiotemporally controlled delivery via coaxial electrospinning (Liu et al. [103]). While many studies confirm the feasibility of these approaches, only a subset introduces true conceptual innovation, with others serving as important but incremental validations.

Future progress will depend on improving mechanistic understanding, long-term efficacy, and clinical translatability, particularly through studies that integrate structural design, biochemical function, and immune regulation into unified therapeutic strategies.

4.3. Multi-Component Composites

Cell-based strategies represent a critical advancement in electrospun scaffold design for SCI, as they directly address the limited intrinsic regenerative capacity of the central nervous system. While electrospun scaffolds can provide structural guidance and localized biochemical cues, they are inherently unable to replace lost neurons or glial cells, nor can they actively participate in tissue remodeling. Therefore, the incorporation of exogenous cells or modulation of endogenous cell behavior has emerged as an essential strategy for achieving functional recovery.

However, effective implementation of cell-based therapies in SCI remains challenging. The post-injury microenvironment is characterized by inflammation, inhibitory extracellular matrix components, and glial scar formation, all of which severely limit cell survival, differentiation, and integration. As a result, successful therapeutic strategies must not only deliver cells but also provide a supportive niche that enables long-term functionality.

4.3.1. Structural Regulation of Cell Behavior

An important early breakthrough in this field was the recognition that electrospun fiber architecture can directly regulate neural cell behavior. Rather than acting as passive substrates, electrospun scaffolds can provide topographical cues that guide cell alignment and neurite extension, which is essential for re-establishing neural connectivity across lesion sites.

For instance, Xie et al. [104] have demonstrated that neurite outgrowth can be strongly guided along aligned electrospun nanofibers, establishing a direct correlation between fiber orientation and axonal growth direction. This guidance effect is largely attributed to contact guidance, whereby aligned nanofibers provide topographical cues that influence cell adhesion and cytoskeletal organization, thereby directing neurite extension along the fiber axis. This finding is particularly significant in the context of SCI, where disorganized axonal regeneration remains a major barrier to functional recovery, As shown in Figure 46. By providing directional guidance and mimicking the anisotropic architecture of native neural tissue, aligned electrospun scaffolds can bridge lesion gaps and promote oriented axonal regrowth, ultimately facilitating organized neural reconnection.

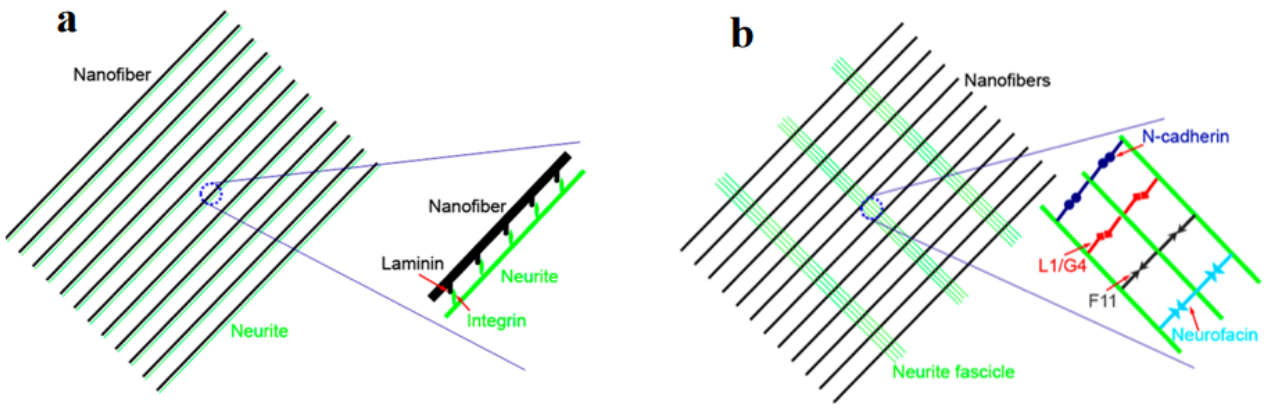

Figure 46. A strong interaction between neurites and nano-fibers could lead to parallel growth of neurites along the fibers, while those neurites that interacted with fibers poorly showed perpendicular growth. Schematic illustration of two different modes of neurite outgrowth on uniaxially aligned nanofibers: (**a**) parallel growth, and (**b**) perpendicular growth.

Building on this concept, Yao et al. [105] further demonstrated that matrix elasticity, when combined with aligned fiber topography, can synergistically regulate stem cell fate. This effect is believed to be mediated by mechanotransduction pathways, in which cells sense and respond to both substrate stiffness and topographical cues via integrin-mediated adhesion and cytoskeletal tension. The coordinated regulation of these mechanical and structural signals enables cells to reorganize their cytoskeleton and activate downstream signaling pathways, ultimately directing lineage specification, As shown in Figure 47. This work represents an important conceptual advance, moving beyond structural guidance toward mechanobiological regulation and highlighting that both mechanical properties and fiber alignment jointly influence cell differentiation. Such insights are critical for designing scaffolds that can actively direct cell behavior rather than support it.

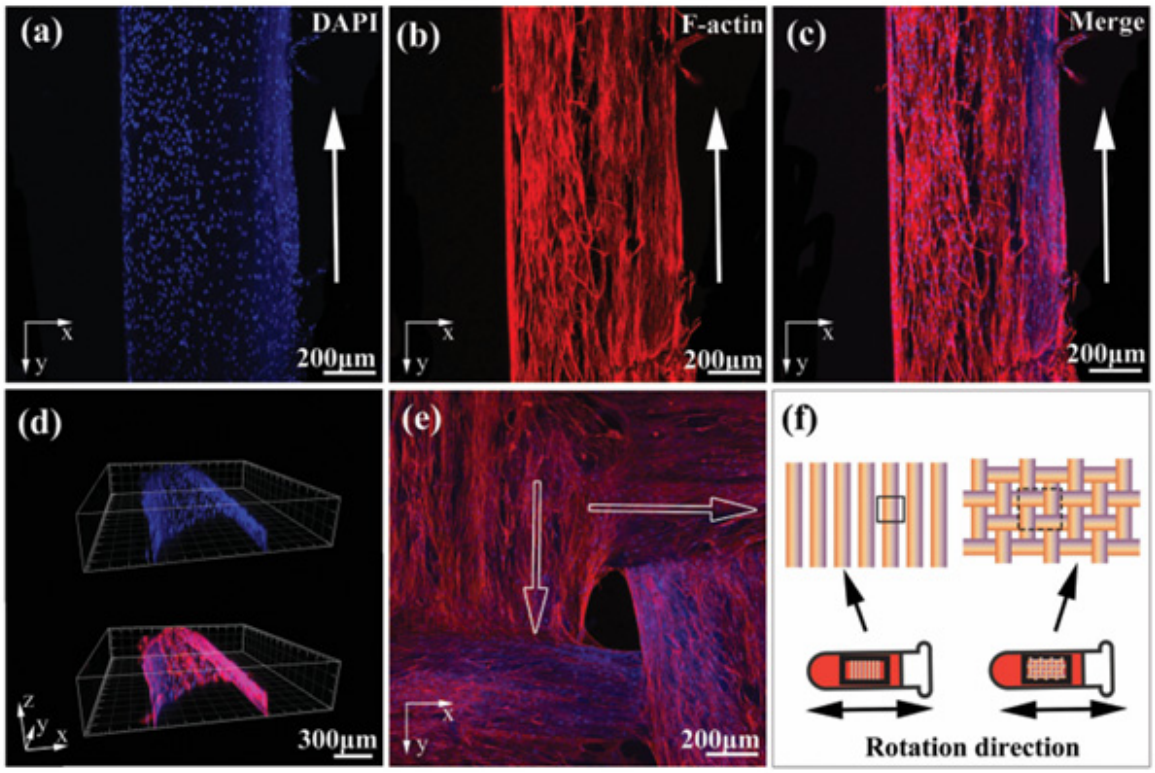

Figure 47. Aligned cell cable formation by hUMsCs attached along aligned fibrin hydrogel microfibers *in vitro*. Fluorescent confocal images of hUMSCs seeded onaligned fibrin hydrogel microfibers after 7 days of culture. (**a**) Fluorescent DAPInuclei

staining, (**b**) rhodamine-phalloid in F-actin staining. and (**c**) merged images (**a**) + (**b**). (**d**) Reconstructed image of the cross-section of AFG microfibers. (**e**) Fluorescent confocal images of hUMSCs seeded on plain fibrin fabric with DAPl nuclei and rhodamine-phalloidin F-acting staining after 7 days of culture. (**f**) Schematic diagram showing the rotation direction during cel seeding on the aligned fibrin hydrogel microfibers and plain fibrin fabric. White arrows indicate the long axis of AFG microfibers.

Earlier work by Xie et al. [50] also demonstrated that embryonic stem cells cultured on electrospun nanofibers can undergo lineage-specific differentiation, providing foundational evidence that electrospun scaffolds can function as cell-instructive microenvironments. This instructive effect is likely mediated by the interplay of biochemical and biophysical cues presented by the nanofibrous architecture, which can modulate cell–material interactions and activate intracellular signaling pathways associated with lineage commitment, As shown in Figure 48. Together, these studies establish that electrospun scaffolds are not merely structural supports, but active regulators of cellular behavior that can dynamically influence cell fate decisions.

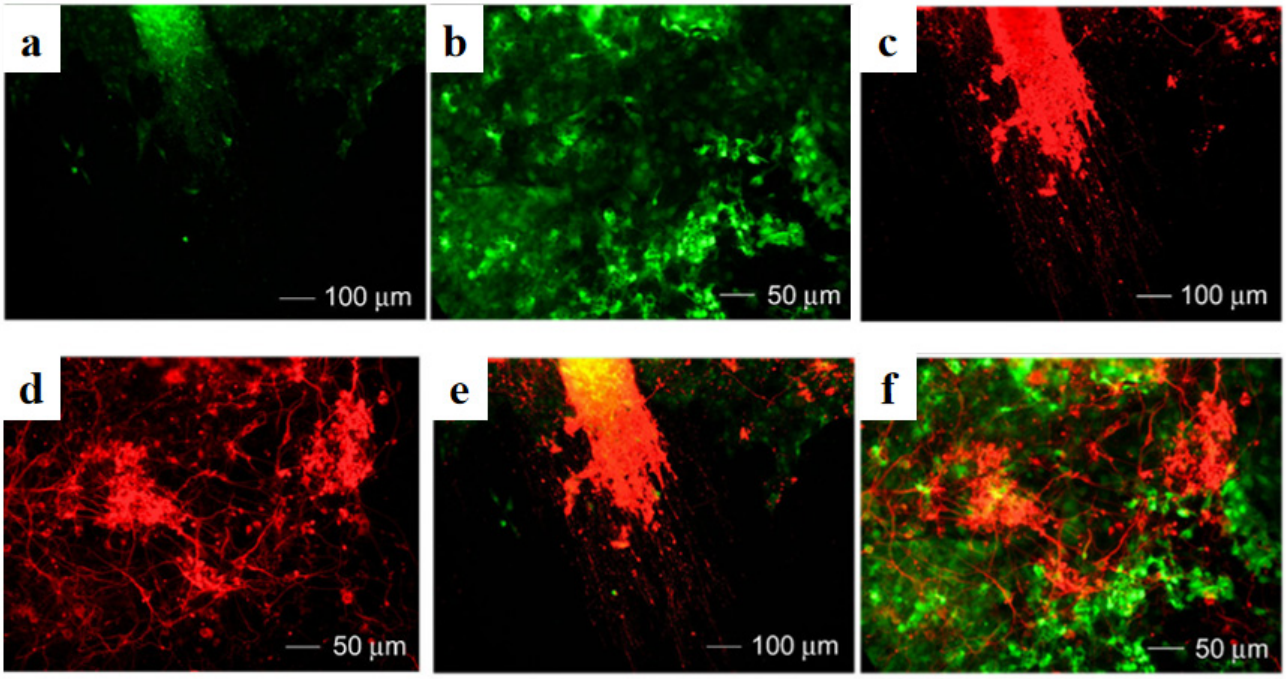

Figure 48. Neuronal differentiation of CE3 cells seeded on (**a**,**c**,**e**) aligned and (**b**,**d**,**f**) random PCL nanofibers directly without forming EBs induced by retinoic acid using 4−/4+ and incubated with neurobasal medium with B27 as a supplement for 14 days. (**a**,**b**) Fluorescence micrographs of CE3 cells. (**c**,**d**) Neuron marker Tujl staining of the same regions as in (**a**,**b**). (**e**) A superimposed image of (**a**,**c**). (**f**) A superimposed image of (**b**,**d**).

Recent studies have further advanced electrospun systems toward multifunctional platforms that integrate sustained drug delivery with structural and cellular regulation. Song et al. [106] found that PLGA loaded microspheres had the best morphology at a concentration of 7 wt% and a water-oil ratio of 1:200. The drug release time was up to 14 days with a final release rate of about 60%. These microspheres maintained drug activity and were non-toxic. Oil-soluble PLGA microspheres were easily prepared and exhibited good drug release performance. They can be used for SCI repair and treatment when combined with other biomaterials. The team also studied a sandwich structure prepared by electrospinning and electrostatic spray for long-term controlled drug release. The NGF-PLGA/P407/P188/SA composite gel was temperature-sensitive, injectable, and achieved long-term sustained drug release, As shown in Figure 49. It was non-toxic in cell co-culture and induced PC-12 cell differentiation into neurons, showing potential in neural repair. Xu et al. established a benchmark for PLGA microsphere optimization, but the current study

advances this paradigm by engineering a multifunctional, long-acting composite scaffold. This work not only extends the duration of drug release but also integrates cell therapy and structural guidance.

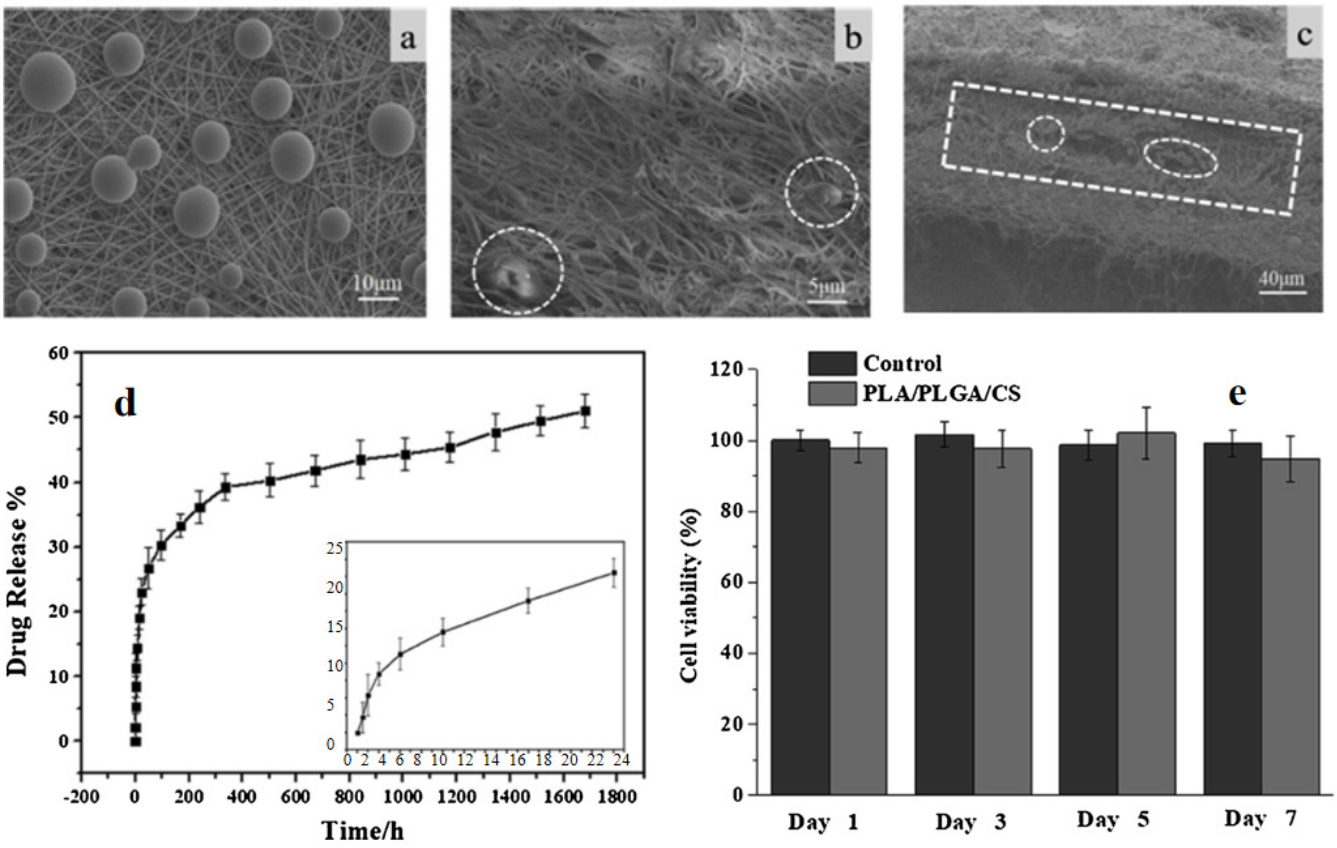

Figure 49. (**a**) SEM images of the NGF-PLGA microspheres on the surface of PLA membrane; (**b**,**c**) cross section of the sandwich composite membrane. (**d**) NGF release plot from PLA/NGF-PLGA/CS composite membrane; (**e**) Cytotoxicity of PLA/PLGA/CS composite membrane *in vitro*. Dashed rectangular box: focusing on the observation range of specific structural interactions or distribution patterns; Dashed circle: used to mark "discrete feature units" (such as particles, pores, defects, *etc.*), highlighting individual objects that require detailed analysis.

Extending beyond delivery-focused strategies, recent efforts have also emphasized microenvironment-responsive scaffold design to actively regulate oxidative stress and cellular behavior. Zhu et al. [107] studied the use of hydrogel surface grafting and microsol electrospinning technology to construct a composite biomimetic stent, which has the dual regulation function of "exogenous-endogenous" ROS. The outer hydrogel enhances local autophagy by degradation and release of rapamycin, neutralizing and inhibiting ROS production, and reducing neuronal apoptosis. Internal fibers provide brain-derived neurotrophic factors that guide axonal growth. *In vitro* experiments showed that the scaffold doubled neuronal autophagy levels, reduced apoptosis, and increased neural stem cell differentiation. *In vivo* experiments have shown that stents reduce ROS levels and scarring. RNA sequencing showed scaffold up-regulation of associated proteins and genes, As shown in Figure 50. This stent represents a therapeutic strategy to achieve neurological recovery. Zhu et al. innovations have been made in "mechanical gradient + fiber orientation", but more sophisticated gradient design tools and long-term mechanical characterization are needed for large-scale applications.

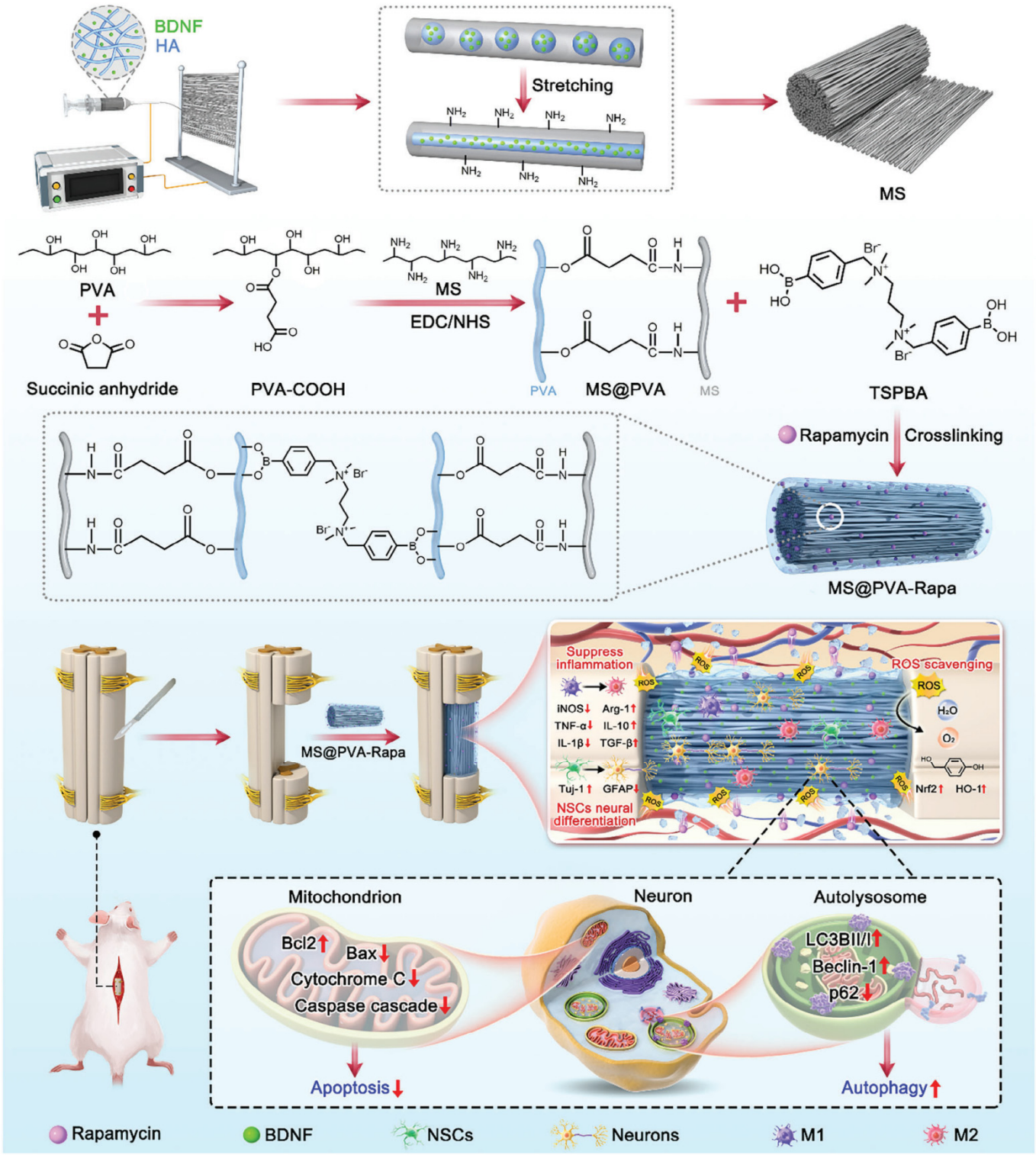

Figure 50. The schematic illustration shows the construction process of the compositefibers and the mechanism for precise regulation of the ROS cascade reaction to promote nerve regeneration after implantation at the injured site.

4.3.2. Scaffold-Assisted Cell Delivery and Retention

A major advancement in this field is the integration of cell delivery with electrospun scaffold systems. Direct injection of therapeutic cells into the injury site typically results in poor cell survival and rapid dispersion due to the hostile microenvironment. In contrast, electrospun scaffolds can serve as protective niches, enhancing cell retention, survival, and functional integration. Carlson et al. [108] demonstrated that

stem cells seeded on electrospun nanofibers exhibit improved adhesion, proliferation, and viability compared to conventional culture systems. This enhancement is largely attributed to the ability of electrospun fibers to recapitulate key structural features of the native extracellular matrix, thereby facilitating integrin-mediated cell–matrix interactions and promoting focal adhesion formation. Such interactions can activate downstream signaling pathways that regulate cytoskeletal organization and cell survival. This highlights the importance of scaffold-mediated microenvironment stabilization in supporting cell-based therapies, As shown in Figure 51. By providing a physical substrate that mimics aspects of the extracellular matrix, electrospun fibers help maintain cell localization and prevent cell loss from the injury site, ultimately improving the efficiency of tissue repair strategies.

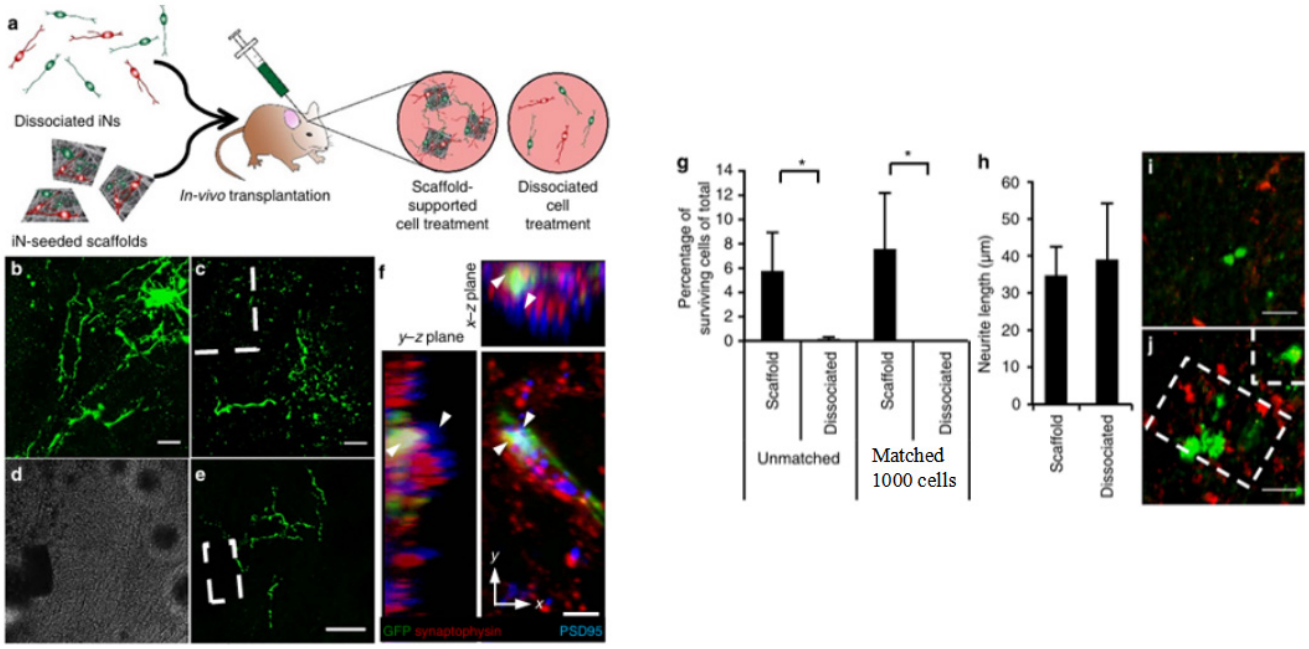

Figure 51. Scaffold-supported induced neurons (iNs) promote axonal growth and survival *in vivo*. (**a**) Schematic diagram of experimental design. (**b**) Survival status of dispersedly transplanted iNs. (**c**–**e**) Survival status of scaffold-transplanted iNs. (**f**) Evidence of synaptic integration. Multi color microstructure observation (white arrows indicate key areas): Localization of specific cellular or subcellular structures in biological/medical research (**g**) Quantitative analysis of survival rate. (**h**) Comparison of neuronal protrusion length. (**i**) Survival status of dispersed transplantation. (**j**) Cell preservation in scaffold co-transplantation. * $p < 0.05$ by one-way ANOVA, all error bars presented as mean±1 s.d. There was no significant difference in neurite length between the two modes of transplanted cells.

A more clinically relevant advance was reported by Koffler et al. [109] who developed biomimetic scaffolds capable of supporting cellular infiltration and integration in SCI models. The key innovation of this work lies in integrating a precisely engineered structural architecture with favorable biological properties, thereby creating a permissive microenvironment that supports host cell infiltration and tissue integration. In particular, the scaffold architecture can provide physical guidance cues that facilitate axonal extension and cellular migration across lesion gaps, thereby enhancing organized tissue regeneration. This study represents a significant step toward translational application, demonstrating that engineered scaffolds can support both structural repair and functional recovery *in vivo*, thereby bridging the gap between experimental design and clinical relevance, As shown in Figure 52.

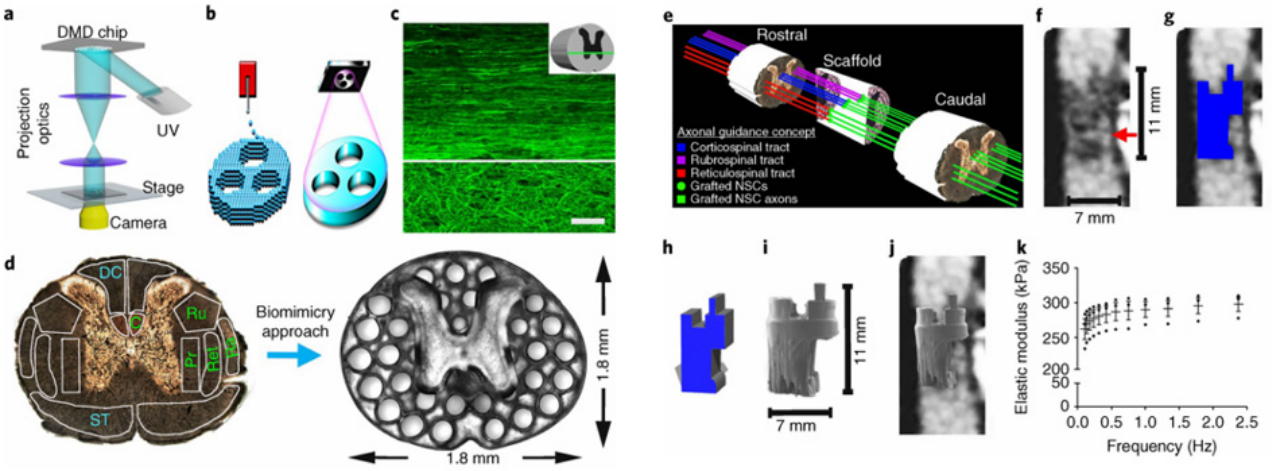

Figure 52. 3D-printed scaffold mimicking spinal cord structure. (**a**) Composition of 3D printing system; (**b**) Layered *vs*. non-layered printing principles; (**c**) Normal spinal cord axonal structure; (**d**) Spinal cord functional zoning and scaffold design; (**e**) Axonal alignment and guidance hypothesis; (**f**) Clinical imaging of human spinal cord injury; (**g**) Contour tracing of lesion cavity; (**h**) Computer-aided design model of scaffold; (**i**) Printed scaffold; (**j**) Hypothetical fit of scaffold *in vivo*; (**k**) Mechanical property testing of scaffold.

Recent advances have further pushed electrospun scaffolds toward highly integrated platforms that combine structural guidance with gene delivery, cell transplantation, and microenvironmental regulation. Zhang et al. [59] found a 3D fiber hydrogel scaffold that can be directly implanted into rats with spinal cord transection. The scaffold is composed of oriented electrospun fibers (providing topographic clues to guide axonal regeneration) and collagen matrix (achieving sustained delivery of miRNAs). Axon miRNAs (*i.e.*, miR-132/miR-222/miR-431 combination) treatment significantly enhanced axonal regeneration. When used in combination with the anti-inflammatory drug methylprednisolone, it synergistically enhances functional recovery, reduces pro-inflammatory gene expression, and enhances extracellular matrix deposition related gene expression. Increasing the dose of Axon miRNAs in combination with methylprednisolone significantly promotes functional recovery and myelin regeneration, As shown in Figure 53. Therefore, the combination therapy of stent mediated Axon miR and methylprednisolone is a promising treatment for spinal cord injury.

In parallel, efforts to incorporate external or stimulus-responsive regulation have introduced additional layers of control over scaffold function. Vashisth et al. [110] developed patterned hybrid nanofiber scaffolds (HANFs) via electrospinning using anisotropic nanofibers (ANFs) embedded in a biocompatible gelatin hydrogel matrix. The ANF rings provided structural reinforcement and directional guidance for neural cell adhesion and growth, while quercetin-functionalized nanofibers delivered sustained neurotrophic support. The cylindrical conduit architecture exhibited enhanced mechanical stability, promoting axonal alignment and outgrowth *in vitro* without cytotoxicity. The dual-mode "photothermal-growth factor" regulation system demonstrated spatiotemporal control over neural regeneration, As shown in Figure 54. However, clinical translation requires addressing the limitations of photothermal penetration depth and the long-term biocompatibility of ANF-derived nanosheets.

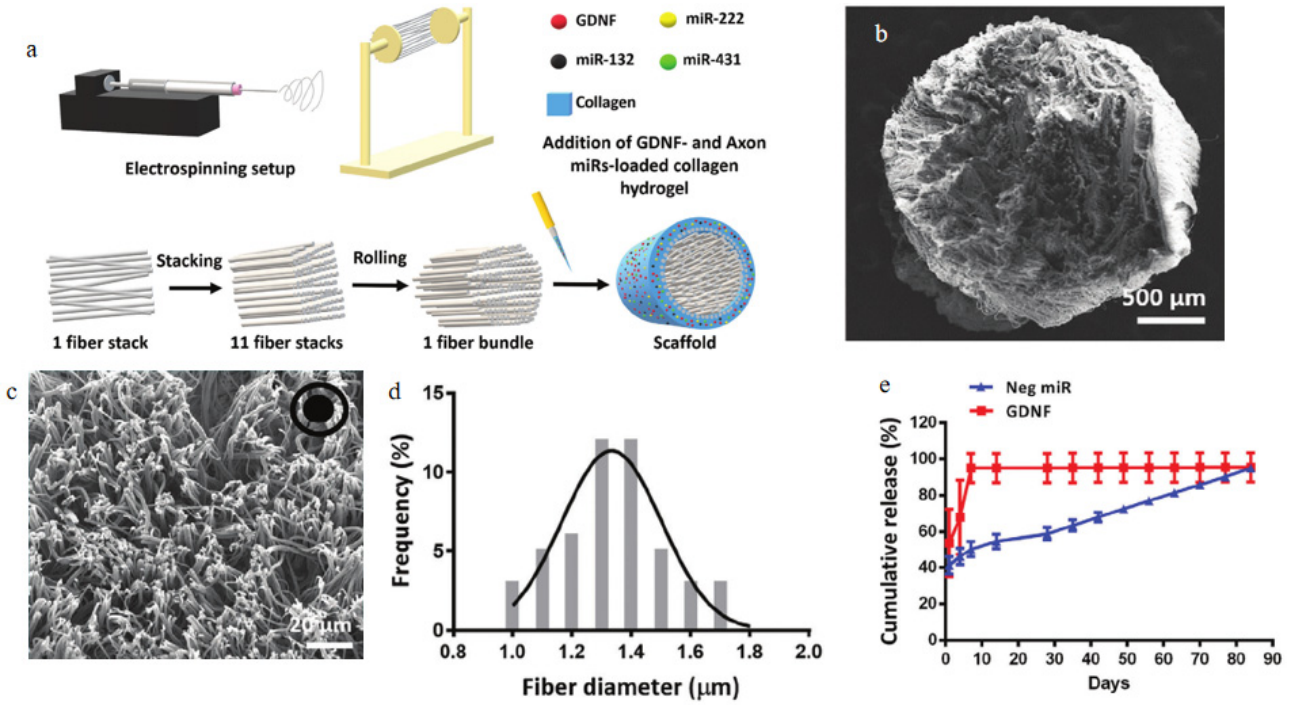

Figure 53. Fiber-hydrogel scaffold was successfully fabricated. (**a**) Scaffold fabrication schematic diagram. (**b**–**d**) Image of the entire scaffold and highmagnification of PCL electrospunfibers. (**e**) Cumulative release of Neg miR and GDNF over time 4.8 h in combination with cell therapy.

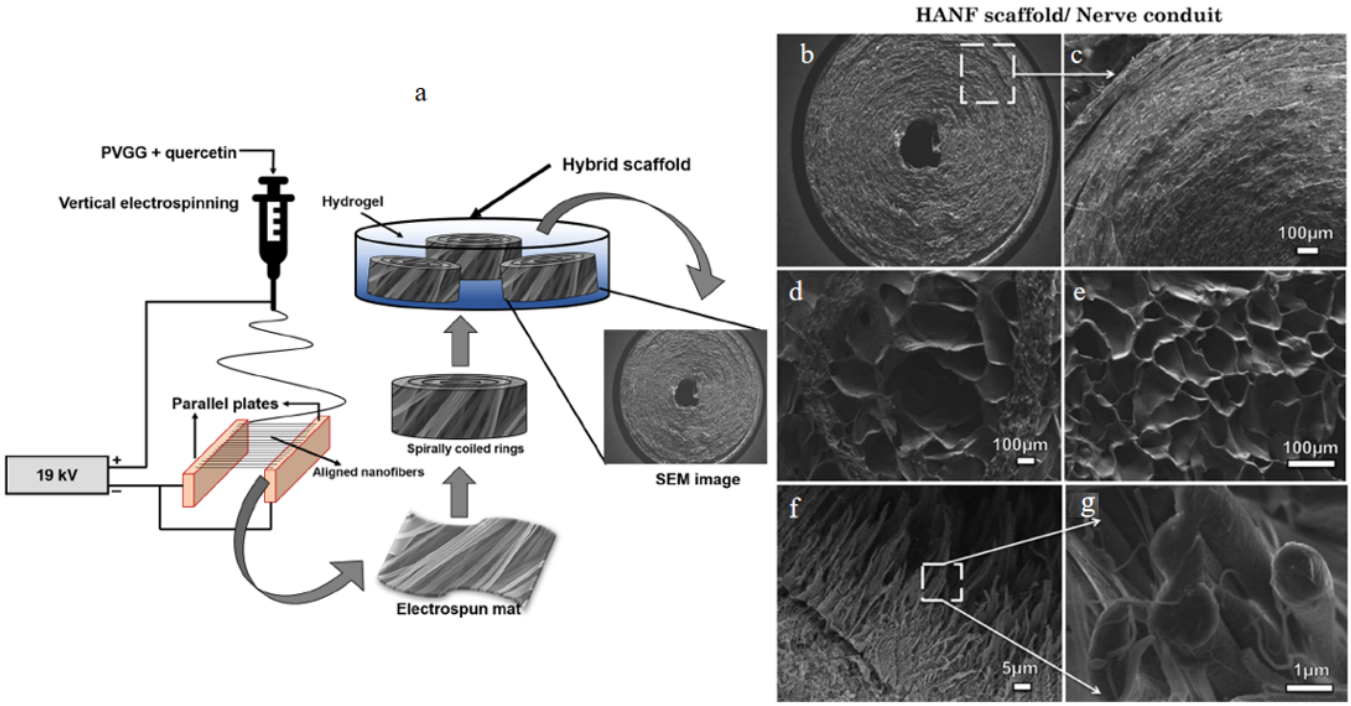

Figure 54. (**a**) Schematic of the fabrication process for biomimetic circular conduit (HANF) or neural tissue regeneration. (**b**,**c**) Micrographs of cross-sectioned ANF circular conduit, (**d**) HANF, (**e**) hydrogel, and (**f**,**g**) ANFs.

Beyond biochemical and external regulation, the integration of living cells into electrospun scaffolds represents another critical direction. Lee et al. [111] studied the feasibility of an electrospun PVDF-Trifluoroethylene (TrFE) catheter combined with Schwann cells (SCs) transplantation for repair of spinal cord transection injury using a full cross-sectional model. The PVDF TrFE catheter has good biocompatibility and potential piezoelectricity. Meanwhile, the catheter supports the survival and axonal

regeneration of SCs. Experiments found that directional catheters are more effective at promoting uniform distribution of SCs and directional axonal growth than random catheters. The processes of astrocytes (GFAP+) can cross the spinal cord/SC bridging interface, co localize with SCs, and promote axonal regeneration, As shown in Figure 55. And specific types of axons, such as noradrenergic dopamine-beta-hydroxylase (DβH+) and calcitonin gene-related peptide (CGRP+) axons, can regenerate in the conduit and cross the interface into the SCs bridge. This study marks the inaugural demonstration of the potential utility of electrospun PVDF-TrFE aligned fiber conduits for repairing spinal cords using SCs.

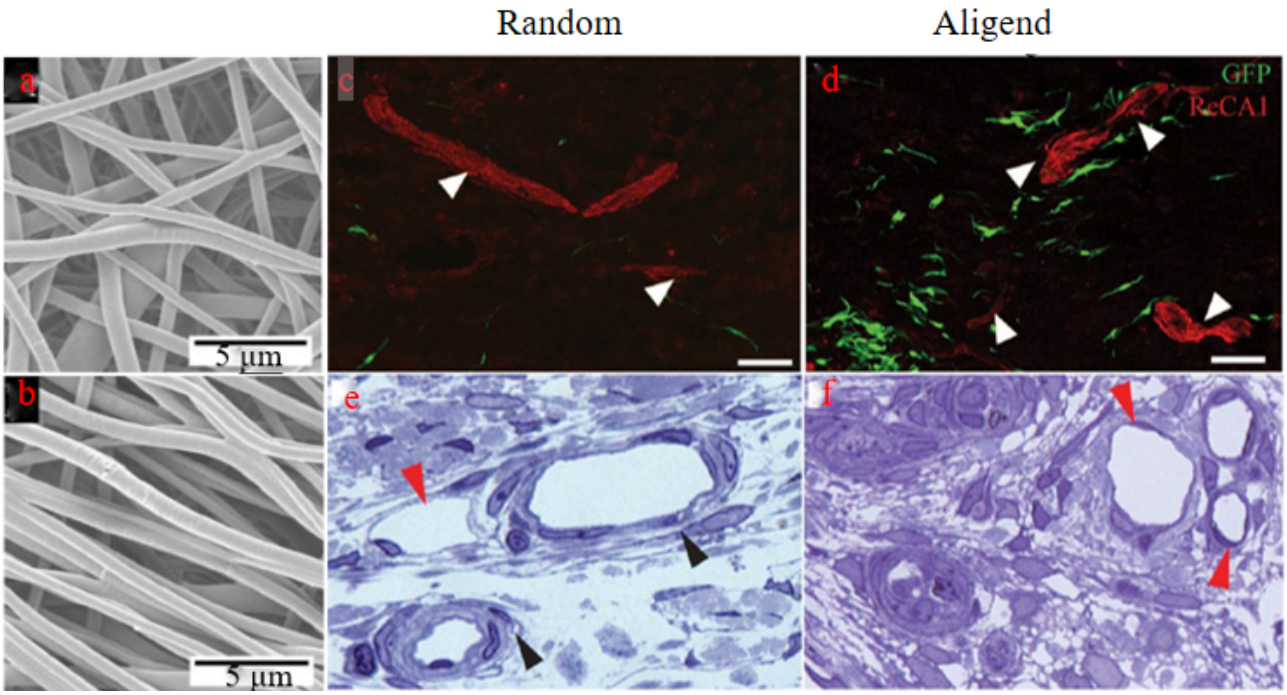

Figure 55. Fiber morphology diagram of (**a**) PVDF, (**b**) TrFE stent(10,000x). Blood vessels in the mid-bridge regions, immunostained with anti-ReCA1 antibody, were observed in both random (**c**) and aligned (**d**) conduits (white arrowheads) (confocal fluorescence images, scale bars: 50 mm). Venules (red arrowheads) and arterioles (black arrowheads) vessels were observed in the mid-bridge region in random (**e**) andaligned (**f**) conduits (1 mm plastic sections, toluidine blue stain, 60x).

Pushing integration even further, stem cell–laden electrospun systems have been developed to simultaneously regulate inflammation, cell differentiation, and tissue reconstruction. Xu et al. [112] investigated the use of micro-alcohol electrospinning and collagen assembly techniques to construct an oriented active fiber bundle loaded with BMSC. A directional active fiber scaffold can leverage the advantages of stem cells in the early period of SCI to regulate the local inflammatory microenvironment and further influence stem cell differentiation. At the same time, it can continuously release BDNF and promote neuronal regeneration by up-regulation of neurotransmitter related genes (e.g., Tuj-1, NF-200). Furthermore, the electrospun fibers of the fiber bundle have the main characteristics of a natural extracellular matrix, capable of uniformly and efficiently loading growth factors and stem cells, As shown in Figure 56. It simulates the three-dimensional structure of the central nervous system, accurately controls the spatial arrangement of stem cells, guides axonal connections, and fills gaps in the spinal cord. *In vivo* induction of fiber bundles by stem cells provides a novel method for the treatment of SCI.

Collectively, these studies illustrate a shift from simple cell transplantation to integrated scaffold–cell therapeutic systems, in which the scaffold actively enhances the effectiveness of cell-based interventions.

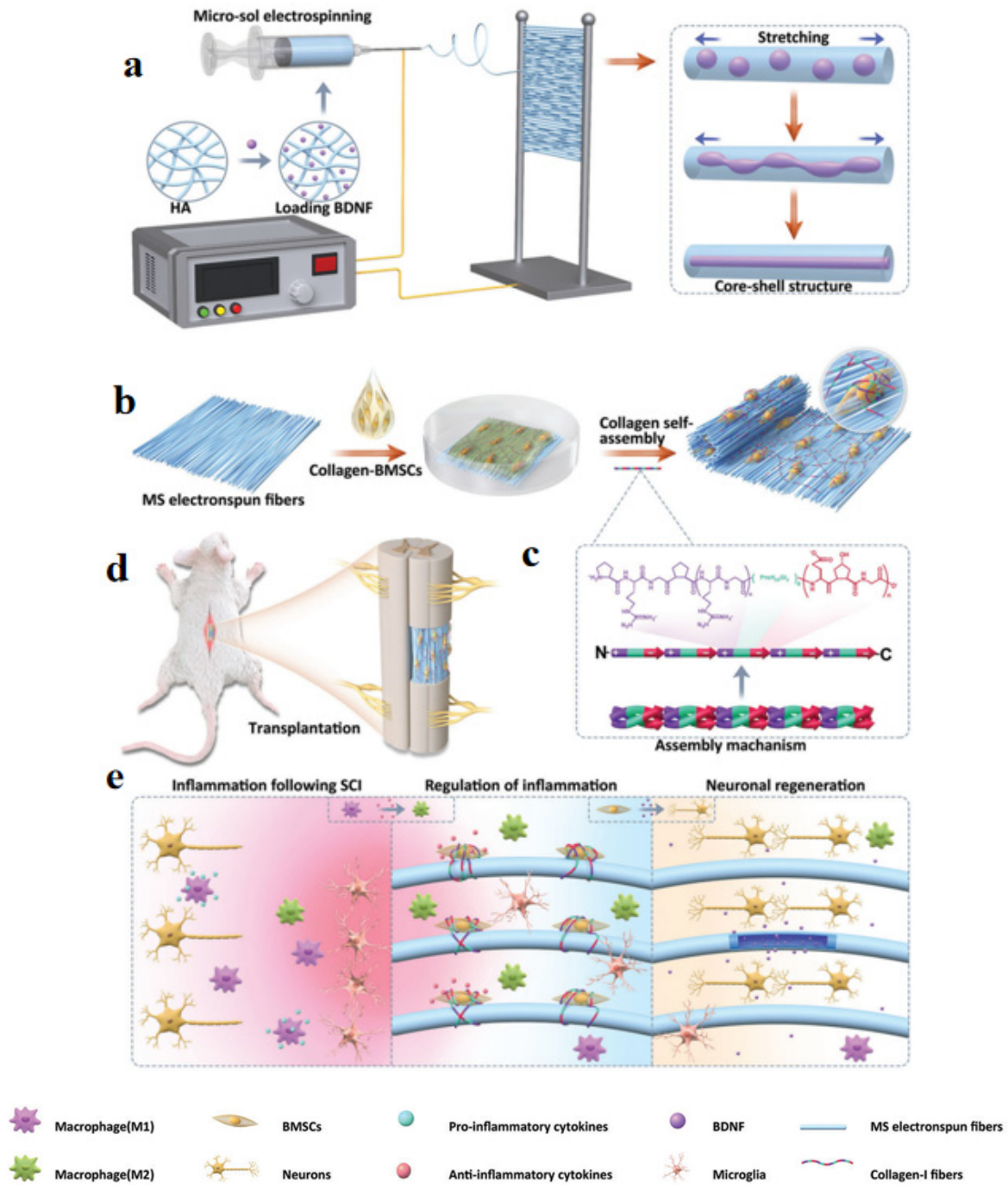

Figure 56. Schematic illustration. (**a**) The building process of the stem cell engineered living oriented electrospun fibers. (**b**) The illustration of the assembly mechanism. (**c**) Construction of a spinal cord hemisection model. (**d**) Mechanism of scaffolds in different periods after spinal cord injury. (**e**) Mechanism of scaffolds in different periods after SCI.

4.3.3. Regulation of the Cell–Material Microenvironment

Beyond delivery and structural guidance, regulating the interaction between transplanted cells and the injury microenvironment has emerged as a critical factor in SCI repair. The lesion site is highly inhibitory, with factors such as glial scar formation and inflammatory signaling limiting regenerative outcomes. Therefore, effective scaffolds must not only host cells but also modulate the surrounding microenvironment.

A growing body of work highlights that effective spinal cord repair requires not only structural support or cell delivery, but precise regulation of the cell–material microenvironment. Zuidema et al. [113] highlighted that biomaterials can influence glial scar formation and astrocyte behavior, which are key

barriers to regeneration in SCI. Their work suggests that the physicochemical properties of biomaterials can modulate astrocyte activation and inflammatory responses, thereby regulating the extent of extracellular matrix deposition and glial scar formation at the injury site, As shown in Figure 57. This emphasizes that precise control over the cell–material interface is essential for creating a permissive microenvironment that supports neural repair. Rather than focusing solely on cell transplantation, this approach integrates material design with biological regulation, enabling the coordinated modulation of cellular responses and tissue-level regeneration.

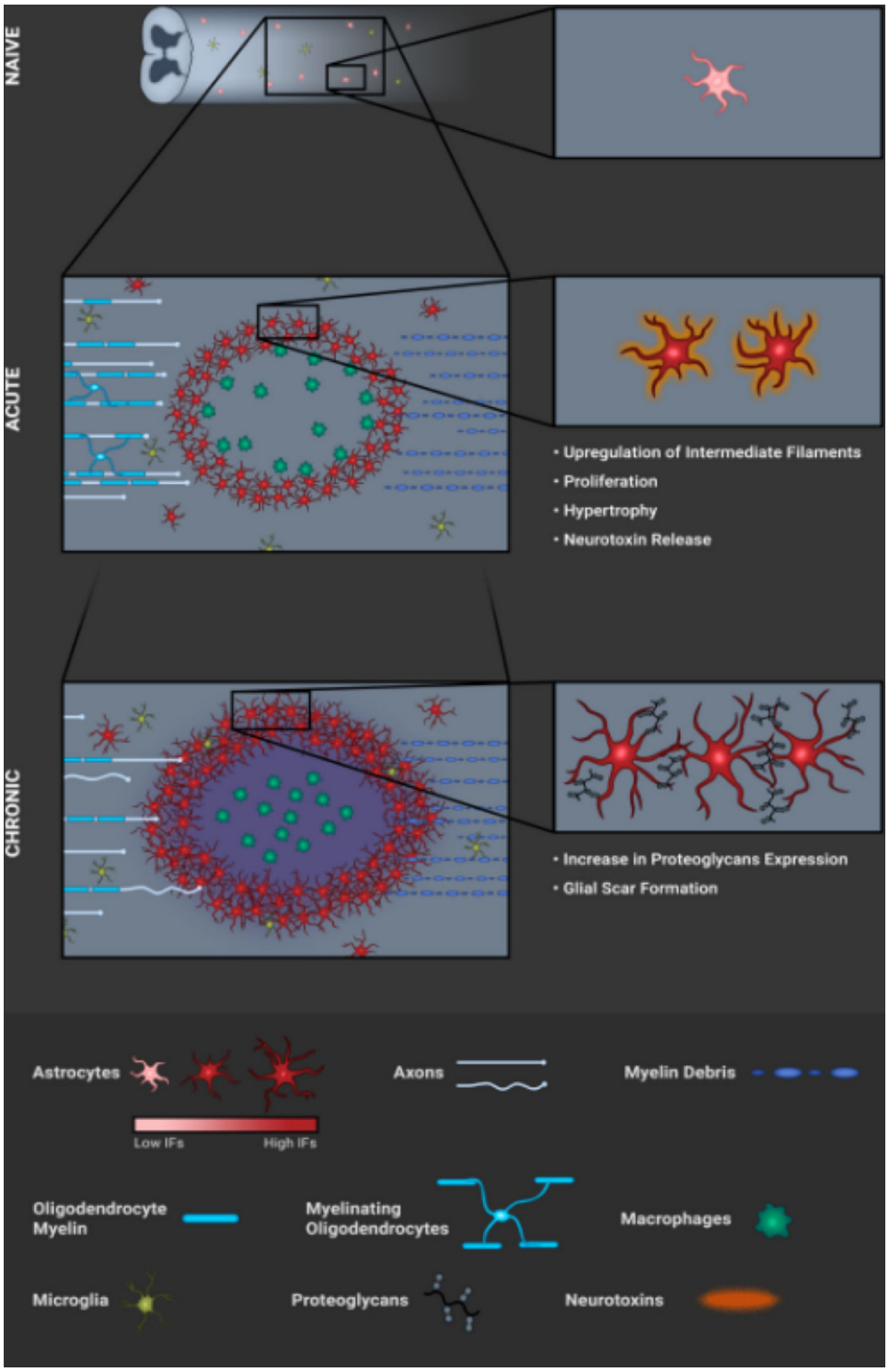

Figure 57. This schematic depicts the temporal astrocyte response to spinal cord injury across 3 core stages: NAIVE (uninjured): Astrocytes in white matter, organized into non-overlapping domains; microglia distributed. ACUTE (early post-contusion):

Microglia/macrophage infiltration + astrocyte activation (hypertrophy, increased intermediate filaments, proliferation, neurotoxin release), with axonal dieback and myelin debris. CHRONIC (long-term): Reactive astrocytes increase proteoglycans to form a thick glial scar; persistent inflammation.

Building on this principle, subsequent studies have demonstrated that scaffold-derived physical cues can further regulate cellular organization across multiple scales. Aligned electrospun scaffolds have been shown to influence cell organization and tissue architecture, as demonstrated by Wang et al. [114] further supporting the concept that scaffold-derived physical cues can regulate cellular interactions across multiple scales. The aligned topographical features of these scaffolds can provide contact guidance and modulate cell–matrix interactions, thereby directing cellular alignment and coordinated tissue organization, As shown in Figure 58. These findings reinforce the concept that cell fate is determined not only by intrinsic cellular properties but also by extrinsic cues provided by the scaffold and its microenvironment, highlighting the importance of integrating material design with biological regulation to achieve precise control over cell behavior.

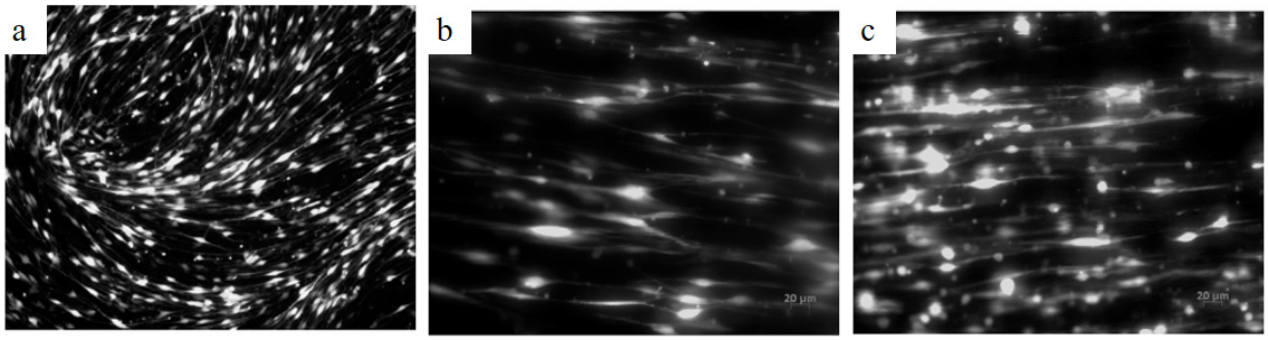

Figure 58. Schwann cell morphology on different substrates. (**a**) Fluorescent image of SCs grown on a poly-L-lysine coated dish, which displays the bipolar, swirling, but undirected growth of SCs. (**b**,**c**) Fluorescent images of Schwann cells cultured on low and high-density fibers, respectively for 2 days. On the fibers, Schwann cells grew along the fibers in a directed manner. Scale bar = 20 µm.

At the material design level, efforts have been made to construct biomimetic architectures that more closely replicate the native extracellular matrix. Forouharshad et al. [115] developed a cell vector by cultivating NSCs on both 2D and 3D structures composed of specially cross-linked and functionalized self-assembled peptides (SAPs) that exhibit improved biological and biomechanical properties. The scaffold's morphology, structure, and secondary structure were analyzed in solid-state and electrospun solutions. Morphological studies revealed that the incorporation of mixed peptides and surfactants as additives promoted the formation of thinner, uniform, and defect-free fibers. Notably, the β-folded conformation was predominant, indicating self-assembly, except in the electrospun solution. When compared to the gold standard, NSCs cultivated on electrospun SAP scaffolds in both 2D and 3D environments exhibited satisfactory proliferation, viability, and differentiation abilities *in vitro,* As shown in Figure 59. *In vivo* biocompatibility experiments further validated the feasibility of inserting fiber channels, as evidenced by a minimal foreign body reaction. The findings suggest that fibrous electrospun SAP scaffolds, in the shape of microchannels and available in both 2D and 3D configurations, may facilitate NSC regeneration in the aftermath of SCI.

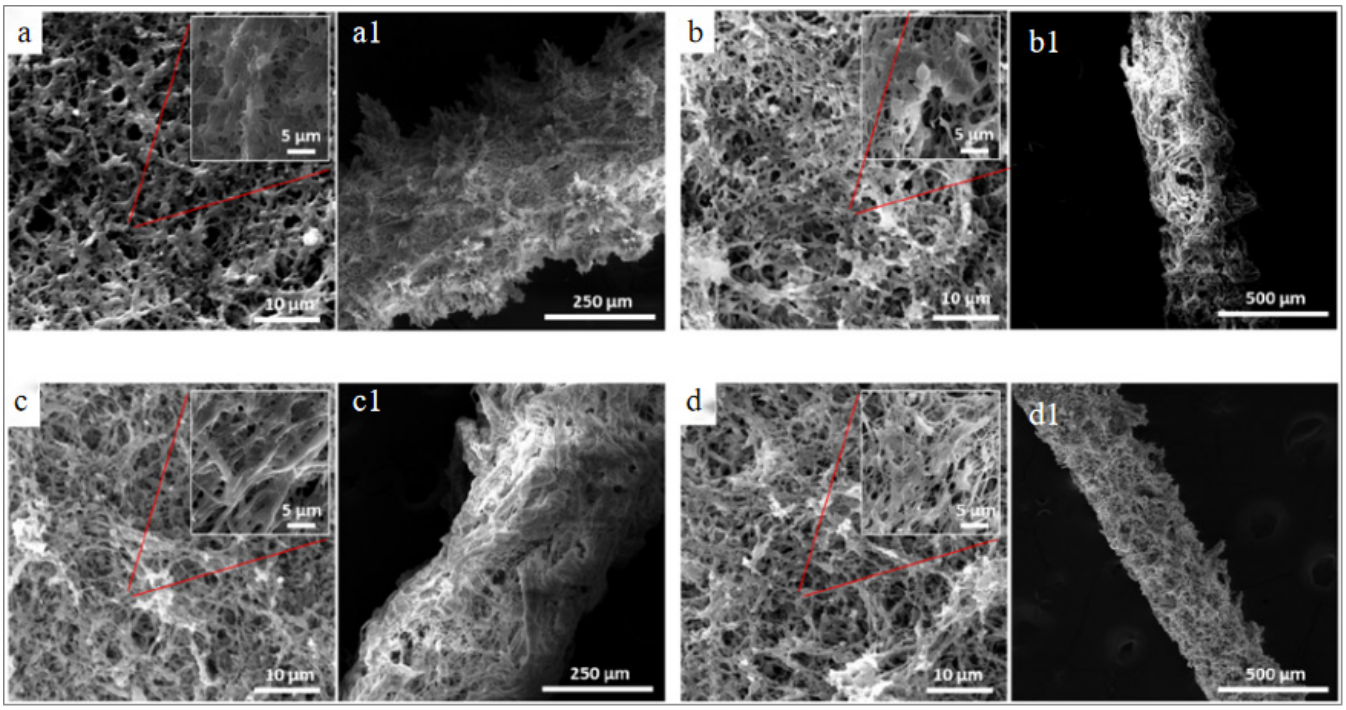

Figure 59. Images of electrospun 2D and 3D scaffolds after post-treatment (annealing and crosslinking): (**a**) electrospun Ac-FAQRVPP-GGG-(LDLK)3-CONH2(FAQ(LDLK)3) gp lamina and channel show rough surface with fibers connection, (**b**) electrospun FAQ (LDLK)3 gp-sds lamina and channel with more uniformity of fibers and surface after adding a surfactant, (**c**) electrospun FAQ (LDLK)3 gp-Hydrogel self-assembled peptide (HYDROSAP) gp lamina and channel comprise defect-free fibers and even surface, (**d**) electrospun FAQ (LDLK)3 gp-HYDROSAPgp-sds lamina and channel reveals very uniform fibers and surface after adding SDS and HYDROSAP. (**a**–**d**) 2D lamina; (**a1**–**d1**) 3D microchannels.

More recently, integrated strategies have combined biochemical signaling with structural guidance to engineer highly functional cell-supportive microenvironments. Yang et al. [116] developed an aligned fibrin nanofiber hydrogel modified with N-cadherin human Fc chimeric protein (AFGN) via electrospinning and biochemical coupling technology for optimized stem cell transplantation in SCI. The AFGN scaffold provided directional guidance, mechanical support, and specific cell-binding ligands to enhance NSC survival, neuronal differentiation, and integration with endogenous neural networks. In a rat model of 2 mm complete spinal cord transection, AFGN hydrogel-delivered NSCs demonstrated improved retention, immune modulation, and axonal regeneration, resulting in functional recovery via reconstructed neural relays. This strategy integrates chemical (N-cadherin-mediated cell adhesion) and mechanical (aligned nanofiber topography) cues to engineer NSC microenvironments, As shown in Figure 60. However, clinical translation requires addressing immunocompatibility challenges and optimizing multiscale mechanical coupling between scaffolds and host tissues.

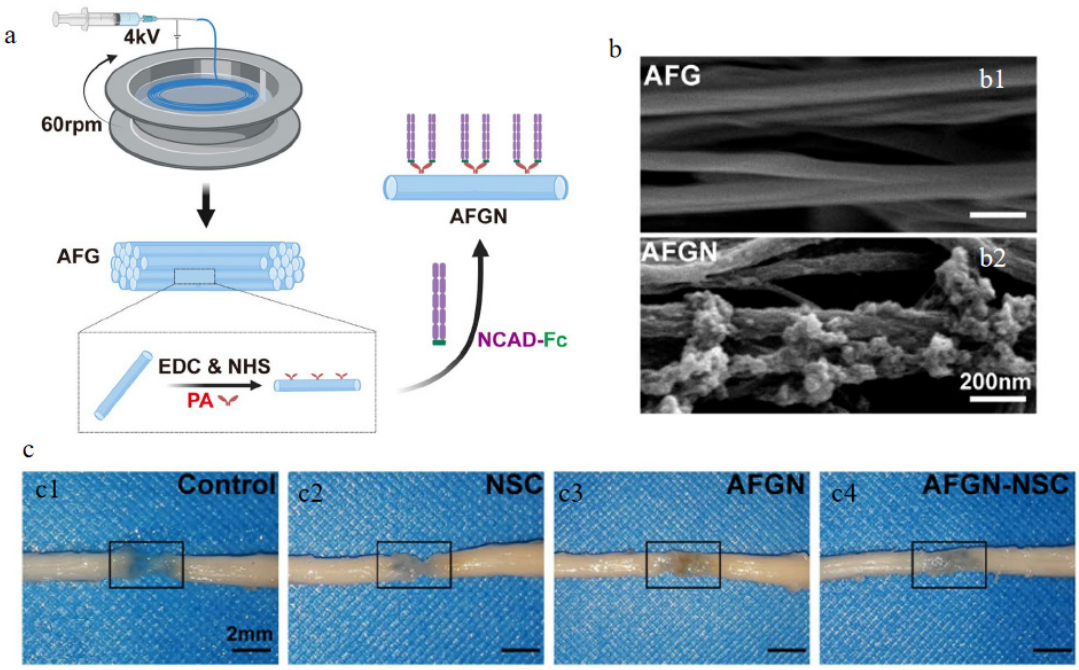

Figure 60. (**a**) Schematic diagram of the fabrication of AFGN hydrogel. (**b**) Images of (**b1**) AFG and (**b2**) AFGN hydrogels. (**c**) Specimens of the spinal cords of all experimental groups 12 weeks postsurgery: (**c1**) Control; (**c2**) NSC; (**c3**) AFGN; (**c4**) AFGN-NSC.

4.3.4. Supporting Studies, General Trends, and Critical Perspective

In addition to the representative studies discussed above, numerous investigations have explored the combination of electrospun scaffolds with various cell types, including mesenchymal stem cells, neural stem cells, and Schwann cells. These studies consistently report improvements in cell survival, differentiation, and functional recovery.

Despite differences in cell sources and scaffold compositions, the overall trend is clear: electrospun scaffolds can enhance the therapeutic efficacy of cell-based strategies by providing structural support and regulating the local microenvironment. These effects are primarily achieved by modulating cell–material interactions, which, in turn, influence cellular behavior and tissue responses. However, many of these studies follow similar design principles and therefore primarily serve as supporting evidence rather than introducing fundamentally new conceptual advances.

Overall, cell-based electrospinning strategies represent a major step toward the development of biologically active systems for spinal cord injury SCI repair. Key advances include structural regulation of cell behavior, mechanobiological control of differentiation, scaffold-assisted cell delivery, and modulation of the microenvironment.

Despite these promising developments, several critical challenges remain. First, cell survival after transplantation is still limited, particularly within the inflammatory microenvironment of acute SCI. Second, long-term functional integration of transplanted cells has not been consistently demonstrated. Third, most studies rely on small-animal models, with limited validation in clinically relevant or large-animal systems.

Future research should therefore focus on integrating cell delivery, scaffold design, and immune regulation into unified therapeutic platforms, with an emphasis on improving long-term functional outcomes and enhancing translational feasibility.

4.4. Cell Electrospinning

Although conventional electrospun scaffolds have been widely investigated for SCI repair, their densely packed fibrous networks may limit homogeneous cell infiltration. This limitation has stimulated the development of C-ES, a biofabrication strategy first introduced in 2006 to encapsulate living cells within

electrospun microthreads and scaffolds [117,118]. Early follow-up work demonstrated that highly concentrated primary cells could also be processed into viable cell-bearing threads and scaffolds [117], indicating that C-ES was not only a conceptual advance but also a technically feasible route for generating cell-laden fibrous constructs.

From an application standpoint, one of the representative demonstrations of C-ES was reported by Sampson et al. [118], who demonstrated the feasibility and in vivo safety of cell electrospinning for generating cell-laden scaffolds, As shown in Figure 61. Subsequent work further expanded this concept through aerodynamically assisted bio-threading and related bioplatforms, enabling the fabrication of large quantities of organized living architectures such as three-dimensional sheets and vessel-like structures.

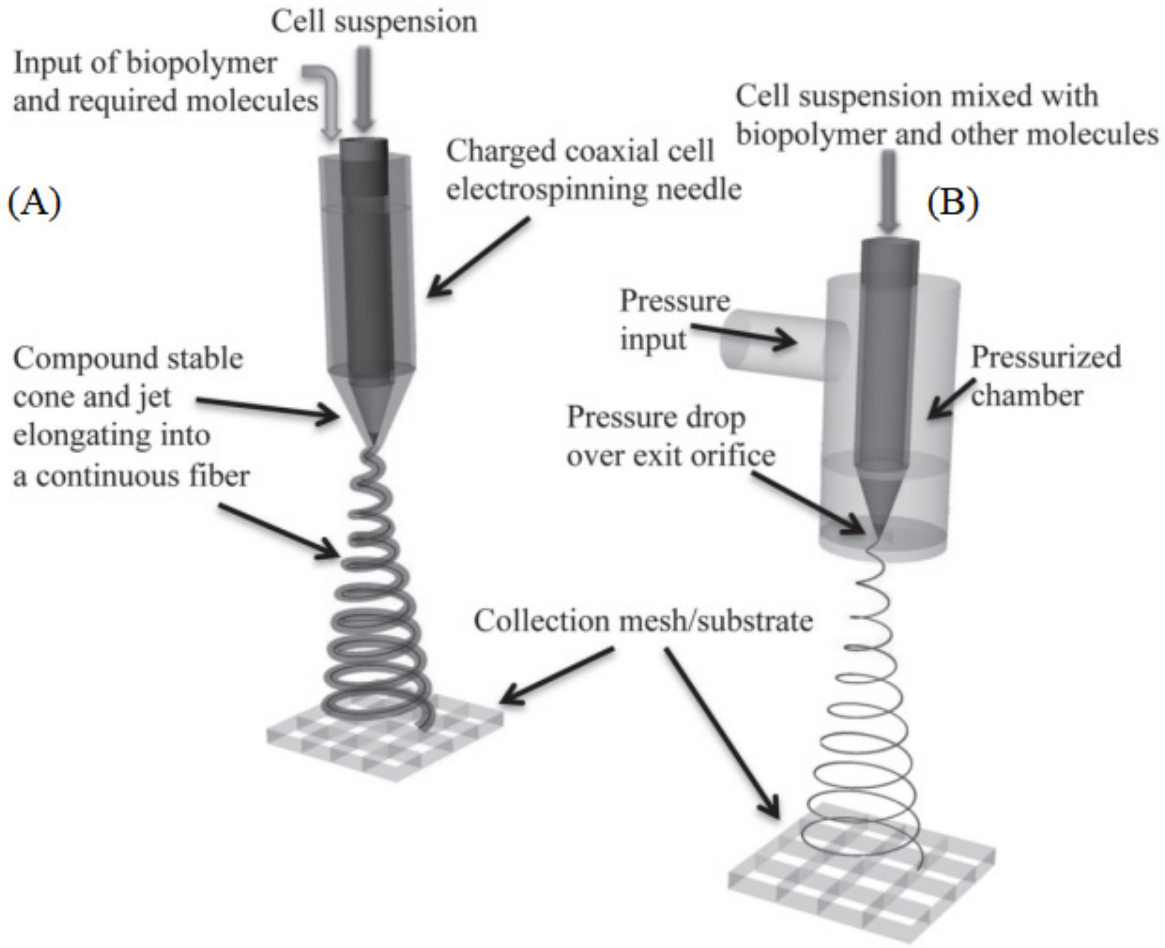

Figure 61. Schematic depiction of the two direct cell spinning approaches, (**A**) cell electrospinning and (**B**) aerodynamically assisted bio-threading.

In a broader regenerative medicine context, later reviews summarized C-ES as a functional platform for regenerative biology and medicine [119,120], and further clarified its critical processing parameters and biofabrication methodologies [121,122]. These studies collectively indicate that C-ES has evolved from an early experimental idea into a distinct and increasingly mature biofabrication branch.

More recent work has further strengthened the practical relevance of C-ES. Maurmann et al. [123] developed a reactive cell electrospinning strategy based on dynamic covalent cross-linking, enabling direct cell loading during electrospinning and the fabrication of nonaligned, aligned, and cross-aligned hydrogel nanofiber networks. In that study, the resulting scaffolds supported C2C12 myoblast viabilities greater than 85% over 14 days, and aligned scaffolds increased cell aspect ratio by approximately 27% relative to

nonaligned scaffolds. Notably, the authors also showed that cell-loaded bilayer scaffolds with perpendicular fiber alignments could guide localized directional cell responses while avoiding delamination between layers, suggesting clear potential for constructing complex tissues such as smooth muscle, neural, or tendon tissues， As shown in Figure 62. These features are particularly relevant to SCI because they provide a route toward scaffolds that combine cell incorporation, directional guidance, and hierarchical architecture in a single construct.

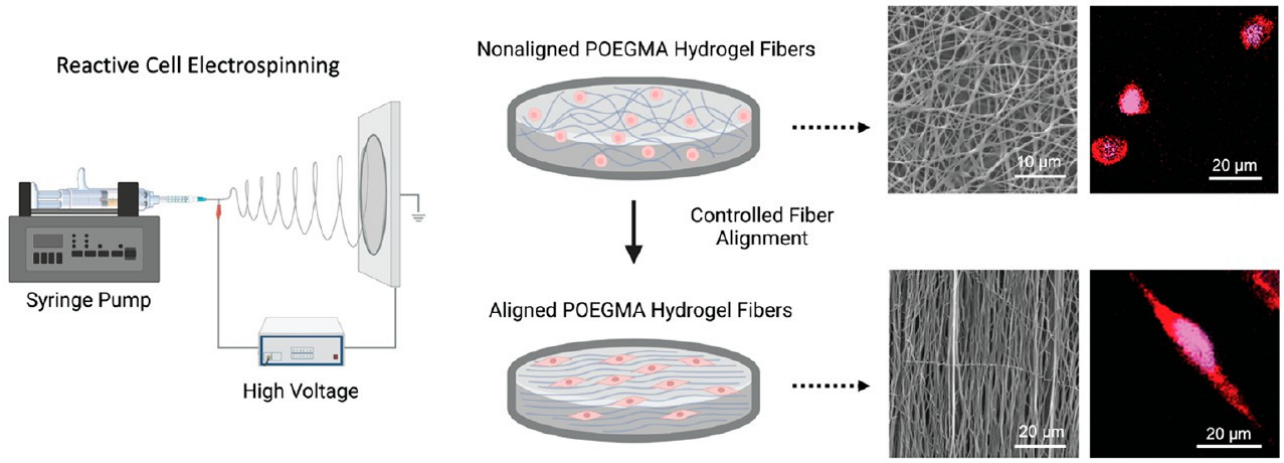

Figure 62. Reactive Cell Electrospinning for Fabricating Aligned/Nonaligned POEGMA Hydrogel Fibers with *In Situ* Cell Incorporation.

More recent work has further extended C-ES from a delivery platform into a practical *in situ* fabrication strategy for direct cell loading at injury sites. Liu et al. [124] developed a handheld *in situ* cell electrospinning device capable of directly preparing cell-loaded nanofiber scaffolds at target sites. Using human umbilical cord mesenchymal stem cells (HUCMSCs) as a model, they demonstrated minimal impact on cellular viability and dryness-related characteristics, achieving non-contact, high-efficiency cell delivery. This work holds significant implications for *in situ* tissue repair and direct cell delivery, serving as a representative foundational study for the practical application of cell electrospinning, as shown in Figure 63. For SCI, its value lies in providing a migratory strategy of "fibroblast formation concurrent with cell loading".

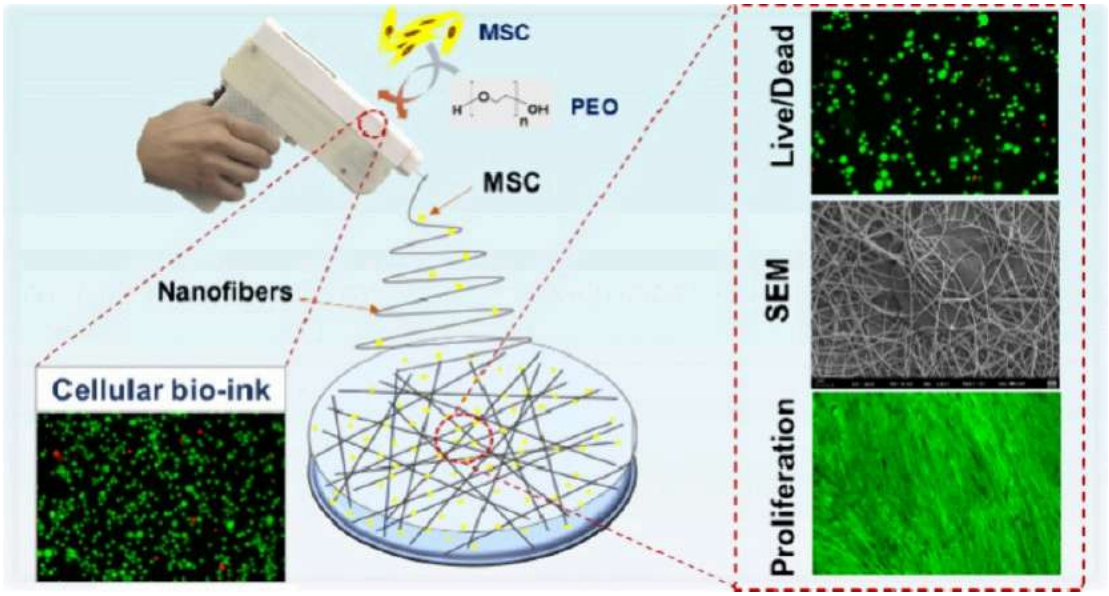

Figure 63. Construction of MSC/PEO Cell-Laden Nanofiber Scaffolds via Manual *In-Situ* Electrospinning (IS-CE) and Evaluation of Cell Activity.

Building on this concept, subsequent studies have shown that C-ES can be combined with biomaterials to achieve simultaneous cell delivery, local shaping, and microenvironment modulation. Chen et al. [125] reported *in situ* electrospinning of live cells loaded with gelatin-dopamine fibers for diabetic wound repair. The study combined human umbilical cord mesenchymal stem cells with Gel-DA as "bioinks", achieving >90% cellular viability and metabolic activity under optimized voltage conditions. Animal experiments demonstrated enhanced wound closure, collagen deposition, and angiogenesis. This approach holds promise for stem cell delivery combined with biomaterials for synergistic repair， As shown in Figure 64. Although not applicable to spinal cord injury models, the study effectively illustrates that cell electrospinning can simultaneously perform three functions: cell delivery, local shaping, and microenvironment modulation.

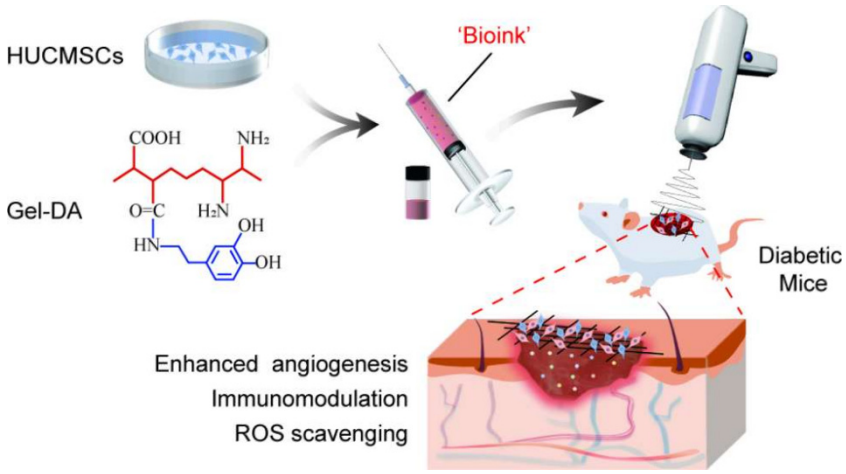

Figure 64. *In-situ* Electrospinning for Constructing HUCMSCs/Gel-DA Bioink-Laden Scaffolds to Promote Wound Healing in Diabetic Mice (with Effects on Angiogenesis, Immunomodulation, and ROS Elimination).

More recently, *in situ* C-ES has also been used to improve cell retention and localized repair on complex tissue surfaces, highlighting its translational potential for surgery-oriented regeneration. Xue et al. [126] employed handheld *in situ* electrospinning to directly immobilize MSCs onto the bone wall surface in an osteoporotic bone defect model. The results demonstrated that this method had minimal impact on MSC viability while enhancing cell retention, upregulating osteogenic marker proteins, and improving bone repair, involving CCL2-associated homing and TSG6-mediated immune regulation. This approach holds significant implications for *in situ* cell immobilization on complex curved surfaces， As shown in Figure 65. For SCI, this study best illustrates how cell electrospinning is transitioning from "proof-of-concept" to "*in situ* cell immobilization and localized repair during surgery".

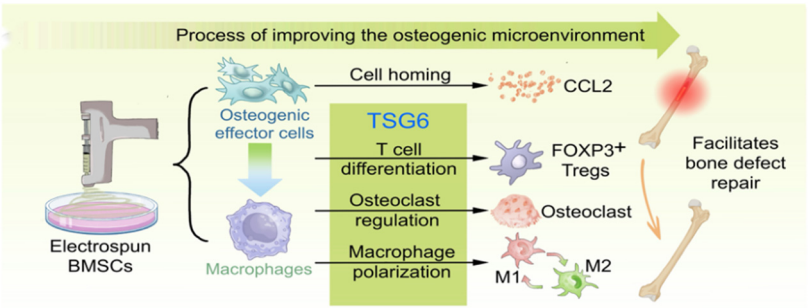

Figure 65. Schematic illustration of the mechanism by which ESG treatment modulates the bone regeneration microenvironment *in vivo*. On the one hand, this microenvironment increases local stem cell abundance by upregulating the expression of the homing factor CCL2; on the other hand, it increases the number of regulatory T cells (Tregs) by promoting TSG6 secretion by

MSCs. In addition, TSG6 regulates macrophage polarisation (M1/M2) and suppresses osteoclast differentiation, thereby synergistically improving the osteogenic microenvironment.

Although direct SCI-specific studies of C-ES are still limited, the broader biomedical literature shows that the strategy is already being explored in other repair contexts, including wound healing. Taken together, these examples suggest that C-ES may serve as a promising extension of conventional electrospinning for future SCI scaffold design, especially where simultaneous control over cellular placement, fiber alignment, and microarchitectural complexity is required.

5. Conclusions

This review thoroughly explores the mechanism, application and progress of electrospinning for SCI, and draws the following main conclusions.

5.1. Mechanism Innovation: From Single-Function to Multi-Regulation

Electrospun scaffolds establish multi-layered repair mechanisms through biomimetic design, dynamic responsiveness, and precise delivery:

a. Biomimetic Microenvironment Reconstruction: The physical properties (diameter, alignment) of nanofibers mimic natural ECM, guiding axonal extension directionally while regulating cellular behaviors (e.g., neural stem cell differentiation).
b. Immune-Inflammatory Homeostasis: Scaffolds loaded with ROS scavengers (e.g., IL-4, melatonin) suppress M1 macrophage polarization, reduce secondary injury, and promote angiogenesis and tissue remodeling.
c. Spatiotemporal Drug Delivery Control: Core-shell structures and light/magnetic-responsive carriers enable gradient release of neurotrophic factors (BDNF, GDNF), synergizing with gene therapy (AAV vectors) to enhance neuronal survival.

5.2. Technological Breakthroughs: From Static Scaffolds to Intelligent Systems

Cutting-edge research drives electrospun scaffolds toward multifunctional and intelligent platforms:

a. Multi-Material Composite Strategies: Hydrogel-electrospun hybrid scaffolds integrate mechanical support (PLGA) with bioactivity (growth factors), addressing traditional scaffold brittleness and uncontrollable degradation.
b. Conductive Functionalization: Carbon nanotube-doped scaffolds restore electrical signal conduction in injured areas, promoting corticospinal tract regeneration. Combined with electrical stimulation, this approach enhanced motor function recovery by 40% in rat models.
c. 4D Printing Technology: Shape-memory polymer scaffolds autonomously deploy *in vivo* to match spinal canal morphology, eliminating the need for secondary surgeries.
d. Cell Electrospinning as an Emerging Extension: C-ES enables the direct incorporation of living cells into fibrous scaffolds and may improve the poor cell infiltration of conventional electrospun structures. Although SCI-related studies are still limited, it shows promise for combining cell delivery with structural guidance in neural repair.

5.3. Clinical Translation: Key Challenges from Lab to Bedside

Despite technological promise, clinical adoption faces critical hurdles:

a. Standardization and Scalability: Minor variations in electrospinning parameters (voltage, collector distance) cause batch-to-batch performance fluctuations, restricting GMP-grade production.

b. Long-Term Biocompatibility: Degradation of synthetic materials (e.g., PLGA) generates localized acidic microenvironments that may exacerbate neuroinflammation, necessitating natural-derived alternatives (e.g., silk fibroin, chitosan).
c. Evidence Gap in Translation: Current studies predominantly use rodent models, lacking long-term follow-up data in large animals (e.g., non-human primates) and established efficacy evaluation gold standards.

Future Directions:

1. Patient-Specific Design: Customized layered scaffolds (e.g., gradient porosity structures) tailored to injury-level mechanical demands via 3D bioprinting integrated with patient MRI data.
2. Closed-Loop Intelligent Systems: Integration of flexible electronic sensors and self-powered devices for real-time monitoring of pH and inflammatory cytokines in injury zones, coupled with wireless drug release modulation.
3. Organoid Co-Culture Models: iPSC-derived neuron-astrocyte co-culture systems to simulate SCI pathophysiology, accelerating scaffold performance screening.
4. Nanorobot-Mediated Delivery: Magnetic nanoparticle systems for targeted blood-spinal cord barrier penetration, enhancing drug delivery efficiency while minimizing systemic toxicity.
5. Future studies should also clarify the applicability of C-ES in SCI-relevant models, particularly with respect to cell survival, directional fiber construction, long-term functional integration, and translational manufacturability, so that its advantages can be effectively incorporated into clinically relevant scaffold design.

Author Contributions

C.Y. and S.Z. completed the initial draft of the paper. M.Y. played a central driving role in the overall content, conducting a comprehensive review and editing of the manuscript. C.L. (Chuankun Li) and Y.S.D. conducted an in-depth analysis of the research background, comprehensively combing through the development context of related fields. X.M. and X.Z. collected the literature relevant to this study, laying a solid theoretical foundation and providing theoretical support for the research. C.L. (Changhe Li) and Y.Z. (Yanbin Zhang) revised the format of the paper, ensuring that the paper conformed to academic norms in form and enhancing its readability and professionalism. Y.Z. (Yongxing Zang) and P.Y. summarized the research of this paper, distilling the core points and clearly presenting the key conclusions of the study.

Ethics Statement

Not applicable.

Informed Consent Statement

Not applicable.

Data Availability Statement

Not applicable.

Funding

This study was financially supported by the Support plan for Outstanding Youth Innovation Team in Universities of Shandong Province (2023KJ114), Young Talent of Lifting engineering for Science and Technology in Shandong, China (SDAST2024QTA043), Qingdao postdoctoral researchers applied research project funding (QDBSH20230102050).

Declaration of Competing Interest

The authors declare that they have no known competing financial interests or personal relationships that could have appeared to influence the work reported in this paper.

Nomenclature

Nomenclature			
SCI	Spinal cord injury	PPC	Poly (propylene carbonate)
MP	Corticosteroid hormone	CS	Chitosan
BDNF	Brain-derived neurotrophic factor	ChABC	Chondroitinase ABC
CGRP+	Calcitonin gene-related peptide	dbcAMP	Dibutyryl cyclic adenosine monophosphate
GM-1	Injection of gangliosides	VPA	Valproic acid
EPO	Erythropoietin	AFG	A 3D layered fibrin hydrogel
TMP	Tetramethylpyrazine	TrFE	Trifluoroethylene
CT	Computed Tomography	SCs	Schwann cells
GDNF	Glial cell-derived neurotrophic factor	ECM	Extracellular matrix
CNS	Central nervous system	DβH+	Dopamine-beta-hydroxylase
NSCs	Neural stem cells	OLS	Oligodendrocytes
SF	Silk fibroin	SAPs	Self-assembled peptides
ANF	Aligned nanofibers	PLA	Poly lactic acid
AMF	Aligned microfibers	PDS	Polymer dots
PCL-PLGA	Poly (ε-caprolactone) and poly (D, L-lactide-co-glycolide)	DSC	Porcine acellular spinal cord matrix
RMF	Random microfibers	NSLCs	Neural Stem-LikeCells
PLLA	Polylactic acid	HB-9	Hemoglobin-9
db-cAMP	Dibutyryl cyclic adenosine monophosphate	RNF	Random nanofibers
PCL	Polycaprolactone	FGF-2	Fibroblast growth factor-2
PSA	Prostate specific antigen	MNS-G	Nerve-manganese sulfide
PMMA	Polymethyl methacrylate	PPy	Polypyrrole
SEM	Scanning electron microscope	GelMA	Gelatin methacryloyl
PHBV	Poly3-hydroxybutyrate-co-3-hydroxyvalerate	COL	Collagen
A-NF	Oriented PHBV fiber membrane	HDAC6	Histone deacetylase 6
R-NF	Non oriented PHBV fiber membrane	AC	Astrocyte
FAQ $(LDLK)_3$	Ac-FAQRVPP-GGG-$(LDLK)_3$-$CONH_2$	pIL10-LNP	Interleukin-10 plasmid (pIL10) wasloaded into lipid nanoparticles
HYDROSAP	Hydrogel self-assembled peptide	CAMs	Cell adhesion molecules
FTIR	Fourier transform infrared spectroscopy	MP	Methylprednisolone
TUBA	Tubastatin A	BSA	Bovine serum albumin
Islet-1	Sc-1616, sc-21248, sc-19057, sc-22542, sc-23590, all from Santa Cruz Biotech, Dallas, TX, USA	Sodium borohydride	$NaBH_4$
SC	Single-channel	Ibu	Ibuprofen
MgO	Magnesium oxide	T3	Triiodothyronine
PLCL	Lactide-caprolactone copolymer	PPDO	Polydioxycyclohexanone
NMDA	N-methyl-D-aspartic	DEXP	Dexamethasone sodium phosphate
PUR	Puromycin	MS	Microsol
RA	Retinoic acid	HA	Hyaluronic acid
CCK-8	Cell counting kit-8	PVDF	Polyvinylidene fluoride
MAP2	Microtubule associated protein	FeOOH	Iron hydroxide oxide
DMSO	Dimethyl sulfoxide	NS@COP	Ceria nanofiber scaffolds
IgG	Immunoglobulin G	BBB	Basso Beattie Bresnahan
DMF	N-Dimethylformamide	TGFβ3	Transforming growth factor β3
CD80mAb	CD80 antibody	AA	Acetic acid

GFAP	Glial fibrillary acidic protein	NGF	Nerve growth factor
HFIP	Hexafluoroisopropyl alcohol	HE	Histological evaluation
DCM	Methylene chloride	NSs	Nanofiber sponges
PCLEEP	Poly (caprolactone-co-ethyl ethylene phosphate)	(ISL@RBC NPs)	Red blood cell membrane nanoparticles loaded with isoliquiritigenin
NPC	Neural progenitor cell	ALG	Alginate
PVA	Polyvinyl alcohol	UA	Uric acid
GIE	Glutamate-induced excitotoxicity	ROS	Reactive oxygen species
PEGDA	Poly (ethylene glycol) diacrylate	PBS	Phosphate-buffered saline
CNTs	Carbon nanotubes	pDOPA	Poly (3,4-dihydroxy-L-phenylalanine)
NT-3	Neurotrophin-3	Ψ	Pseudouridine-modified
IPC	Interfacial polyelectrolyte complex	AsC	Acid-soluble chitosan
WsC	Water-soluble chitosan	PEO	Polyethylene oxide
EMSCs	Ectodermal mesenchymal stem cells	CS	Chitosan
SPIONs	Superparamagnetic iron oxide nanoparticles	GA	Glutamic acid
SC	Schwann cells	DRG	Dorsal root ganglion
TEM	Transmission electron microscopy	DHA	Docosahexaenoic acid
CSFMs	Core-shell fibrous membranes	MeHA	Methacrylate hyaluronic acid
MICM	M1 macrophage-conditioned media	GFs	Growth factors
GMS	Gelatin microspheres	αSMA	α-smooth muscle actin
MRI	Magnetic resonance imaging	DTT	Diffusion tensor tractography
HANFs	Hybrid scaffolds	OMT	Oxymatrine
AFGN	Aligned fibrin nanofiber hydrogel-N-cadherin human Fc chimeric protein	UC-MSCs	Umbilical cord mesenchymal stem cells
PU-Gel	Poly (ester polyurethane urea)	NF70	Neuronal filament protein

References

1. Wu M, Feng X. The Research Progress of "Tongdu Yisui" Acupuncture Therapy for Spinal Cord Injury Based on the Theory of Governor Vessel. *Chin. Ethn. Folk. Med.* **2024**, *33*, 72–75. DOI:10.3969/j.issn.1007-8517.2024.14.zgmzmjyyzz202414013
2. Walsh CM, Wychowaniec JK, Brougham DF, Dooley D. Functional hydrogels as therapeutic tools for spinal cord injury: New perspectives on immunopharmacological interventions. *Pharmacol. Ther.* **2022**, *234*, 108043. DOI:10.1016/J.PHARMTHERA.2021.108043
3. Zhang C, Li H, Xu R, Xu T. Research progress of biological 3D printing in the field of neurosurgery. *Chin. J. Neurotraumatic Surg.* **2020**, *6*, 57–60. DOI:10.3877/cma.j.issn.2095-9141.2020.01.014
4. Arsalan A, Scott MD, Soheila KA. Traumatic Spinal Cord Injury: An Overview of Pathophysiology, Models and Acute Injury Mechanisms. *Front. Neurol.* **2019**, *10*, 282. DOI:10.3389/fneur.2019.00282
5. Wagner FB, Mignardot JB, Le Goff-Mignardot CG, Demesmaeker R, Komi S, Capogrosso M, et al. Targeted neurotechnology restores walking in humans with spinal cord injury. *Nature* **2018**, *563*, 65–71. DOI:10.1038/s41586-018-0649-2
6. Chin JS, Milbreta U, Becker DL, Chew SY. Targeting connexin 43 expression via scaffold mediated delivery of antisense oligodeoxynucleotide preserves neurons, enhances axonal extension, reduces astrocyte and microglial activation after spinal cord injury. *J. Tissue Eng.* **2023**, *14*, 20417314221145789. DOI:10.1177/20417314221145789
7. Jazayeri SB, Beygi S, Shokraneh F, Hagen EM, Rahimi-Movaghar V. Incidence of traumatic spinal cord injury worldwide: A systematic review. *Eur. Spine J.* **2015**, *24*, 905–918. DOI:10.1007/s00586-014-3424-6
8. Ning GZ, Yu TQ, Feng SQ, Zhou XH, Ban DX, Liu Y, et al. Epidemiology of traumatic spinal cord injury in Tianjin, China. *Spinal Cord* **2010**, *49*, 386–390. DOI:10.1038/sc.2010.130
9. Wan C, Feng Z, Gao Y, Yu J, Wu Z, Yang Z, et al. Self-Healing and Shear-Stiffening Electrodes for Wearable Biopotential Sensing and Gesture Recognition. *ACS Sens.* **2024**, *9*, 5253–5263. DOI:10.1021/ACSSENSORS.4C01445
10. Ren M, Wu Q, Huang X. Flexible tactile sensors inspired by bio-mechanoreceptors. *Biosens. Bioelectron.* **2025**, *267*, 116828. DOI:10.1016/j.bios.2024.116828
11. Shen H, Fan C, You Z, Xiao Z, Zhao Y, Dai J. Advances in Biomaterial-Based Spinal Cord Injury Repair. *Adv. Funct. Mater.* **2021**, *32*, 2110628. DOI:10.1002/ADFM.202110628

12. Chai Y, Jia Q, Dai Y, Wang Y, Ye M, Wu J, et al. Meta integration of neuropathic pain experience in patients with spinal cord injury. *Chin. Nurs. Manag.* **2024**, *24*, 1071–1076. DOI:10.3969/j.issn.1672-1756.2024.07.021
13. Jiang K, Sun Y, Chen X. Mechanism underlying acupuncture therapy in spinal cord injury: A narrative overview of preclinical studies. *Front. Pharmacol.* **2022**, *13*, 875103. DOI:10.3389/fphar.2022.875103
14. Zhang D, Wang R, Zhou L, Jiang H, Sun Z, Yin H. Research progress on electroacupuncture promoting motor function recovery after spinal cord injury. *Chin. Emerg. Med.* **2023**, *32*, 361–363. DOI:10.3969/j.issn.1004-745X.2023.02.046
15. Tian T, Zhang S, Yang M. Recent progress and challenges in the treatment of spinal cord injury. *Protein Cell* **2023**, *14*, 635–652. DOI:10.1093/procel/pwad003
16. Liu W, Tang L, Wang M, Wang C, Dong Z. Characterization and Drug Release Study of Electrospun MNZ/PLGA Nanofiber Membrane Preparation. *Chin. J. Antibiot.* **2024**, *49*, 75–82. DOI:10.13461/j.cnki.cja.007622
17. Nguyen LH, Gao M, Lin J, Wu W, Wang J, Chew SY. Three-dimensional aligned nanofibers-hydrogel scaffold for controlled non-viral drug/gene delivery to direct axon regeneration in spinal cord injury treatment. *Sci. Rep.* **2017**, *7*, 42212. DOI:10.1038/srep42212
18. Qi G, Jiang Q, Wu Y, Qi W. Experimental research progress of seed cells and biological scaffolds in spinal cord tissue engineering. *Chin. Rehabil. Theory Pract.* **2021**, *27*, 677–686. DOI:10.3969/j.issn.1006-9771.2021.06.008
19. Kong Y, Wang Y, Zhao H, Tan S, Huang W. Research Status and Prospects of 3D Printing in Spinal Cord Injury Repair. *Chin. J. Clin. Anat.* **2024**, *42*, 480–483. DOI:10.13418/j.issn.1001-165x.2024.4.22
20. Jiang Z, Zhang H, Yuan X, Duan M, Tang C, Li L. Hydrogel-based treatments for spinal cord injuries. *Heliyon* **2023**, *9*, e19933. DOI:10.1016/J.HELIYON.2023.E19933
21. Cheng Y, Zhang Y, Wu H. Polymeric Fibers as Scaffolds for Spinal Cord Injury: A Systematic Review. *Front. Bioeng. Biotechnol.* **2022**, *9*, 807533. DOI:10.3389/fbioe.2021.807533
22. Jiao E, Sun Z, Xu M, Wu Z, Liu Y, Guo K, et al. Research progress of electrospinning polyurethane fiber in the field of biomedical tissue engineering. *J. Biomed. Eng.* **2024**, *41*, 840–847. DOI:10.7507/1001-5515.202305051
23. Gao X, Gao H. Research progress of biological nanomaterials in bone tissue engineering. *Oral. Med. Res.* **2019**, *35*, 524–526. DOI:10.13701/j.cnki.kqyxyj.2019.06.004
24. Xie J, MacEwan MR, Liu W, Jesuraj N, Li X, Hunter D, et al. Nerve guidance conduits based on double-layered scaffolds of electrospun nanofibers for repairing the peripheral nervous system. *ACS Appl. Mater. Interfaces* **2014**, *6*, 9472–9480. DOI:10.1021/am5018557
25. Ma X, Lv G, Wang Y, Yu D, Huang T. The effect of high-dose methylprednisolone on the expression of c-fos and HSP 70 after acute spinal cord injury in rats. *J. China Med. Univ.* **2007**, *36*, 35–37. Available online: https://qikan.cqvip.com/Qikan/Article/Detail?id=24040403 (accessed on 1 May 2026).
26. Lan X, Feng G, Qin S, Zhong L, Li Q. New ideas and opportunities for polyurethane materials in peripheral nerve repair. *Chin. J. Tissue Eng. Res.* **2025**, *29*, 6127–6137. DOI:10.12307/2025.470
27. Kong M, Zhou R, Yang M, Zhang J, Ma X, Gao T, et al. Mechanism and Performance Evaluation of a Strain Sensor Made from a Composite Hydrogel Containing Conductive Fibers of Thermoplastic Polyurethane and Polyvinyl Alcohol. *ACS Omega* **2024**, *9*, 43743–43755. DOI:10.1021/acsomega.4c06328
28. Kong M, Yang M, Li R, Long YZ, Zhang J, Huang X, et al. Graphene-based flexible wearable sensors: Mechanisms, challenges, and future directions. *Int. J. Adv. Manuf. Technol.* **2024**, *131*, 3205–3237. DOI:10.1007/s00170-023-12007-7
29. Chung YK, Hoon YK, Woon JK, Yong HK. Transplantation of Mesenchymal Stem Cells for Acute Spinal Cord Injury in Rats: Comparative Study between Intralesional Injection and Scaffold Based Transplantation. *J. Korean Med. Sci.* **2016**, *31*, 1373–1382. DOI:10.3346/jkms.2016.31.9.1373
30. Bonner JF, Steward O. Repair of spinal cord injury with neuronal relays: From fetal grafts to neural stem cells. *Brain Res.* **2015**, *1619*, 115–123. DOI:10.1016/j.brainres.2015.01.006
31. Kong W, Li R, Xia P, Pan S, Qi Z, Zhao C, et al. AuNPs@PDA-PLGA nanomembrane combined with electrical stimulation promotes spinal cord injury recovery. *Mater. Des.* **2022**, *216*, 110585. DOI:10.1016/j.matdes.2022.110585
32. Luo Y, Li W, Lin Q, Zhang F, He K, Yang D, et al. A Morphable Ionic Electrode Based on Thermogel for Non-Invasive Hairy Plant Electrophysiology. *Adv. Mater.* **2021**, *33*, 2007848. DOI:10.1002/ADMA.202007848
33. Liu Z, Shi J, Chen L, He X, Weng Y, Zhang X, et al. 3D printing of fish-scale derived hydroxyapatite/chitosan/PCL scaffold for bone tissue engineering. *Int. J. Biol. Macromol.* **2024**, *274*, 133172. DOI:10.1016/J.IJBIOMAC.2024.133172
34. Townsend-Nicholson A, Jayasinghe SN. Cell electrospinning: A unique biotechnique for encapsulating living organisms for generating active biological microthreads/scaffolds. *Biomaterials* **2006**, *7*, 3364–3369. DOI:10.1021/bm060649h
35. Chew SY, Wen J, Yim EKF, Leong KW. Sustained release of proteins from electrospun biodegradable fibers. *Biomacromolecules* **2005**, *6*, 2017–2024. DOI:10.1021/bm0501149

36. Xie J, MacEwan MR, Schwartz AG, Xia Y. Electrospun nanofibers for neural tissue engineering. *Nanoscale* **2010**, *2*, 35–44. DOI:10.1039/B9NR00243J
37. Prabhakaran MP, Venugopal JR, Chyan TT, Hai LB, Chan CK, Lim AY, et al. Electrospun biocomposite nanofibrous scaffolds for neural tissue engineering. *Tissue Eng. Part A* **2008**, *14*, 1787–1797. DOI:10.1089/ten.tea.2007.0393
38. Wang HB, Mullins ME, Cregg JM, McCarthy CW, Gilbert RJ. Varying the diameter of aligned electrospun fibers alters neurite outgrowth and Schwann cell migration. *Acta Biomater.* **2010**, *6*, 2970–2978. DOI:10.1016/j.actbio.2010.02.020
39. Hurtado A, Cregg JM, Wang HB, Wendell DF, Oudega M, Gilbert RJ, et al. Robust CNS regeneration after complete spinal cord transection using aligned poly-L-lactic acid microfibers. *Biomaterials* **2011**, *32*, 6068–6079. DOI:10.1016/j.biomaterials.2011.05.006
40. Cnops V, Chin JS, Milbreta U, Chew SY. Biofunctional scaffolds with high packing density of aligned electrospun fibers support neural regeneration. *J. Biomed. Mater. Res. Part A* **2020**, *108*, 2473–2483. DOI:10.1002/jbm.a.36998
41. Tai Z, Liu J, Wang B, Chen S, Liu C, Chen X. The Effect of Aligned and Random Electrospun Fibers Derived from Porcine Decellularized ECM on Mesenchymal Stem Cell-Based Treatments for Spinal Cord Injury. *Bioengineering* **2024**, *11*, 772. DOI:10.3390/bioengineering11080772
42. Li Z, Qi Y, Sun L, Li Z, Chen S, Zhang Y, et al. Three-dimensional nanofibrous sponges with aligned architecture and controlled hierarchy regulate neural stem cell fate for spinal cord regeneration. *Theranostics* **2023**, *13*, 4762–4780. DOI:10.7150/thno.87288
43. Nisbet DR, Forsythe JS, Shen W, Finkelstein DI, Horne MK. Review paper: A review of the cellular response on electrospun nanofibers for tissue engineering. *J. Biomater. Appl.* **2009**, *24*, 7–29. DOI:10.1177/0885328208099086
44. Johnson CD, D'Amato AR, Puhl DL, Wich DM, Vesperman A, Gilbert RJ. Electrospun fiber surface nanotopography influences astrocyte-mediated neurite outgrowth. *Biomed. Mater.* **2018**, *13*, 054101. DOI:10.1088/1748-605X/aac4de
45. Puhl DL, Funnell JL, Nelson DW, Gottipati MK, Gilbert RJ. Electrospun Fiber Scaffolds for Engineering Glial Cell Behavior to Promote Neural Regeneration. *Bioengineering* **2020**, *8*, 4. DOI:10.3390/bioengineering8010004
46. Podder AK, Mohamed MA, Tseropoulos G, Nasiri B, Andreadis ST. Engineering Nanofiber Scaffolds with Biomimetic Cues for Differentiation of Skin-Derived Neural Crest-like Stem Cells to Schwann Cells. *Int. J. Mol. Sci.* **2022**, *23*, 10834. DOI:10.3390/ijms231810834
47. Al-Hadeethi Y, Nagarajan A, Hanuman S, Mohammed H, Vetekar AM, Thakur G, et al. Schwann cell-matrix coated PCL-MWCNT multifunctional nanofibrous scaffolds for neural regeneration. *RSC Adv.* **2023**, *13*, 1392–1401. DOI:10.1039/D2RA05368C
48. Zha F, Chen W, Zhang L, Yu D. Electrospun natural polymer and its composite nanofibrous scaffolds for nerve tissue engineering. *J. Biomater. Sci.* **2020**, *31*, 519–548. DOI:10.1080/09205063.2019.1697170
49. Keshvardoostchokami M, Majidi SS, Huo P, Ramachandran R, Chen M, Liu B. Electrospun Nanofibers of Natural and Synthetic Polymers as Artificial Extracellular Matrix for Tissue Engineering. *Nanomaterials* **2021**, *11*, 21. DOI:10.3390/nano11010021
50. Xie J, Willerth SM, Li X, MacEwan MR, Rader A, Sakiyama-Elbert SE, et al. The differentiation of embryonic stem cells seeded on electrospun nanofibers into neural lineages. *Biomaterials* **2009**, *30*, 354–362. DOI:10.1016/j.biomaterials.2008.09.046
51. Hu X, Wang G. Research progress of electrospun nanofibers scaffold in nerve tissue engineering. *Chin. J. Reparative Reconstr. Surg.* **2010**, *24*, 1133–1137. Available online: https://europepmc.org/article/med/20939490 (accessed on 1 May 2026).
52. Wang G, Hu X, Lin W, Dong C, Wu H. Electrospun PLGA-silk fibroin-collagen nanofibrous scaffolds for nerve tissue engineering. *Vitr. Cell. Dev. Biol. Anim.* **2011**, *47*, 234–240. DOI:10.1007/s11626-010-9381-4
53. Mutepfa AR, Hardy JG, Adams CF. Electroactive Scaffolds to Improve Neural Stem Cell Therapy for Spinal Cord Injury. *Front. Med. Technol.* **2022**, *4*, 693438. DOI:10.3389/fmedt.2022.693438
54. Zhang J, Zhang X, Wang C, Li F, Qiao Z, Zeng L, et al. Conductive Composite Fiber with Optimized Alignment Guides Neural Regeneration under Electrical Stimulation. *Adv. Healthc. Mater.* **2021**, *10*, 2000604. DOI:10.1002/adhm.202000604
55. Sun Y, Wu J, Zhou L, Wang W, Wang H, Sun S, et al. Genetically engineered electrospinning contributes to spinal cord injury repair by regulating the immune microenvironment. *Front. Bioeng. Biotechnol.* **2024**, *12*, 1415527. DOI:10.3389/fbioe.2024.1415527
56. Guo J, Cao J, Wu J, Gao J. Electrical stimulation and conductive materials: Electrophysiology-based treatment for spinal cord injury. *Biomater. Sci.* **2024**, *12*, 5704. DOI:10.1039/D4BM00959B
57. Zhang S, Wang XJ, Li WS, Xu XL, Hu JB, Kang XQ, et al. Polycaprolactone/polysialic acid hybrid, multifunctional nanofiber scaffolds for treatment of spinal cord injury. *Acta Biomater.* **2018**, *77*, 15–27. DOI:10.1016/j.actbio.2018.06.038

58. Zhou XH, Shi G, Fan B, Cheng X, Zhang X, Wang X, et al. Polycaprolactone electrospun fiber scaffold loaded with iPSCs-NSCs and ASCs as a novel tissue engineering scaffold for the treatment of spinal cord injury. *Int. J. Nanomed.* **2018**, *13*, 6265–6277. DOI:10.2147/IJN.S175914
59. Zhang N, Lin J, Lin VPH, Milbreta U, Chin JS, Chew EGY, et al. A 3D Fiber-Hydrogel Based Non-Viral Gene Delivery Platform Reveals that microRNAs Promote Axon Regeneration and Enhance Functional Recovery Following Spinal Cord Injury. *Adv. Sci.* **2021**, *8*, 2100805. DOI:10.1002/advs.202100805
60. Milbreta U, Nguyen LH, Diao HJ, Lin J, Wu W, Sun CY, et al. Three-Dimensional Nanofiber Hybrid Scaffold Directs and Enhances Axonal Regeneration after Spinal Cord Injury. *ACS Biomater. Sci. Eng.* **2016**, *2*, 1319–1329. DOI:10.1021/acsbiomaterials.6b00248
61. Kim TG, Lee DS, Park TG. Controlled protein release from electrospun biodegradable fiber mesh composed of poly(epsilon-caprolactone) and poly(ethylene oxide). *Int. J. Pharm.* **2007**, *338*, 276–283. DOI:10.1016/j.ijpharm.2007.01.040
62. Liu T, Xu J, Chan BP, Chew SY. Sustained release of neurotrophin-3 and chondroitinase ABC from electrospun collagen nanofiber scaffold for spinal cord injury repair. *J. Biomed. Mater. Res. Part A* **2012**, *100*, 236–242. DOI:10.1002/jbm.a.33271
63. Colello RJ, Chow WN, Bigbee JW, Lin C, Dalton D, Brown D, et al. The incorporation of growth factor and chondroitinase ABC into an electrospun scaffold to promote axon regrowth following spinal cord injury. *J. Tissue Eng. Regen. Med.* **2016**, *10*, 656–668. DOI:10.1002/term.1805
64. Hong MH, Hong HJ, Pang H, Lee HJ, Yi S, Koh WG. Controlled Release of Growth Factors from Multilayered Fibrous Scaffold for Functional Recoveries in Crushed Sciatic Nerve. *ACS Biomater. Sci. Eng.* **2018**, *4*, 576–586. DOI:10.1021/acsbiomaterials.7b00801
65. Ullrich MM, Pulipaka B, Yin J, Hlinková J, Zhang F, Chan MW, et al. Neuroprotective Riluzole-Releasing Electrospun Implants for Spinal Cord Injury. *Mol. Pharm.* **2025**, *22*, 2905–2916. DOI:10.1021/acs.molpharmaceut.4c01270
66. Christopherson GT, Song H, Mao HQ. The influence of fiber diameter of electrospun substrates on neural stem cell differentiation and proliferation. *Biomaterials* **2009**, *30*, 556–564. DOI:10.1016/j.biomaterials.2008.10.004
67. Zhang D, Ni N, Chen J, Yao Q, Shen B, Zhang Y, et al. Electrospun SF/PLCL nanofibrous membrane: A potential scaffold for retinal progenitor cell proliferation and differentiation. *Sci. Rep.* **2015**, *5*, 14326. DOI:10.1038/srep14326
68. Liu T, Houle DJ, Xu J, Chan PB, Chew YS. Nanofibrous Collagen Nerve Conduits for Spinal Cord Repair. *Tissue Eng. Part A* **2012**, *18*, 1057–1066. DOI:10.1089/ten.TEA.2011.0430
69. Johnson CDL, Zuidema JM, Kearns KR, Maguie BA, Desmond PG, Thompson MD, et al. The Effect of Electrospun Fiber Diameter on Astrocyte-Mediated Neurite Guidance and Protection. *ACS Appl. Bio Mater.* **2019**, *2*, 104–117. DOI:10.1021/acsabm.8b00432
70. Chen C, Tang J, Gu Y, Liu L, Liu X, Deng L, et al. Bioinspired Hydrogel Electros pun Fibers for Spinal Cord Regeneration. *Adv. Funct. Mater.* **2019**, *29*, 1806899. DOI:10.1002/adfm.201806899
71. Xia T, Huang B, Ni S, Gao L, Wang J, Chen A, et al. The combination of db-cAMP and ChABC with poly(propylene carbonate) microfibers promote axonal regenerative sprouting and functional recovery after spinal cord hemisection injury. *Biomed. Pharmacother.* **2017**, *86*, 354–362. DOI:10.1016/j.biopha.2016.12.045
72. Xie J, Li J, Ma J, Li M, Wang X, Fu X, et al. Magnesium Oxide/Poly (L-lactide-co-ε-caprolactone) Scaffolds Loaded with Neural Morphogens Promote Spinal Cord Repair through Targeting the Calcium Influx and Neuronal Differentiation of Neural Stem Cells. *Adv. Healthc. Mater.* **2022**, *11*, e2200386. DOI:10.1002/ADHM.202200386
73. Xue J, Zhu C, Li J, Li H, Xia Y. Integration of Phase-Change Materials with Electrospun Fibers for Promoting Neurite Outgrowth under Controlled Release. *Adv. Funct. Mater.* **2018**, *28*, 1705563. DOI:10.1002/adfm.201705563
74. Vieira T, Silva JC, Kubinova S, Borges JP, Henriques C. Evaluation of Gelatin-Based Poly (Ester Urethane Urea) Electrospun Fibers Using Human Mesenchymal and Neural Stem Cells. *Macromol. Biosci.* **2024**, *24*, 2400014. DOI:10.1002/mabi.202400014
75. Xia H, Xia Y. An *in vitro* study of non-aligned or aligned electrospun poly (methyl methacrylate) nanofibers as primary rat astrocytes-loading scaffold. *Mater. Sci. Eng. C* **2018**, *91*, 228–235. DOI:10.1016/j.msec.2018.05.050
76. Subramanian A, Krishnan UM, Sethuraman S. Fabrication, characterization and *In Vitro* Evaluation of Aligned PLGA–PCL Nanofibers for Neural Regeneration. *Ann. Biomed. Eng.* **2012**, *40*, 2098–2110. DOI:10.1007/s10439-012-0592-6
77. Sánchez MM, Giraldo E, Gisbert F, Alastrue A, Martinez C, Monleón PM, et al. Acute transplantation of NPC on electrospun poly-lactic acid membranes containing curcumin into the injured spinal cord reduces neuronal degeneration. *Front. Biomater. Sci.* **2023**, *2*, 1298894. DOI:10.3389/FBIOM.2023.1298894
78. Liao S, Liu Y, Kong Y, Shi H, Xu B, Tang B, et al. A bionic multichannel nanofiber conduit carrying Tubastatin A for repairing injured spinal cord. *Mater. Today Bio* **2022**, *17*, 100454. DOI:10.1016/j.mtbio.2022.100454

79. Wu S, Chen MS, Maure P, Lee Y, Bunge MB, Arinzeh TL. Aligned fibrous PVDF-TrFE scaffolds with Schwann cells support neurite extension and myelination *in vitro*. *J. Neural Eng.* **2018**, *15*, 056010. DOI:10.1088/1741-2552/aac77f
80. Sun B, Sun Y, Han S, Zhang R, Wang X, Meng C, et al. Electroactive Hydroxyapatite/Carbon Nanofiber Scaffolds for Osteogenic Differentiation of Human Adipose-Derived Stem Cells. *Int. J. Mol. Sci.* **2022**, *24*, 530. DOI:10.3390/ijms24010530
81. Vismara I, Papa S, Veneruso V, Mauri E, Mariani A, Paola DM, et al. Selective Modulation of A1 Astrocytes by Drug-Loaded Nano-Structured Gel in Spinal Cord Injury. *ACS Nano* **2010**, *14*, 360–371. DOI:10.1021/acsnano.9b05579
82. Reis KP, Sperling EL, Teixeira C, Paim A, Alcantara B, Vizcay-Barrena G. Application of PLGA/FGF-2 coaxial microfibers in spinal cord tissue engineering: An *in vitro* and *in vivo* investigation. *Regen. Med.* **2018**, *13*, 785–801. DOI:10.2217/rme-2018-0060
83. Sun X, Zhang C, Xu J, Zhai H, Liu S, Xu Y, et al. Neurotrophin-3-Loaded Multichannel Nanofibrous Scaffolds Promoted Anti-Inflammation, Neuronal Differentiation, and Functional Recovery after Spinal Cord Injury. *Acs Biomater. Sci. Eng.* **2020**, *6*, 1228–1238. DOI:10.1021/acsbiomaterials.0c00023
84. Zhao T, Jing Y, Zhou X, Wang J, Huang X, Gao L, et al. PHBV/PLA/Col-Based Nanofibrous Scaffolds Promote Recovery of Locomotor Function by Decreasing Reactive Astrogliosis in a Hemisection Spinal Cord Injury Rat Model. *J. Biomed. Nanotechnol.* **2018**, *14*, 1921–1933. DOI:10.1166/jbn.2018.2622
85. Zheng G, Yu W, Xu Z, Yang C, Wang Y, Yue Z, et al. Neuroimmune modulating and energy supporting nanozyme-mimic scaffold synergistically promotes axon regeneration after spinal cord injury. *J. Nanobiotechnol.* **2024**, *22*, 399. DOI:10.1186/s12951-024-02594-2
86. Ni S, Xia T, Li X, Zhu X, Qi H, Huang S, et al. Sustained delivery of chondroitinase ABC by poly(propylene carbonate)-chitosan micron fibers promotes axon regeneration and functional recovery after spinal cord hemisection. *Brain Res.* **2015**, *1624*, 469–478. DOI:10.1016/j.brainres.2015.08.018
87. Shu B, Sun X, Liu R, Jiang F, Yu H, Xu N, et al. Restoring electrical connection using a conductive biomaterial provides a new therapeutic strategy for rats with spinal cord injury. *Neurosci. Lett.* **2019**, *692*, 33–40. DOI:10.1016/j.neulet.2018.10.031
88. He L, Liao S, Quan D, Ma K, Chan C, Ramakrishna S, et al. Synergistic effects of electrospun PLLA fiber dimension and pattern on neonatal mouse cerebellum C17.2 stem cells. *Acta Biomater.* **2010**, *6*, 2960–2969. DOI:10.1016/j.actbio.2010.02.039
89. Singh NK, Khaliq S, Patel M, Wheeler N, Vedula S, Freeman JW, et al. Uric Acid Released from Poly(ε-Caprolactone) Fibers as a Treatment Platform for Spinal Cord Injury. *J. Tissue Eng. Regen. Med.* **2020**, *15*, 14–23. DOI:10.1002/term.3153
90. Mogas Barcons A, Chowdhury F, Chari DM, Adams C. Systematic alignment analysis of neural transplant cells in electrospun nanofibre scaffolds. *Materials* **2022**, *16*, 124. DOI:10.3390/ma16010124
91. Faccendini A, Vigani B, Rossi S, Sandri G, Bonferoni M, Caramella C, et al. Nanofiber Scaffolds as Drug Delivery Systems to Bridge Spinal Cord Injury. *Pharmaceuticals* **2017**, *10*, 63. DOI:10.3390/ph10030063
92. Wang Q, Liu K, Cao X, Rong W, Shi W, Yu Q, et al. Plant-derived exosomes extracted from *Lycium barbarum* L. loaded with isoliquiritigenin to promote spinal cord injury repair based on 3D printed bionic scaffold. *Bioeng. Transl. Med.* **2024**, *9*, e10646. DOI:10.1002/btm2.10646
93. Zeng X, Wei QS, Ye JC, Rao JH, Zheng MG, Ma YH, et al. A biocompatible gelatin sponge scaffold confers robust tissue remodeling after spinal cord injury in a non-human primate model. *Biomaterials* **2023**, *299*, 122161. DOI:10.1016/j.biomaterials.2023.122161
94. Lee YS, Arinzeh TL. Electrospun Nanofibrous Materials for Neural Tissue Engineering. *Polymers* **2011**, *3*, 413–426. DOI:10.3390/polym3010413
95. Xia T, Ni S, Li X, Yao J, Qi H, Fan X, et al. Sustained delivery of dbcAMP by poly(propylene carbonate) micron fibers promotes axonal regenerative sprouting and functional recovery after spinal cord hemisection. *Brain Res.* **2013**, *1538*, 41–50. DOI:10.1016/j.brainres.2013.09.027
96. Rasti Boroojen F, Mashayekhan S, Abbaszadeh HA. The Controlled Release of Dexamethasone Sodium Phosphate from Bioactive Electrospun PCL/Gelatin Nanofiber Scaffold. *Iran. J. Pharm. Res.* **2019**, *18*, 111–124. DOI:10.22037/ijpr.2019.2319
97. Mays EA, Ellis EB, Hussain Z, Parajuli P, Sundararaghavan HG. Enzyme-Mediated Nerve Growth Factor Release from Nanofibers Using Gelatin Microspheres. *Tissue Eng. Part A* **2023**, *29*, 333–343. DOI:10.1089/ten.TEA.2022.0205
98. Dolci LS, Perone RC, Di Gesù R, Kurakula M, Gualandi C, Zironi E, et al. Design and *In Vitro* Study of a Dual Drug-Loaded Delivery System Produced by Electrospinning for the Treatment of Acute Injuries of the Central Nervous System. *Pharmaceutics* **2021**, *13*, 848. DOI:10.3390/pharmaceutics13060848

99. Xi K, Gu Y, Tang J, Chen H, Xu Y, Wu L, et al. Microenvironment-responsive immunoregulatory electrospun fibers for promoting nerve function recovery. *Nat. Commun.* **2020**, *11*, 4504. DOI:10.1038/s41467-020-18265-3
100. Funnell JL, Fougere J, Zahn D, Dutz S, Gilbert RJ. Delivery of TGFβ3 from Magnetically Responsive Coaxial Fibers Reduces Spinal Cord Astrocyte Reactivity *In Vitro*. *Adv. Biol.* **2024**, *8*, 2300531. DOI:10.1002/adbi.202300531
101. Gunes M, Öcal GK, Kılıclı B, Ozturk AM, Armagan G, Karavana SY. N-acetylcysteine loaded electrospun core/shell nanofibers: A promising system for ferroptosis in spinal cord injury. *Eur. J. Pharm. Biopharm.* **2026**, *218*, 114938. DOI:10.1016/j.ejpb.2025.114938
102. Reis KP, Sperling LE, Teixeira C, Sommer L, Colombo M. VPA/PLGA microfibers produced by coaxial electrospinning for the treatment of central nervous system injury. *Braz. J. Med. Biol. Res.* **2020**, *53*, e8993. DOI:10.1590/1414-431X20208993
103. Liu ZH, Huang YC, Kuo CY, Chuang CC, Chen CC, Chen NY, et al. Co-Delivery of Docosahexaenoic Acid and Brain-Derived Neurotropic Factor from Electrospun Aligned Core–Shell Fibrous Membranes in Treatment of Spinal Cord Injury. *Pharmaceutics* **2022**, *14*, 321. DOI:10.3390/pharmaceutics14020321
104. Xie J, MacEwan MR, Liu W, Jesuraj N, Li X, Hunter D, et al. Neurite outgrowth on electrospun nanofibers with uniaxial alignment: The effects of fiber density, surface coating, and supporting substrate. *ACS Nano* **2014**, *8*, 1878–1885. DOI:10.1021/nn406363j
105. Yao S, Liu X, Yu S, Wang X, Zhang S, Wu Q, et al. Co-effects of matrix low elasticity and aligned topography on stem cell neurogenic differentiation and rapid neurite outgrowth. *Biomaterials* **2016**, *102*, 33–44. DOI:10.1039/C6NR01169A
106. Song X, Xu Y, Wu J, Shao H, Gao J, Feng X, et al. A sandwich structured drug delivery composite membrane for improved recovery after spinal cord injury under longtime controlled release. *Colloids Surf.* **2021**, *199*, 111529. DOI:10.1016/j.colsurfb.2020.111529
107. Zhu H, Zhou L, Tang J, Xu Y, Wang W, Shi W. Reactive Oxygen Species-Responsive Composite Fibers Regulate Oxidative Metabolism through Internal and External Factors to Promote the Recovery of Nerve Function. *Small* **2024**, *20*, 2401241. DOI:10.1002/smll.202401241
108. Carlson A, Bennett NK, Francis NL, Halikere A, Clarke S, Moore JC, et al. Generation and transplantation of reprogrammed human neurons in the brain using 3D microtopographic scaffolds. *Nat. Commun.* **2016**, *7*, 10862. DOI:10.1038/ncomms10862
109. Koffler J, Zhu W, Qu X, Platoshyn O, Dulin JN, Brock J, et al. Biomimetic 3D-printed scaffolds for spinal cord injury repair. *Nat. Med.* **2019**, *25*, 263–269. DOI:10.1038/s41591-018-0296-z
110. Vashisth P, Kar N, Gupta D, Bellare JR. Three dimensional quercetin-functionalized patterned scaffold: Development, characterization, and *in vitro* assessment for neural tissue engineering. *ACS Omega* **2020**, *5*, 22325–22334. DOI:10.1021/acsomega.0c02678
111. Lee YS, Wu S, Arinzeh TL, Bunge MB. Enhanced noradrenergic axon regeneration into schwann cell-filled PVDF-TrFE conduits after complete spinal cord transection. *Biotechnol. Bioeng.* **2017**, *114*, 444–456. DOI:10.1002/bit.26088
112. Xu J, Xi K, Tang J, Wang J, Tang Y, Wu L, et al. Engineered living oriented electrospun fibers regulate stem cell para-secretion and differentiation to promote spinal cord repair. *Adv. Healthc. Mater.* **2023**, *12*, e2202785. DOI:10.1002/adhm.202202785
113. Zuidema JM, Gilbert RJ, Gottipati MK. Biomaterial Approaches to Modulate Reactive Astroglial Response. *Cells Tissues Organs.* **2018**, *205*, 372–395. DOI:10.1159/000494667
114. Wang HB, Mullins ME, Cregg JM, Hurtado A, Oudega M, Trombley MT, et al. Creation of highly aligned electrospun poly-L-lactic acid fibers for nerve regeneration. *J. Neural Eng.* **2009**, *6*, 016001. DOI:10.1088/1741-2560/6/1/016001
115. Forouharshad M, Raspa A, Marchini A, Ciulla MG, Magnoni A, Gelain F. Biomimetic Electrospun Self-Assembling Peptide Scaffolds for Neural Stem Cell Transplantation in Neural Tissue Engineering. *Pharmaceutics* **2023**, *15*, 2261. DOI:10.3390/PHARMACEUTICS15092261
116. Yang K, Yang J, Man W, Meng Z, Yang CY, Cao Z, et al. N-cadherin-functionalized nanofiber hydrogel facilitates spinal cord injury repair by building a favorable niche for neural stem cells. *Adv. Fiber Mater.* **2023**, *5*, 1349–1366. DOI:10.1007/s42765-023-00272-W
117. Jayasinghe SN, Irvine S, McEwan JR. Cell electrospinning highly concentrated cellular suspensions containing primary living organisms into cell-bearing threads and scaffolds. *Nanomedicine* **2007**, *2*, 555–567. DOI:10.2217/17435889.2.4.555
118. Sampson SL, Saraiva L, Gustafasson K, Jayasinghe SN, Robertson BD. Cell electrospinning: An *in vitro* and *in vivo* study. *Small* **2013**, *10*, 78–82. DOI:10.1002/smll.201300804
119. Hong Y, Huber A, Takanari K, Amoroso NJ, Hashizume R, Badylak SF, et al. Mechanical properties and *in vivo* behavior of a biodegradable synthetic polymer microfiber–extracellular matrix hydrogel biohybrid scaffold. *Biomaterials* **2011**, *32*, 3387–3394. DOI:10.1016/j.biomaterials.2011.01.025

120. Elveren B, Kurecic M, Maver T, Maver U. Cell Electrospinning: A Mini-Review of the Critical Processing Parameters and Its Use in Biomedical Applications. *Adv. Biol.* **2023**, *7*, e2300057. DOI:10.1002/adbi.202300057
121. Jayasinghe SN. Cell Electrospinning: Revolutionising Cell Scaffolding for Healthcare. *Mater. Today Bio.* **2023**, *19*, 100602. DOI:10.1002/adbi.202300224
122. Hu X, Liu S, Zhou G, Huang Y, Xie Z, Jing X. Electrospinning of polymeric nanofibers for drug delivery applications. *J. Control. Release* **2014**, *185*, 12–21. DOI:10.1016/j.jconrel.2014.04.018
123. Maurmann N, Franca FS, Giron J, Pranke P. Cell electrospinning: A review of materials and methodologies for biofabrication. *Adv. Biol.* **2023**, *7*, 2300058. DOI:10.1002/adbi.202300058
124. Liu H, Zhang Y, Gao C, Dai Q, Lu C, Sun W, et al. *In situ* cell electrospinning to produce cell-laden nanofiber scaffolds for a contactless delivery technology. *ACS Appl. Nano Mater.* **2024**, *7*, 22723–22737. DOI:10.1021/acsanm.4c03690
125. Chen Y, Chai L, Zhang M, Chen H. *In situ* electrospinning of mesenchymal stem cell-laden gelatin-dopamine fibers for accelerated diabetic wound healing. *ACS Appl. Bio Mater.* **2025**, *8*, 10185–10194. DOI:10.1021/acsabm.5c01508
126. Xue Y, Ran X, Zhao D, Han D, Cao Y, Jiang H, et al. *In situ* electrospinning at the operating table to immobilise mesenchymal stem cells on the bony wall for the regeneration of osteoporotic bone defects. *J. Nanobiotechnol.* **2026**, *24*, 277. DOI:10.1186/s12951-026-04165-z